PNC TN9410 97-057



# Pu Vector Sensitivity Study for a Pu Burning Fast Reactor

## Part II : Rod Worth Assessment and Design Optimization

May. 1997

OARAI ENGINEERING CENTER

POWER REACTOR AND NUCLEAR FUEL DEVELOPMENT CORPORATION

PNC TN9410 97 – 057
May, 1997

# Pu Vector Sensitivity Study for a Pu Burning Fast Reactor
## Part II: Rod Worth Assessment and Design Optimization

Stuart Hunter*

Abstract

This study was based on a 'pancake' type fast reactor core design of 600 MW(e), which had been optimized for Pu burning with a feed Pu vector appropriate to once-through irradiation of MOX fuel in a PWR. The purpose of the study was to investigate the effects of varying the Pu vector, examining various methods of offsetting the effects of such a change, and finally to produce fuel cycles optimized for the different qualities of Pu vector within the same basic design. In addition to the reference (once-through) Pu vector, two extreme Pu vectors were examined: high quality Pu from military stockpiles; low quality Pu corresponding to the equilibrium point of multiple recycling in a Pu burning fast reactor.

Variations in Pu quality were overcome by changing the fuel inventory - replacing some of the fuel by diluent material, and altering the fuel pin size. Using absorber material ($^{10}B_4C$) as diluent improves the rod worth shutdown margin but degrades the Na void and Doppler safety parameters, a non-absorber diluent has the opposite effects, so a mix of the 2 material types was used to optimize the core characteristics. Of the non-absorber diluent materials examined, ZrH gave significantly better performance than all others; $^{11}B_4C$ was the second choice for non-absorber diluent, because of its compatibility with $^{10}B_4C$ absorber. It was not possible to accommodate the lower quality (multi-recycled) Pu vector without a significant increase in the fuel pin volume. It was not generally possible, especially with the increased fuel pin size, to achieve positive rod worth shutdown margins - this was overcome by increasing the number of control rods. For the higher quality Pu vectors to maintain ratings within limits, it was necessary to adopt hollow fuel pellets, or else to use the diluent material as an inert matrix in the fuel pellets.

It proved possible to accommodate both extremes of Pu vector within a single basic design, maintaining key characteristics within safe limits; changes from the original reference design could be limited to an increase in pin size and in the number of control rods (both are practical alterations); it was not necessary to resort to any of the 'advanced' fuel concepts currently under development. That these results could be produced within such restrictions is a clear demonstration of the design flexibility of fast reactors for Pu burning and associated roles.

* Reactor Physics Research Section, Advanced Technology Division, O-arai Engineering Center, PNC, Japan

公　開　資　料
PNC TN9410 97－057
１９９７　年　５　月

# Ｐｕ燃焼型高速炉におけるＰｕ同位体組成比変化の影響評価
## －制御棒価値及び最適炉心検討－

スチュアート・ハンター＊

## 要旨

本研究の目的は、高速炉におけるＰｕ同位体組成比（Ｐｕベクター）変化の炉心特性に与える影響を調べ、そしてそれに対応する方策を検討し、最終的には、同一炉心において色々なＰｕベクターの燃料を燃焼できる最適炉心を構築することにある。本研究では、ＰＷＲでのＭＯＸ燃料照射によって得られたＰｕベクターを持つＰｕ燃料を燃焼するために最適化された６００ＭＷｅクラス高速炉炉心をベースとした。このレファレンスＰｕベクターに加えて、２つの極端なＰｕベクター（高フィッサイルＰｕ：解体核Ｐｕ、劣化Ｐｕ：多重リサイクルＰｕ）の場合について解析評価した。

Ｐｕベクターの変化に対して、燃料体積比の調整（幾つかの燃料ピンを希釈ピンで置き換えたり、燃料ピン径を変更する方策）により対応できることが分かった。希釈材として、ＺｒＨを使用した場合、炉心性能が大幅に改善されることが分かった。ただ、劣化Ｐｕにたいしては、燃料体積比を大幅に増加させることに加えて、制御棒ワースのマージンを確保するために、制御棒本数の増加が必要となることが分かった。

今回の検討により、燃料ピン径の増大や制御棒本数の増加により、ラッパー管サイズを変更せずに、１つの炉心で幅広いＰｕベクターを持つ燃料を燃焼できる炉心概念を構築することができた。これにより、高速炉のＰｕ燃焼における柔軟性を示すことができた。

---

＊動燃　大洗工学センター基盤技術開発部　炉心技術開発室　国際特別研究員

CONTENTS

LIST OF TABLES

LIST OF FIGURES

# 1 INTRODUCTION

A significant area in the nuclear fuel cycle which has yet to be definitively resolved is the final disposal of long lived radiotoxic waste. It is undesirable from ethical, political, ecological and economic viewpoints to leave unnecessarily large stocks of materials which may remain a potential hazard, whether real or perceived, for many future generations. Transmutation of those radiotoxic nuclides - plutonium (Pu), minor actinides and long lived fission products - which produce the long term radiotoxicity of the waste stream, is an attractive option for greatly reducing the long term waste produced by the nuclear fuel cycle.

Considerable investigation has been taking place, both in Japan[1-1 to 1-5] and elsewhere[1-6 to 1-9], into the use of fast reactors to transmute Pu, minor actinides and long lived fission products. The intense, hard neutron spectrum in a fast reactor makes it particularly suitable for such a transmutation role. When Pu and minor actinides are transmuted (fissioned) in a fast reactor, they become a valuable fuel resource rather than a waste product liability.

This document is the second of two reports, which between them present the results of a reactor physics study that was undertaken to investigate the feasibility, within a single design of core, for a Pu burning fast reactor to utilize the full range of Pu isotopic compositions that may become available. The potential flexibility of a fast reactor to burn all grades of Pu is a further advantage over other methods of Pu transmutation - at the one extreme it allows stockpiles of military Pu to be used directly, whilst at the other the use of multiple recycling can minimize the Pu remaining in the waste stream.

The study was based on a 600 MW(e) fast reactor core design - this design was taken from an earlier study, in which a core had been optimized for Pu burning with a fixed Pu vector. The data and methods for the calculations presented in the current report are in general the same as those presented in the report on Part I of the current study.

Part I of the current study was a sensitivity analysis carried out to determine the most significant characteristics of cores with different Pu vectors, and to assess the effectiveness of methods of allowing the cores to compensate for the effects of those differences. In Part II of the study, the subject of the current report, the sensitivity study was extended, primarily by the addition of calculations of rod group worths and shutdown margins. In addition, the results of the sensitivity study were used to produce a single optimized core design, appropriate for burning the range of Pu vectors.

Section 2 gives a brief summary of the results of Part I of the sensitivity study (which was the subject of a previous report). The original conclusions of Part I of the study are emphasized and made clearer by the inclusion a small number of calculations additional to those of the original report.

The sensitivity study has been extended to incorporate the 3D calculations necessary to make direct calculations of rod group worths, and thus shutdown margins. Section 3 presents the methods used in such calculations. Section 4 shows the results of the shutdown margin analysis, and how they cause the conclusions from Part I of the study to be modified. Also in Section 4 is an assessment of improving the shutdown margins by increasing the number of control rods, and other changes found necessary as a consequence of the results of the shutdown margin calculations.

To produce the final optimized core designs, it was considered appropriate to employ more detailed calculations than had been used in the sensitivity studies. Section 6 presents the changes that were made to models and methods. The production of and results for the final optimized design are given in Section 7.

## 2 SUMMARY OF PREVIOUS SENSITIVITY STUDIES

The following gives basic information on the assessment carried out for, and the results and conclusions obtained in, the sensitivity study of Part I of the analysis. (For more detailed information see the previous report.)

The reactor design used as a basis for the study has a power of 600 MW(e). The core has a 'pancake' shape, which gives it a good Na void characteristic. The fuel is MOX; in order to allow a high Pu enrichment - and thus a high Pu burning rate - the core has a low fuel volume fraction and a high Na volume fraction. (Reprocessing considerations limit the Pu enrichment to no more than ~45%.) The core has a high rate of reactivity loss with burn-up, this is a consequence of the high Pu enrichment, it is offset by a short cycle length. Table 2.1 and Figure 2.1 give further details of the design. This reactor design was initially produced as part of a previous study[1-10], in which the design was optimized for Pu burning (with the reference Pu vector described below).

Three Pu vectors were analyzed, encompassing the extremes that might be encountered in practice; the compositions are given in Table 2.2. The high quality Pu vector is military grade Pu. The reference quality Pu corresponds to that produced by once-through irradiation of MOX fuel in an LWR. The low quality Pu vector is an equilibrium composition obtained by multiple recycling in a Pu burner core, using the reference Pu as make-up feed.

In assessing the acceptability of the core variants analyzed, three types of parameters were most important: transient safety parameters, the reactivity loss per cycle and the peak linear rating. A peak linear rating limit of 430 W/cm was used; for the remaining parameters, values calculated for the reference Pu core were used as targets against which all the core variants could be assessed - values are given in Table 2.3.

There are 4 parameters of particular import to safety transients: Na void worth and Doppler coefficient, and to a lesser extent prompt neutron lifetime ($\tau$) and delayed neutron fraction ($\beta$). Composite parameters were used for ease of comparison: the ratio

Na void-to-Doppler and, where values of $\tau$ and $\beta$ were available, the following parameters:

$$\frac{Void}{Doppler.\tau}$$ (from boiling faults)

$$\frac{\beta}{Doppler.\tau}$$ (from non-boiling faults)

Reactivity loss per cycle is a major and variable component of the rod worth margin calculation. It was used as an indicator of the rod worth margin, in the absence of the 3D calculations needed to evaluate rod worths.

Two types of pin rating value were calculated. 'Type A' is based on the assumption that all the diluent material in a fuel S/A is mixed in the fuel pellets, so all 217 pins contain fuel. 'Type B' rating corresponds to the complete segregation of fuel and diluent into separate pins.

The Part I sensitivity study examined the high and low quality Pu vectors separately, the results are summarized in the 2 following sub-sections.

## 2.1 HIGH QUALITY Pu VECTOR

To compensate for the high reactivity of the Pu, the fuel fraction was reduced by replacing some of it with a diluent material. At first just three categories of diluent material were examined: void, which corresponds to either empty fuel pins or hollow fuel pellets; materials transparent to neutrons (MgO, BeO, $CeO_2$ and $Al_2O_3$); moderating materials ($^{11}B_4C$, $ZrH_{1.7}$). All these different diluent materials had the same general effects:

safety parameters were improved,
reactivity loss per cycle was degraded (increased),
'type B' pin ratings were increased.

There was one particular diluent material, ZrH, which gave significantly better results than any other, most especially by increasing the Doppler constant. All the other diluent materials

were similar in effect, $^{11}B_4C$ and BeO being slightly better than the others.

A fourth class of diluent material was examined: absorber, in the form of $^{10}B_4C$. The nuclear data calculations did not explicitly model heterogeneity effects; to approximate these for $^{10}B_4C$ diluent, it was represented as $B_4C$ with some of the $^{10}B$ replaced by $^{11}B$. For all plausible $^{10}B$ fractions the same general results were obtained:

safety parameters were degraded,

reactivity loss per cycle was improved (reduced),

the fraction of $^{10}B_4C$ required was much lower than was the case for other diluents.

It was clear that it would be possible to optimize a core design, in terms of the safety parameters and reactivity loss per cycle, by using a mixture of absorber and non-absorber materials as diluent. Optimization would be achieved by varying the fractions of the 2 components. Figure 2.2 illustrates the optimization, showing how varying the absorber/non-absorber fractions alters the balance between Na void-to-Doppler ratio and reactivity loss per cycle for several different non-absorber diluents, all for a fuel cycle of 4 batches of 6 months. The cases for ZrH as non-absorber diluent are additional to those presented in Part I; they clearly demonstrate the superior performance of this material.

As demonstrated by Figure 2.2, only for ZrH as non-absorber diluent was it possible to simultaneously achieve the targets for safety parameters and reactivity loss (with a fuel cycle of 4 batches of 6 months). A number of sensitivities were assessed, using $^{11}B_4C$ as non-absorber diluent and varying both cycle length and number of batches. It was determined that, with $^{11}B_4C$ non-absorber diluent, it would be possible to meet targets if the cycle length were reduced, either to 5.3 months, or to 5.7 months with a 3 batch cycle.

A design variant was assessed, in which a uniform Pu enrichment of 45% was used, with the balancing of rating between the inner and outer core zones being achieved by using different diluent fractions in the 2 zones. The intent of the design was to maximize the Pu enrichment, and thus to maximize the Pu burning rate. Results were

produced for a core with an optimized mixture of ZrH and $^{10}B_4C$ as diluent, they are given in Table 2.3.

Table 2.3 gives results for the various optimized cases, and also the reference case. (It is necessary to interpolate between the cases for $^{11}B_4C$ non-absorber diluent to obtain the limiting cycle lengths mentioned above.)

In reviewing the results for the various diluent materials assessed, it was concluded that, in addition to $^{10}B_4C$ as absorber diluent, there were 3 non-absorber diluent materials particularly suitable for considering further:

ZrH, because of the significantly better performance (safety parameters and reactivity loss),

$^{11}B_4C$ because it raises no questions of compatibility with the $^{10}B_4C$ absorber diluent,

void because it can be placed in fuel pins (thus reducing ratings) without raising compatibility questions.

## 2.2 LOW QUALITY Pu VECTOR

To allow criticality targets to be met with the low quality Pu vector it was necessary to increases the fuel inventory, by increasing the pin radius. The basic S/A design of pins supported by grids and a high coolant volume fraction of 65% gives sufficient margin for such a change - Figure 2.3 shows the S/A cross-section for various sizes of fuel pin. Alternative approaches to increasing reactivity, by increasing Pu enrichment or reducing cycle length, were found to be impractical.

A calculation with increased pin size showed that, compared with the reference case, the low quality Pu core had the following characteristics:

safety parameters were degraded,

reactivity loss per cycle was improved.

From the results obtained for the high quality Pu vector, it was deduced that the addition of a small fraction of non-absorber diluent to the low quality Pu core should improve the safety parameters.

Adding the most effective diluent, ZrH, it was seen that a range of options were able to simultaneously satisfy the targets for both safety parameters and reactivity loss. As shown in Figure 2.4 for a 4 batch cycle, an increased fuel pin volume of at least 150% is required (with a 6 month cycle length), but if the pin size is increased to 180% then a cycle length up to 12 months is possible. With a 3 batch fuel cycle the minimum allowable pin size reduces to ~140%.

Limited calculations were also done with other diluent materials (void, $^{11}B_4C$, $Al_2O_3$ and BeO). As with the high quality Pu vector, all were seen to be similarly effective, but rather less so than ZrH. For two of these diluents - $^{11}B_4C$ and $Al_2O_3$ - sufficient calculations were done to define the limits of acceptable conditions. Table 2.4 gives the results (those for $^{11}B_4C$ were not included in Part I): the minimum pin sizes required, for a 4 batch, 6 month cycle, are 200% and 220% for $^{11}B_4C$ and $Al_2O_3$ respectively. With such a large pin size the number of diluent pins required is such that the peak 'Type B' pin ratings are approaching the 430 W/cm limit.

### 2.2.1 EFFECT ON OTHER Pu VECTORS

Since the main purpose of the study was to consider a single reactor design burning various compositions of Pu, it was necessary to consider how the increased pin size necessary for the low quality Pu affected the case for other Pu vectors. One possibility would be to use several alternative sizes of gagging device in the S/A design, so that the same S/A pressure drop and flow can be obtained with different sizes of fuel pin. If such an approach is possible, it would greatly improve the freedom for optimizing a core design for a wider range of Pu compositions. Consideration of whether such an approach is feasible from a thermal hydraulics point of view is beyond the scope of the current study. It was, conservatively, assumed throughout the study that it was necessary to have a uniform pin size for all Pu vectors

The effects of adopting an increased pin size were assessed for both the reference and high quality Pu vectors. Results for some of

these calculations are shown, in Table 2.5 for reference Pu and Table 2.6 for high quality Pu; they show results for 2 different non-absorber diluents - $^{11}B_4C$ and ZrH - and for pin sizes of 150% and 200%. (These pin sizes are minima, taken from the low quality Pu calculations.) As before, a mixture of absorber and non-absorber diluents was used; the tables show cases with the diluent mixture adjusted to produce a near limiting Na void-to-Doppler ratio, this minimizes both reactivity losses and pin ratings. (Several of the cases shown in the two tables were not included in Part I.)

The results of Tables 2.5 and 2.6 show that the safety parameter and reactivity loss targets can be met simultaneously (though for the 150% pin size with $^{11}B_4C$ non-absorber diluent the margins are comparatively small). With ZrH non-absorber diluent the 'type B' peak rating approaches the 430 W/cm limit, and with $^{11}B_4C$ the limit is clearly exceeded. To ensure that the 430 W/cm limit is not exceeded, it would be necessary for the diluent (or at least a fraction thereof) to be placed within fuelled pins. Any questions of fuel-diluent compatibility can be avoided by using void as the diluent positioned in the fuel pins (i.e. hollow fuel pellets) - this need not significantly affect the results, since void and $^{11}B_4C$ were shown to be approximately interchangeable as diluent materials.

## 2.3 CORRECTION

Since Part I of the study was published, a minor error in the PENCIL program has been discovered and corrected. This caused the diluent fractions in certain of the calculations to be slightly different from the reported values. The effect is too small to alter any of the conclusions of Part I of the study, but corrections are listed below, for the record (the table numbers refer to the report on Part I of the study).

In Table 5.8, alter the $B_4C$ fractions,

| | | | | | | |
|---|---|---|---|---|---|---|
| from: | 0 | 4 | 6 | 8 | 10 | 13.2 |
| to: | 0 | 3.23 | 5.07 | 7.08 | 9.28 | 13.2 |

In Table 5.9, the 3 cases do not have identical $B_4C$ fractions:

void diluent 5.07 pins of $B_4C$

$BeO/Al_2O_3$ diluent 6 pins of $B_4C$

In Table 5.11, in the ZrH moderator case,
alter the $B_4C$ fraction from 3 pins to 3.05 pins

In Table 6.12, alter the $B_4C$ fractions,

| | | |
|---|---|---|
| from: | 2 | 5 |
| to: | 2.03 | 5.16 |

Table 2.1 Main parameters of reference core design

| | |
|---|---|
| Reactor Power | 600 MWe / 1560 MWth |
| Core Diameter | 4.0 m |
| Core Height | 0.6 m |
| Fuel Type | MOX |
| Pu Enrichment | 37.5% (inner core)<br>45.0% (outer core) |
| Numbers of S/As | Inner Core 295<br>Outer Core 246<br>Main Rods 27<br>Backup Rods 9 |
| Core Volume Fractions | Fuel 18.00%<br>Steel 16.32%<br>Coolant 64.46% |
| No. of Pins per S/A | 217 |
| Fuel Pellet Diameter | 4.781 mm |
| Clad Thickness | 0.4185 mm |
| Clad Outer Diameter | 5.778 mm |
| Wrapper Thickness | 3.9 mm |
| Inter-Wrapper Gap | 5.8 mm |
| Core Pitch | 158.1 mm (a/f) |
| Pin Support | grids |
| Cycle Length | 6 months |
| Fuel Irradiation | 4 batches |

Table 2.2 Isotopic compositions of the three Pu vectors (w/o)

| Pu Quality | Pu 238 | Pu 239 | Pu 240 | Pu 241 | Pu 242 | Am 241 |
|---|---|---|---|---|---|---|
| High (military) | 0.0 | 94.0 | 6.0 | 0.0 | 0.0 | 0.0 |
| Reference (once through) | 1.8 | 58.2 | 22.3 | 11.1 | 5.5 | 1.1 |
| Low (multi-recycled) | 3.4 | 32.6 | 39.8 | 8.0 | 15.4 | 0.8 |

Table 2.3 Sensitivity study results for reference core and for high quality Pu cases optimized with 100% pin size

| | | Reference Pu Core | Uniform Diluent Fraction | Uniform 45% Pu Enrichment | $B_4C$ Diluent 4 batch * 6 month | | $B_4C$ Diluent 4 batch * 5 month | | $B_4C$ Diluent 3 * 6 mon. |
|---|---|---|---|---|---|---|---|---|---|
| Diluent Material | | None | $ZrH/^{10}B_4C$ | $ZrH/^{10}B_4C$ | $B_4C$ | $B_4C$ | $B_4C$ | $B_4C$ | $B_4C$ |
| $^{10}B$ Fraction | | - | 92% | 92% | 5% | 3% | 5% | 3% | 3% |
| Diluent Fraction (pins) | | - | 23/4.08 | 52/3.05 I<br>26/3.05 O | 40.91 | 46.04 | 43.70 | 49.43 | 50.75 |
| Fuel Cycle | | 4*6 month | 4*6 month | 4*6 month | 4*6 month | 4*6 month | 4*5 month | 4*5 month | 3*6 month |
| Pu Enrichment (%) | (inner) | 37.5 | 39.07 | 45.0 | 38.97 | 39.14 | 38.34 | 38.46 | 38.54 |
| | (outer) | 45.0 | 44.84 | 45.0 | 45.00 | 44.98 | 44.96 | 45.00 | 44.99 |
| Na Void (%Δk/kk') | | 1.631 | 1.548 | 0.887 | 1.489 | 1.395 | 1.474 | 0.995 | 0.980 |
| Doppler Constant | | -.00573 | -.00572 | -.00730 | -.00434 | -.00506 | -.00429 | -.00510 | -.00506 |
| Void:Doppler Ratio | | -285 | -271 | -122 | -343 | -276 | -344 | -195 | -194 |
| Peak Pin Rating (W/cm) | ('type A') | 279.9 | 287.2 | 280.3 | 292.4 | 294.4 | 288.4 | 289.6 | 296.3 |
| | ('type B') | 279.9 | 328.2 | 375.6 | 360.3 | 373.7 | 361.1 | 375.0 | 386.7 |
| Reactivity Loss/ Cycle (%Δk/kk') | (70gp) | 4.304 | 3.614 | 3.903 | 4.622 | 4.945 | 3.835 | 4.128 | 4.888 |
| | (7gp) | 4.237 | 3.695 | 4.113 | 4.591 | 4.935 | 3.810 | 4.117 | 4.886 |
| EOC Keff | (70gp) | 1.04708 | 1.00124 | 1.00399 | 0.99864 | 0.99976 | 0.99878 | 0.99995 | 1.00005 |
| | (7gp) | 1.05233 | 1.00493 | 1.00399 | 1.00445 | 1.00488 | 1.00444 | 1.00482 | 1.00485 |
| Pu Burn Rate (Kg/TWhe) | (all) | 72.3 | 71.4 | 73.4 | 75.7 | 72.3 | 73.5 | 72.6 | 72.5 |
| | (fissile) | 74.6 | 98.5 | 104.3 | 94.7 | 95.5 | 96.8 | 96.8 | 97.0 |
| Neutron Lifetime (sec x $10^{-6}$) | | 0.619 | | 0.717 | 0.670 | | | | |
| Delayed Neutron Fraction (%) | | 0.2954 | | 0.2352 | 0.2429 | | | | |
| Safety Comparators | V/D.τ | -460 | | -169 | -512 | | | | |
| | β/D.τ | -83 | | -45 | -84 | | | | |
| Average Irradiation (GWd/te) | | 102.1 | 114.1 | 125.0 | 125.7 | 129.5 | 106.5 | 110.1 | 99.9 |

Table 2.4 Sensitivity study results for low quality Pu: variation with pin size for a 4 batch * 6 month cycle, for both $^{11}B_4C$ and $Al_2O_3$ diluents

| Diluent Material | | $^{11}B_4C$ | $^{11}B_4C$ | $Al_2O_3$ | $Al_2O_3$ | $Al_2O_3$ |
|---|---|---|---|---|---|---|
| Pin Size | | 160% | 200% | 180% | 200% | 220% |
| Na Volume (%) | | 48.68 | 38.17 | 43.42 | 38.17 | 32.91 |
| Diluent Fraction (pins) | | 26.7 | 58.5 | 45.4 | 60.1 | 72.1 |
| Pu Enrichment (%) | (inner) | 37.90 | 38.51 | 38.10 | 38.42 | 38.71 |
| | (outer) | 45.00 | 44.97 | 45.00 | 44.99 | 45.01 |
| Na Void (%Δk/kk') | | 2.944 | 2.146 | 2.665 | 2.312 | 1.975 |
| Doppler Constant | | -.00650 | -.00794 | -.00621 | -.00646 | -.00669 |
| Void:Doppler Ratio | | -453 | -270 | -429 | -358 | -295 |
| Peak Pin Ratings (inner/outer) (W/cm) | (A) (BOC) | 282.9 | 285.5/285.0 | 283.3/283.4 | 284.4/285.7 | 285.7/287.8 |
| | (A) (EOC) | | 283.2/283.2 | 281.1/281.5 | 283.6/283.3 | 285.4/285.3 |
| | (B) (BOC) | 322.6 | 390.9/390.2 | 358.3/358.4 | 393.3/395.1 | 427.9/431.0 |
| | (B) (EOC) | | 387.7/387.7 | 355.5/356.0 | 392.2/391.8 | 427.4/427.3 |
| Reactivity Loss per Cycle (%Δk/kk') | (70gp) | 2.468 | 2.342 | 2.414 | 2.359 | 2.310 |
| | (7gp) | 2.430 | 2.324 | 2.388 | 2.333 | 2.306 |
| EOC Keff | (70gp) | 1.00457 | 1.00920 | 1.00787 | 1.01034 | 1.01259 |
| | (7gp) | 1.00465 | 1.00521 | 1.00496 | 1.00496 | 1.00483 |
| Pu Burn Rate (Kg/TWhe) | (all) | 67.7 | 66.2 | 66.9 | 66.6 | 66.4 |
| | (fissile) | 32.9 | 32.6 | 32.8 | 32.6 | 32.5 |
| Neutron Lifetime (sec x $10^{-6}$) | | | | | | 0.458 |
| Delayed Neutron Fraction (%) | | | | | | 0.3152 |
| Safety Comparators | V/D.τ | | | | | -645 |
| | β/D.τ | | | | | -103 |
| Average Irradiation (GWd/te) | | 72.7 | 69.9 | 71.7 | 70.6 | 69.5 |

Table 2.5 Sensitivity study results for reference quality Pu: cases optimized with 150% & 200% pin sizes, for ZrH and $^{11}B_4C$ non-absorber diluents

| Diluent Material | | ZrH | ZrH | $^{11}B_4C$ | $^{11}B_4C$ |
|---|---|---|---|---|---|
| Pin Size | | 150% | 200% | 150% | 200% |
| Na Volume (%) | | 51.34 | 38.17 | 51.34 | 38.17 |
| Diluent Fraction (pins) | | 5 / 32 | 6.5 / 41 | 72.0 (1.6%) | 95.7 (1.9%) |
| Pu Enrichment (%) | (inner) | 40.00 | 41.03 | 39.20 | 39.93 |
| | (outer) | 45.05 | 44.86 | 45.00 | 45.07 |
| Na Void (%Δk/kk') | | 2.077 | 1.610 | 1.699 | 1.569 |
| Doppler Constant | | -.00693 | -.00571 | -.00618 | -.00562 |
| Void:Doppler Ratio | | -300 | -282 | -274 | -279 |
| Peak Pin Ratings (A) | (BOC) | 284.0/273.3 | 283.4/280.5 | 295.6/269.2 | 297.4/276.5 |
| (inner/outer) | (EOC) | 274.6/274.3 | 279.6/280.0 | 273.5/274.0 | 279.5/279.7 |
| (W/cm) (B) | (BOC) | 342.4/329.5 | 362.8/359.2 | 442.4/402.9 | 532.0/494.6 |
| | (EOC) | 331.0/330.7 | 357.9/358.4 | 409.3/410.1 | 500.0/500.4 |
| Reactivity Loss per | (70gp) | 2.340 | 1.606 | 4.006 | 3.193 |
| Cycle (%Δk/kk') | (7gp) | 2.345 | 1.622 | 3.963 | 3.165 |
| EOC Keff | (70gp) | 1.00079 | 1.01117 | 1.00257 | 1.00644 |
| | (7gp) | 1.00475 | 1.00446 | 1.00446 | 1.00514 |
| Pu Burn Rate | (all) | 75.7 | 78.8 | 71.5 | 72.9 |
| (Kg/TWhe) | (fissile) | 80.3 | 84.0 | 75.8 | 78.1 |
| Average Irradiation (GWd/te) | | 79.7 | 62.9 | 101.8 | 91.2 |

Table 2.6 Sensitivity study results for high quality Pu: cases optimized with 150% & 200% pin sizes, for ZrH and $^{11}B_4C$ non-absorber diluents

| Diluent Material | | ZrH | ZrH | $^{11}B_4C$ | $^{11}B_4C$ |
|---|---|---|---|---|---|
| Pin Size | | 150% | 200% | 150% | 200% |
| Na Volume (%) | | 51.34 | 38.17 | 51.34 | 38.17 |
| Diluent Fraction (pins) | | 5.1 / 53 | 5.6 / 65 | 93.1 (2.0%) | 113.8 (2.1%) |
| Pu Enrichment (%) | (inner) | 40.76 | 41.56 | 39.78 | 40.39 |
| | (outer) | 44.90 | 44.75 | 44.84 | 45.09 |
| Na Void (%Δk/kk') | | 1.400 | 1.082 | 1.307 | 1.295 |
| Doppler Constant | | -.00511 | -.00368 | -.00522 | -.00460 |
| Void:Doppler Ratio | | -274 | -294 | -250 | -281 |
| Peak Pin Ratings (A) | (BOC) | 288.2/269.5 | 288.4/277.1 | 302.6/265.4 | 303.8/273.7 |
| (inner/outer) | (EOC) | 272.1/272.3 | 278.3/278.1 | 272.6/272.8 | 278.6/278.9 |
| (W/cm) (B) | (BOC) | 393.6/368.0 | 427.4/410.7 | 530.0/464.8 | 638.8/575.5 |
| | (EOC) | 371.7/371.9 | 412.5/412.2 | 477.4/477.8 | 585.8/586.4 |
| Reactivity Loss per | (70gp) | 2.097 | 1.419 | 4.079 | 3.228 |
| Cycle (%Δk/kk') | (7gp) | 2.205 | 1.463 | 4.112 | 3.250 |
| EOC Keff | (70gp) | 1.01494 | 1.02010 | 1.00062 | 1.00205 |
| | (7gp) | 1.00486 | 1.00436 | 1.00440 | 1.00472 |
| Pu Burn Rate | (all) | 71.4 | 72.4 | 71.7 | 72.5 |
| (Kg/TWhe) | (fissile) | 104.3 | 107.1 | 97.6 | 99.6 |
| Average Irradiation (GWd/te) | | 90.0 | 72.8 | 119.1 | 107.3 |

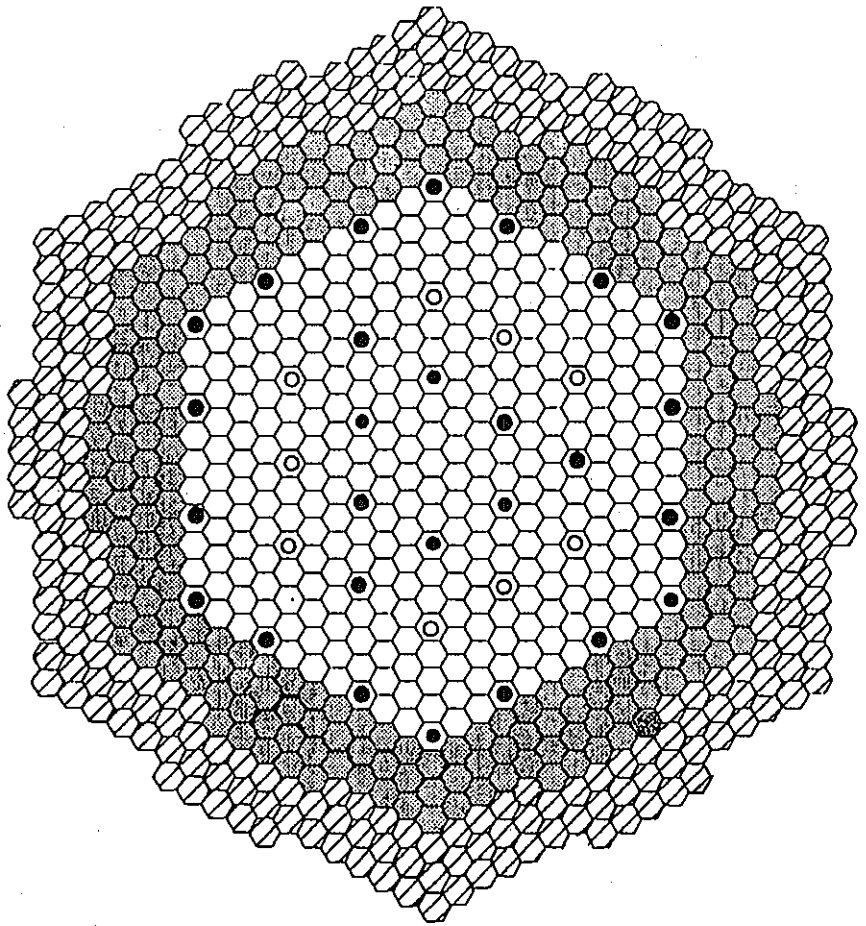

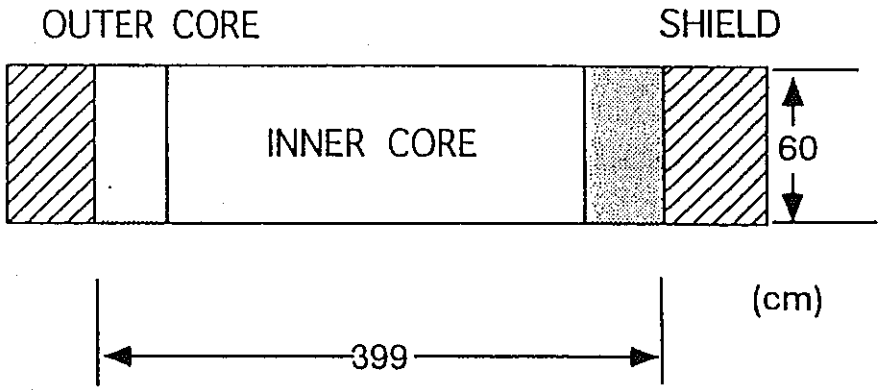


| | |
|---|---|
| INNER CORE | 295 |
| OUTER CORE | 246 |
| SHIELD | 270 |
| PRIMARY CR | 27 |
| BACKUP CR | 9 |

Figure 2.1 Configuration of reference 600MWe Pu burner core

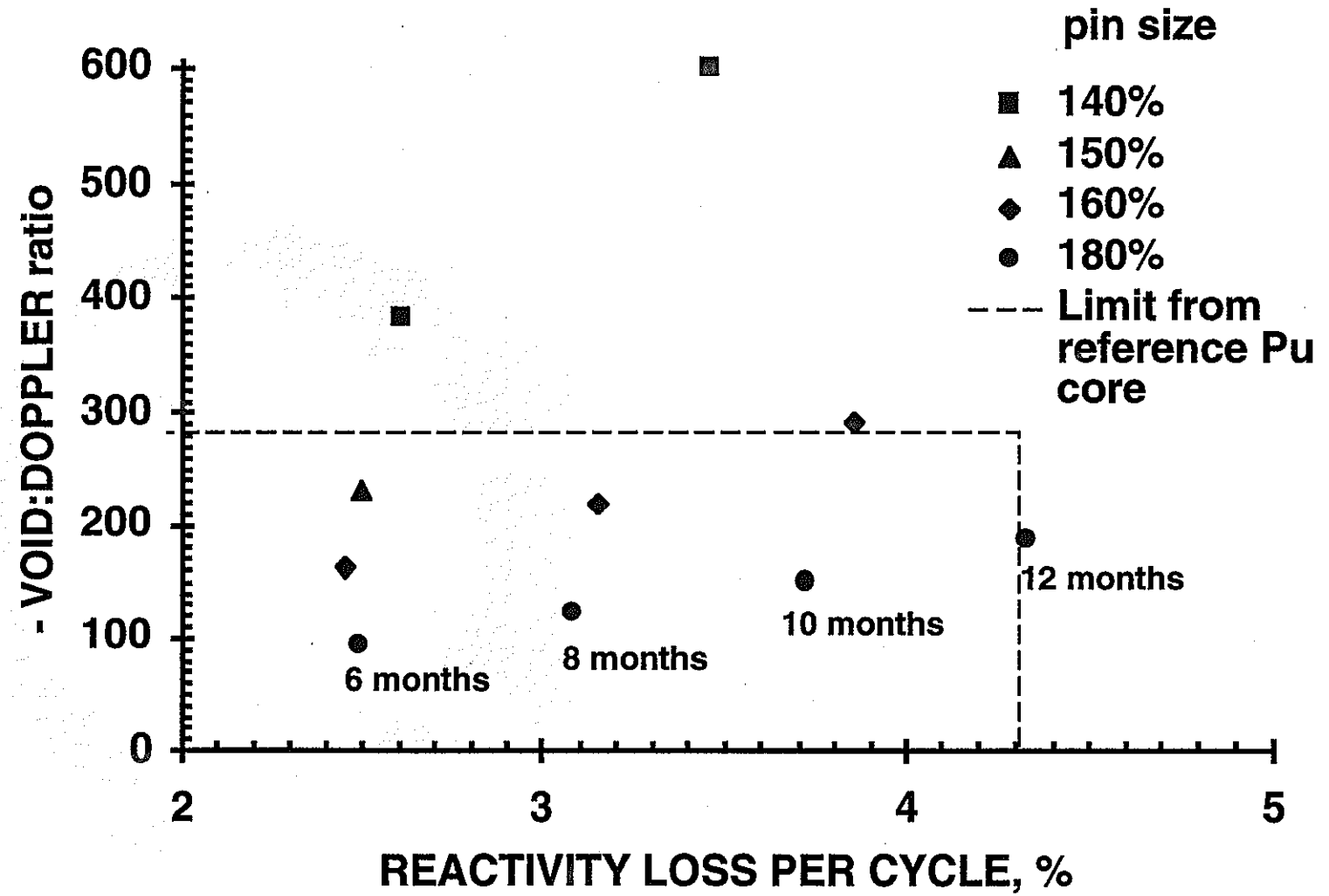


Figure 2.2 High quality Pu sensitivity study: Void:Doppler ratio as a function of reactivity loss, for various non-absorber diluents and a 4 batch * 6 months cycle

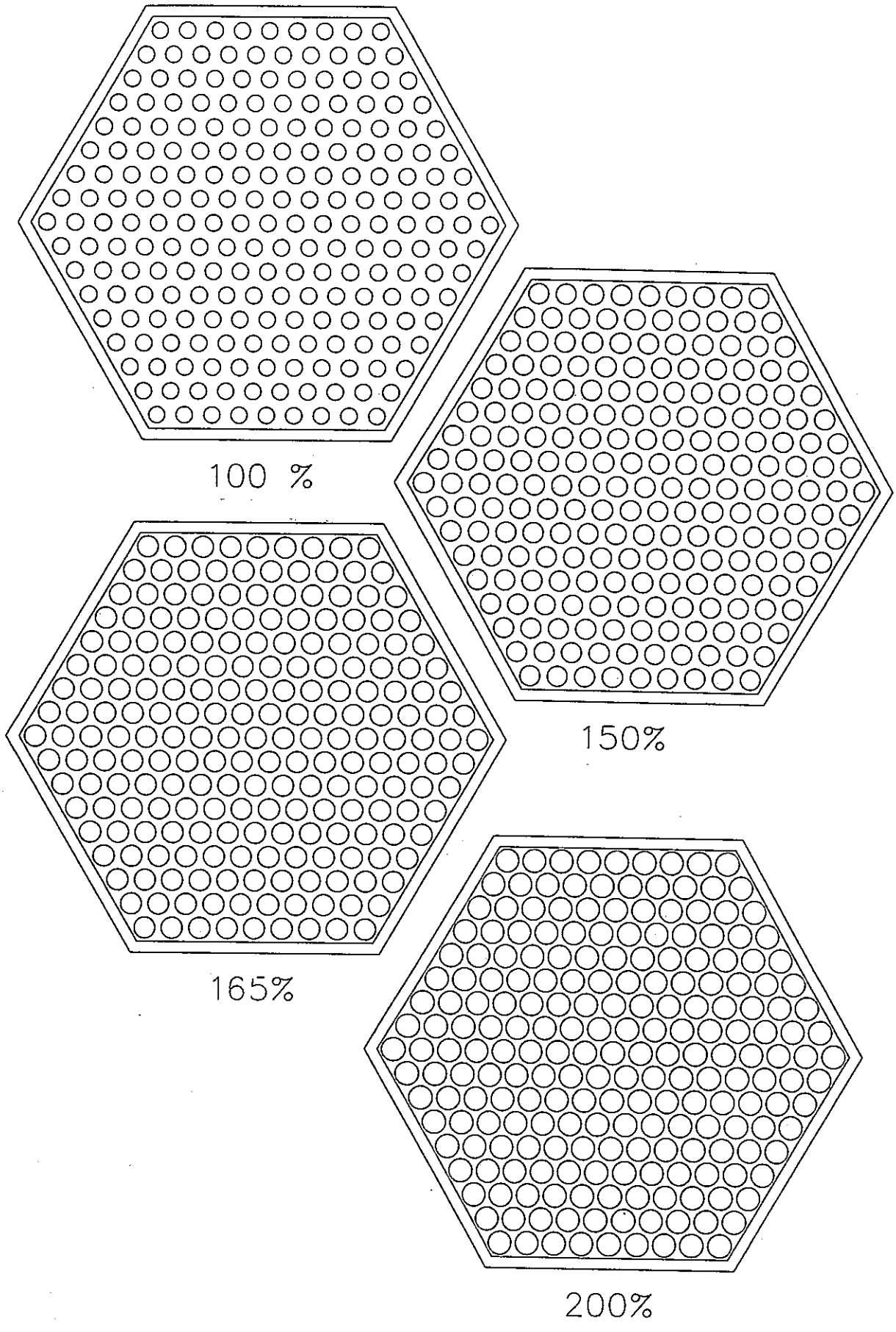


Figure 2.3 S/A cross-section as a function of fuel pin size

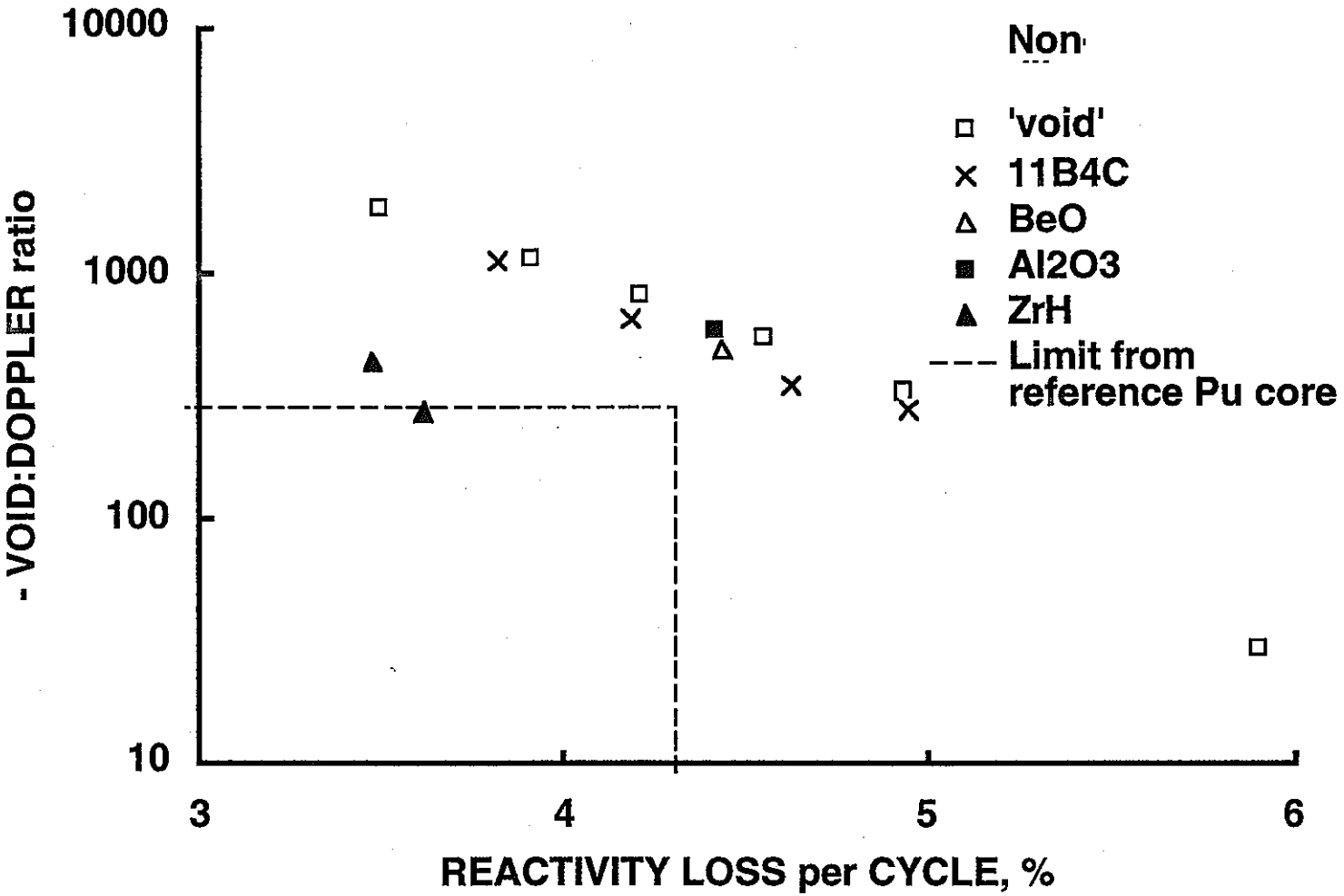


Figure 2.4 Low quality Pu sensitivity study: Void:Doppler ratio as a function of reactivity loss, for 4 batches of varying cycle length and various pin sizes, with ZrH non-absorber diluent

## 3 ROD WORTH AND SHUTDOWN MARGIN - METHODS

In Part I of the study, reactivity loss per cycle was used as an indicator of the margins between rod group worths and the requirements for reactor shutdown. This approximation has now been superseded, by extending the calculations to include explicit assessments of the rod group worths and requirements. This section describes the methods used for those calculations.

Shutdown margins were calculated for the BOC core conditions, since it is at this condition that the shutdown requirements are most difficult to meet. Two different rod configurations were assessed: the worth of the PCR group with the BCRs fully withdrawn; the worth of the BCR group with the PCRs 50% inserted (a nominal BOC insertion). In each case the worth was calculated for the rod group moving from fully in to fully out, with the worst single rod remaining at the fully out position.

The assessments of shutdown margins were restricted to the above two conditions. It should be noted that there is a possibility of other conditions occurring which have the potential to be more restrictive of shutdown margin than those conditions analyzed. During fuel handling operations the following two situations should be considered, since they could be the result of a single operator error: 2 control rods withdrawn at the same time (a second rod being erroneously removed when one is already withdrawn for maintenance); a control rod replaced by a fresh fuel S/A (replacing the wrong S/A type when a rod is removed for maintenance, the outer S/A geometries are the same).

There are several stages to the calculation of shutdown margin. Nominal rod group worths are calculated; these are obtained from the difference in Keff values from flux snapshot calculations - because of the asymmetry associated with one stuck rod, 3D calculations are required and the MOSES program[3-1] was used. A series of adjustments are applied to the nominal rod worth, to cover both calculational uncertainties and systematic errors in the calculational method. The shutdown requirement is the sum of several values, these include the reactivity effects of reducing core temperatures to 200°C (from both nuclear data changes and thermal

expansion) which can be calculated for each case. The shutdown margin is obtained by comparing the adjusted rod worth with the shutdown requirement.

## 3.1 WORTH ADJUSTMENTS AND SHUTDOWN REQUIREMENTS

The various components used in the calculation of rod worths and shutdown margins were taken from calculations used in a design study of a 600 MW(e) fast breeder reactor[6-1].

Table 3.1 shows the various multiplicative factors used to adjust the nominal rod group worths calculated using MOSES. There are a series of factors to compensate for known inaccuracies in the calculational model. A correction for the condensation to 7 energy groups used in the calculation (x0.972). A combined correction factor for mesh and transport effects (x1.021). A correction for not modelling the heterogeneity of the control rod absorber (x0.88). A correction for not modelling the burn-up of $^{10}B$ in the absorber (x0.95). A correction for differences between the MOSES program and that used (CITATION) in the assessment of correction factors (x1.0). A final correction factor obtained from comparing calculated rod worths with experimental values (from the JUPITER experiments on ZPPR-10C) (x1.018). In addition to the above factors a multiplier of x0.9 is applied, as an allowance for calculational uncertainties at the $2\sigma$ level. When combined, the total correction factor is x0.761.

The components of shutdown requirements are given in Table 3.2. They differ between PCR and BCR rod groups, with the only common component the reactivity worth of reducing the core temperatures from the operating conditions to a shutdown state of 200°C. There are two contributions to this temperature effect: one from changing nuclear data (the Doppler effect); the other from thermal expansion effects. These two factors are calculated independently, the calculations are described in Sub-sections 3.3 and 3.4 below.

For the BCR there are just two further components of the shutdown requirement. An allowance of 0.2%$\Delta k/kk'$ to cover the

reactivity inserted during a fault. An uncertainty allowance of 0.24%Δk/kk', a 2σ value based on experimental measurements at JOYO.

The PCR shutdown requirement has several components, in addition to the temperature effect. The reactivity loss per cycle, which at BOC these rods are inserted to offset; obtained from the standard SLAROM-JOINT-CITATION calculations for each core variant. A margin of 0.2%Δk/kk' to allow some rod insertion for control at EOC. An allowance of 0.1%Δk/kk' for reactivity variations between different refuelling batches. An allowance for uncertainty in cycle length, consisting of 3 values all assessed at the 2σ level and combined in quadrature: 0.3%Δk/kk' for fuel fabrication uncertainties; 0.24%Δk/kk' uncertainty in reactor measured power; a fraction (20%) of the calculated reactivity loss per cycle. An allowance for uncertainties in shutdown margin, comprising 2 values combined in quadrature: a 2σ allowance of 0.3%Δk/kk' for uncertainties in fuel fabrication; a 1σ allowance of 0.44%Δk/kk' for uncertainties in the calculated Keff values.

## 3.2 3D MOSES PROGRAM

To produce the Keff values from which nominal rod group worths were calculated, the 3D program MOSES[3-1] was used. A 3D model is required to model the effects of a stuck rod in the withdrawn group; a 360°, full core height core, representation is used.

In most cases a hex-Z mesh structure with one mesh per S/A was used, this incorporates a radial interpolation[3-2] based on the Askew method to give a pseudo-tri-Z representation. MOSES incorporates an option for true tri-Z geometry, in a few cases in which the hex-Z model experienced convergence difficulties, a tri-Z mesh with 6 points per S/A was used. A case was done using both hex-Z and tri-Z geometries, no significant systematic differences in Keff were found.

The calculations were done in 7 energy groups, this was necessary to avoid excessive computer time requirements. Nuclear data is input to MOSES in the form of a microscopic cross-section library file. This is basically the same 7 group datafile as used to

run PENCIL calculations, but it required a modification in the form of adding data for the rod absorber region (absorber was not modelled in the calculations for Part I of the study). To create data for this absorber material, the SLAROM-JOINT-CITATION calculation that created the original 7 group microscopic library file is repeated, but with a central region equal in volume to 1 S/A replaced by control rod absorber: the 7 group data calculated for this absorber region are appended to the original library file.

The calculations used number densities taken from 7 group, PENCIL, burn-up calculations. The rod absorber number densities come from the following composition: volume fractions of 42.5% Na, 22.6% steel and 33.3% $B_4C$, the $B_4C$ has 92 at% $^{10}B$ and 95% of theoretical density. The MOSES calculations used a less detailed number density representation than was used in other calculations of the sensitivity study: rather than the 31 separate regions (20 of them in the core) shown in Figure 3.1 of the report on Part I of the study, just 15 regions (11 in the core) were used, as seen in Figure 3.1.

## 3.3 SHUTDOWN TEMPERATURE - NUCLEAR DATA EFFECTS

The effects of nuclear data changes when reactor temperatures reduce from operational to shutdown values are readily evaluated. The calculations that produced the 7 group microscopic data library used in the MOSES calculations were repeated, but with the material temperatures altered appropriately. This produced a second 7 group library, for the lower (200°C) temperature condition. These two nuclear data libraries were then used in otherwise identical MOSES calculations, and the Keff difference gives the reactivity worth of this component of the temperature change. The MOSES calculations used were for PCRs 50% inserted and BCRs fully withdrawn.

## 3.4 SHUTDOWN TEMPERATURE - THERMAL EXPANSION EFFECTS

The calculation of the effect of thermal expansion on core reactivity consists of three parts. Calculating reactivity coefficients for changing core size at constant number density.

Calculating reactivity coefficients for changing number densities of different core materials (at constant core size). Combining these factors with temperature change and thermal expansion coefficient data, to give an overall reactivity change.

A series of reactivity coefficients, represented $K_X$, are calculated, they are the fractional change in reactivity relative to the fractional change in the parameter indicated by 'x' - either a core dimension or the density of one of the core constituent materials.

The reactivity coefficients of changing core size were obtained from CITATION calculations which repeated cases for the BOC condition, but with either the axial or radial mesh uniformly expanded by a nominal amount (1%). These calculations gave the following reactivity coefficients for height ($K_H$) and radius ($K_R$),

defined by $$K_H = \frac{\Delta k/kk'}{\Delta H/H} \quad , \quad K_R = \frac{\Delta k/kk'}{\Delta R/R}$$

The reactivity coefficients for changing number density were calculated with first order perturbation theory using PERKY, in 18 energy groups. Associated with this usage of PERKY are pre- and post-processor codes PREPK and POSTPK; these transform input and output data into suitable formats, PREPK also initiates a CITATION calculation that produces direct and adjoint fluxes used by PERKY. Since the calculation is in 18 energy groups, SLAROM-JOINT-CITATION calculations were run first to produce nuclear data files condensed to 18 groups. The route calculates separate values of density reactivity coefficients for 3 categories of component materials - fuel, coolant and structure - the calculation method incorporates the diluent within the structure material category. The density reactivity coefficient values are provided for each region of the reactor model; combined values appropriate to the reactor core were obtained, the sum of values for the inner core, outer core and follower regions (the latter reduced by the fraction of that region actually within the core). The values produced are the coefficients $K_F$, $K_C$ and $K_S$,

defined by $K_F = \frac{\Delta k/kk'}{\Delta\rho_F/\rho_F}$ , $K_C = \frac{\Delta k/kk'}{\Delta\rho_C/\rho_C}$ , $K_S = \frac{\Delta k/kk'}{\Delta\rho_S/\rho_S}$

The assessment of thermal expansion effects considers the core to be made up of 5 components - fuel, Na coolant, diluent, clad and wrapper (the last 2 both made of steel) - other minor components (wire/grids) are ignored. There are a number of factors to the core expansion, providing a number of contributions ($F_1$ - $F_5$) to the overall reactivity change with reactor temperatures. In the following expressions, $\Delta T$ is a temperature change, $\alpha$ is a thermal expansion coefficient (a function of temperature), V is a fraction of core volume, and K is a reactivity coefficient as already defined. Where not defined above, subscripts are obvious in meaning.

Overall radial core expansion is controlled by the steel support structure on which the S/As rest - this increases core size, but reduces the number density of all solid materials in proportion, the increased volume is filled by coolant, increasing its number density.

$$F_1 = \Delta T_{sup} \cdot \alpha_{steel}(T_{sup}) \cdot \left( K_R - 2 \cdot (K_F + K_S) + 2 \cdot \frac{(1 - V_{Na})}{V_{Na}} \cdot K_C \right)$$

Within each S/A the wrapper expands radially, as does the clad, each displacing a volume of coolant. For the clad it is actually the pin volume that expands - it is assumed to be the clad expansion, rather than that of its contents, which determines the pin expansion. Since the steel is only being repositioned within the S/A, its density is unaltered.

$$F_2 = -\Delta T_{wrap} \cdot \alpha_{steel}(T_{wrap}) \cdot 2 \cdot \frac{V_{wrap}}{V_{Na}} \cdot K_C - \Delta T_{clad} \cdot \alpha_{steel}(T_{clad}) \cdot 2 \cdot \frac{V_{pin}}{V_{Na}} \cdot K_C$$

The fuel expands axially, this is assumed to be driven by its own expansion (i.e. fuel pellets are not bonded to the clad). This increases the height of the core, but reduces the fuel number density.

$$F_3 = \Delta T_{fuel} \cdot \alpha_{fuel}(T_{fuel}) \cdot (K_H - K_F)$$

The clad, diluent and wrapper all expand axially, decreasing their number densities. The wrapper and clad are both driven by their own thermal expansion. The diluent is assumed to be stuck to the clad and so expands with the clad.

$$F_4 = -\Delta T_{clad} \cdot \alpha_{steel}(T_{clad}) \cdot \left( \frac{V_{clad}}{(V_{clad} + V_{wrap})} \cdot K_{steel} + K_{dil} \right) - \Delta T_{wrap} \cdot \alpha_{steel}(T_{wrap}) \cdot \frac{V_{wrap}}{(V_{clad} + V_{wrap})} \cdot K_{steel}$$

The final component comes from the thermal expansion of the coolant. Note that whilst all other $\alpha$ values are linear expansion coefficients $\alpha_{Na}$ is a density coefficient (and so of opposite sign).

$$F_5 = \Delta T_{Na} \cdot \alpha_{Na}(T_{Na}) \cdot K_C$$

Values of temperature changes and expansion coefficients ($\Delta T$ and $\alpha$) were taken from calculations for the 600 MW(e) fast breeder reactor design study[6-1], rather than assessed specifically for the current study. The temperatures reduce to 200°C, starting from 380, 455, 455, 475 and 1073°C for support, coolant, wrapper, clad and fuel respectively. The temperature averaged expansion coefficients for fuel, clad, wrapper and support are $1.439 \times 10^{-5}$, $2.016 \times 10^{-5}$, $2.003 \times 10^{-5}$ and $1.949 \times 10^{-5}$ $\Delta l/l$ per °C respectively. The coolant density coefficient is $-2.841 \times 10^{-4}$ $\Delta\rho/\rho$ per °C. The values of volume fractions (V) come from the core geometric data. The reactivity coefficient values (K) are calculated as described previously, except that separate $K_{steel}$ and $K_{dil}$ values, as used in $F_4$, are not calculated. However, since $K_S = K_{steel} + K_{dil}$ and $T_{clad} \approx T_{wrap}$ we can modify $F_4$ to -

$$F_4 = -\Delta T_{clad} \cdot \alpha_{steel}(T_{clad}) \cdot \frac{V_{clad}}{(V_{clad} + V_{wrap})} \cdot K_S - \Delta T_{wrap} \cdot \alpha_{steel}(T_{wrap}) \cdot \frac{V_{wrap}}{(V_{clad} + V_{wrap})} \cdot K_S$$

It was to facilitate this approximation that the assumption of diluent being bonded to the clad was made.

Table 3.1 Components of adjustment to nominal rod group worths

| Effect Adjusted | Factor |
|---|---|
| Effect of Condensation to 7 energy groups | x0.972 |
| Combined Mesh and Transport correction factor | x1.021 |
| Control Rod Heterogeneity correction factor | x0.88 |
| Rod $^{10}B$ Burn-up correction factor | x0.95 |
| Difference between MOSES program and reference (CITATION) used in assessing corrections | x1.0 |
| Adjustment for difference from experimental values (based on JUPITER core ZPPR-10C) | x1.018 |
| Allowance for calculational uncertainty (2σ) | x0.9 |
| Total Correction Factor | x0.761 |

Table 3.2 Components of rod group shutdown worth requirements

| Components of Primary Control Rod (PCR) Shutdown Margin | |
|---|---|
| Effect of reducing core temperature to 200°C | α |
| Reactivity loss per cycle | β |
| Margin for control at EOC | 0.2 %Δk/kk' |
| Margin for variations in refuelling batches | 0.1 %Δk/kk' |
| Uncertainties in cycle length # | |
| Reactor measured power uncertainty (2σ) | 0.24 %Δk/kk' |
| Fuel fabrication uncertainties (2σ) | 0.3 %Δk/kk' |
| Uncertainty in reactivity loss/cycle (2σ) | 20% of α |
| Uncertainties in shutdown margin # | |
| Uncertainty in calculated Keff (1σ) | 0.44 %Δk/kk' |
| Fuel fabrication uncertainties (2σ) | 0.3 %Δk/kk' |
| Components of Backup Control Rod (BCR) Shutdown Margin | |
| Effect of reducing core temperature to 200°C | α |
| Margin for reactivity inserted during fault | 0.2 %Δk/kk' |
| Uncertainty, based on JOYO measurements (2σ) | 0.24 %Δk/kk' |

# components are combined in quadrature

values of α,β are evaluated for each case

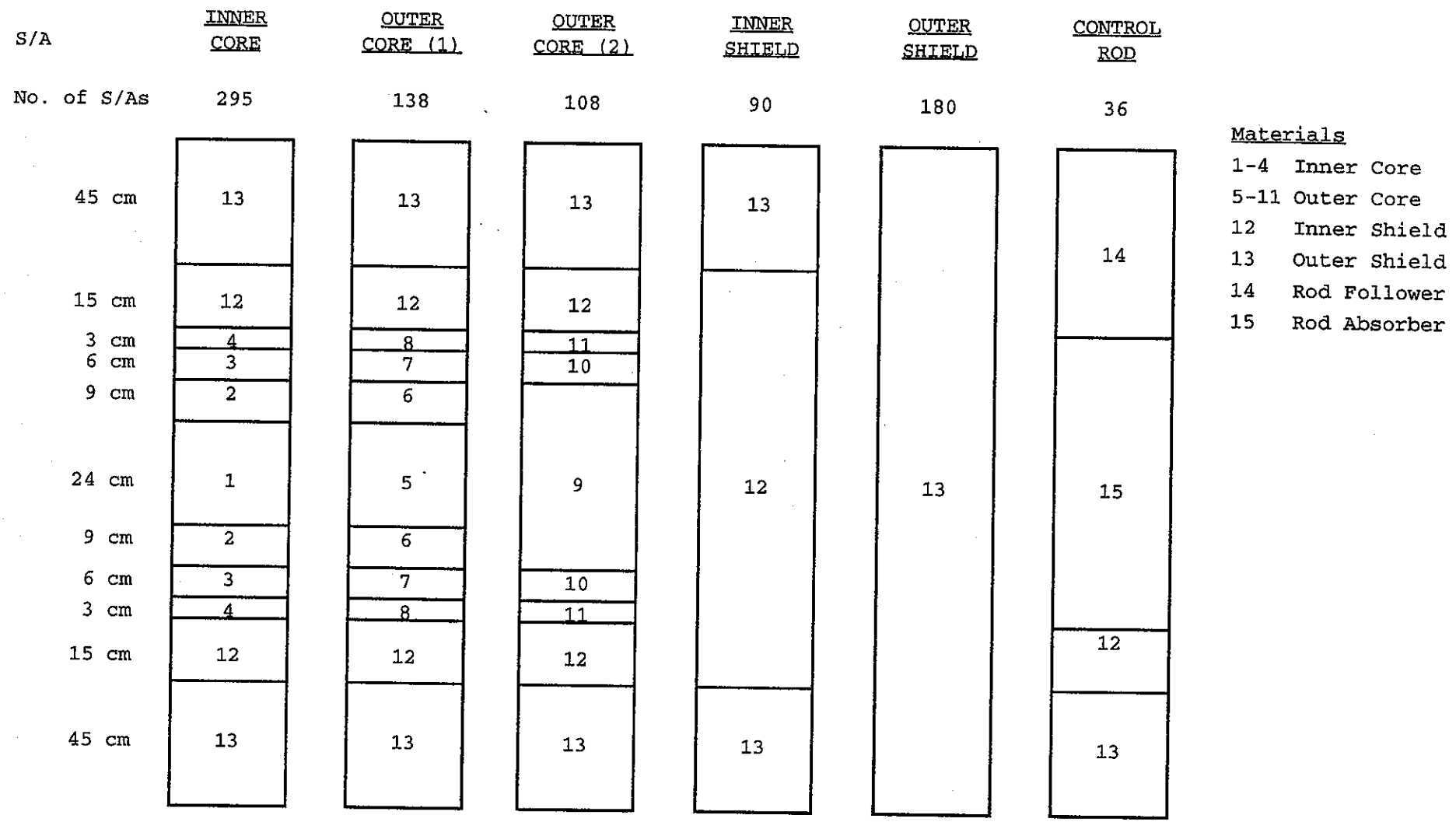


Figure 3.1 Axial mesh representation in sensitivity study MOSES rod worth calculations

# 4 ROD WORTH AND SHUTDOWN MARGIN - CALCULATIONS

The calculations of rod worths and shutdown margins, as described in the previous section, were applied to a range of the cases from Part I of the study. Only those cases with the diluent materials identified as most suitable, ZrH and $B_4C$, were examined. A widespread failure to meet shutdown margins was observed, this was addressed by increasing the number of both control and backup rods in the reactor design (see Section 5). As a consequence of high pin rating results, an additional series of sensitivity calculations was undertaken, using hollow fuel pellets for the high quality Pu vector with a 200% pin size (see Sub-section 4.2).

At this stage of the analysis, the reactivity worth of thermal expansion effects was only calculated for a limited number of cases (the calculations were quite time consuming). Cases done for a range of conditions, see Table 4.1, showed that the effect displayed comparatively little variation between cases. For the purposes of the current section, a nominal value of 0.5%Δk/kk' reactivity worth from thermal expansion was assumed; the error introduced is at most 0.1%Δk/kk'.

The results of the rod worth and shutdown margin calculations are shown in Tables 4.2 to 4.5. The first table is for cases with the nominal pin size; the other 3 tables are for increased pin sizes, with the low quality, reference and high quality Pu vectors respectively. There are two values of rod group worth and shutdown requirement given for each case - for the PCR and the BCR rod groups. The margin is given both as a reactivity difference, and in terms of the rod worth as a fraction of the requirement.

The results for the nominal pin size, in Table 4.2, include the case of the original reference core. The results are in reasonable agreement with the calculations of a preceding study (the source of the 600 MW(e) reference design) which gave PCR worths of 7.3%Δk/kk', BCR worths of 2.1%Δk/kk', and shutdown requirements of 6.7%Δk/kk' and 1.2%Δk/kk' respectively. Table 4.2 also includes several cases for the high quality Pu vector, where a mixture of absorber and non-absorber diluent materials had been used to produce conditions optimized for safety parameters and reactivity loss per cycle. With

$B_4C$ as both absorber and non-absorber diluent, the shutdown requirements were met with margins that were an improvement on those for the reference core. With a mix of ZrH and $^{10}B_4C$ diluent, the margins deteriorated noticeably and shutdown requirements were not met.

Table 4.3 shows rod worth margins for the low quality Pu vector, for a range of increased pin sizes and cycle lengths, and for the two different diluent materials ZrH and $^{11}B_4C$. Although cases were well within the 4.30%$\Delta k/kk'$ target for reactivity loss per cycle (adopted in lieu of calculations of rod worths), the actual rod worths were found in almost all cases to be short of requirements, often significantly so. Thus, the reactivity loss per cycle was not, in practise, a very good predictor of shutdown margins. It is clear from Table 4.3 that, at least for the low quality Pu vector, it would not be possible to achieve shutdown targets with a 6 month cycle length. Whilst the margin for the PCRs could be improved by further reducing the cycle length, this would not improve the margin for the BCRs.

Rod worth margins for the reference and high quality Pu vectors are shown in Tables 4.4 and 4.5 respectively. They are for a range of increased pin sizes with the two non-absorber diluent materials ZrH and $^{11}B_4C$ (all also have $^{10}B_4C$ absorber diluent), all for a 4 batch 6 month fuel cycle. For (almost) every pin size and non-absorber diluent material combination, there is a case with the safety parameters are close to the target of a void-to-Doppler ratio of -285. In Table 4.4, just for the 150% pin size, there are also cases - those with the higher diluent fractions - where the safety parameters are below the limit. As with the low quality Pu, the shutdown requirements are not met, with margins either negative or so low as to be inadequate. It is noted that with $^{11}B_4C$ as diluent the shortfall in rod worth is less than with ZrH, it also reduces as the pin size gets smaller.

## 4.1 RE-EVALUATION OF EARLIER CONCLUSIONS

The earlier results of the sensitivity study are modified by the availability of calculated values of shutdown margin, rather than relying on the reactivity loss per cycle as an indicator of such parameters. As a consequence, some re-evaluation of conclusions drawn in Part I of the study was required.

Summarized in tables 4.6 to 4.8 are the key parameters for the most significant cases, for the low quality, reference and high quality Pu vectors, respectively. The limits set for these values were a positive shutdown margin, a pin rating <430 W/cm, and a void-to-Doppler ratio no less than -285 (this latter limit is less rigid than the others, some flexibility being allowed). With one exception, noted in Table 4.6, the cases are for a 6 month fuel cycle of 4 batches.

In each case for the low quality Pu vector a single diluent material was used, the fraction being adjusted to ensure criticality with the desired peak Pu enrichment of 45%. Possible variations are obtained by altering the fuel pin size: increasing the fuel pin size causes the safety parameters to improve, but both pin rating and shutdown margin to degrade. The cases shown are (near) minimum pin sizes compatible with safety parameters within their chosen limits - in all cases the shutdown margin requirements were not met, demonstrating a requirement for some improvement. The pin ratings remained below 400 W/cm for all options.

The cases presented in Tables 4.7 and 4.8, the reference and high quality Pu vectors, are similar to one another. For the 2 limiting pin sizes as identified in Table 4.6, calculations were done with two different non-absorber diluent materials. As previously, the diluent fraction was adjusted to ensure criticality at a 45% peak Pu enrichment. The diluent was a mixture of absorber (fixed as $^{10}B_4C$) and the non-absorber material (as specified in the tables); the ratio of components was used to vary the conditions: reducing the absorber fraction caused the safety parameter to improve, but made both pin rating and shutdown margin worse. The cases shown are for safety parameters close to the limit. Although shutdown margins are better with $^{11}B_4C$, rather than ZrH, as non-absorber diluent, they are

inadequate in both cases. For ZrH as non-absorber diluent, pin ratings remain below the 430 W/cm limit, though for the larger (200%) pin size they are only just below. For $^{11}B_4C$ as non-absorber diluent the 'type B' (diluent in separate pins) ratings are all >430 W/cm, though the 'type A' (diluent as fuel pellet matrix) ratings barely exceed 300 W/cm.

Although acceptable from linear rating considerations, the 'type A' ratings are based on fuel and diluent materials being mixed together in the same pin. Whilst R & D work to validate the use of such an inert matrix for fuel pellets is currently under way, it was decided that the current study should not presume on the results of such work. Thus the only diluent to be considered in fuel pins was void, in the form of hollow pellets.

The inadequate results, in terms of shutdown margins and also, possibly, pin ratings identified above required some modification to the reference design, the basis of the study, in order for the results to be made acceptable. It had previously been found necessary to adjust the reference design - altering the fuel pin and pellet size, though no other 'fixed' parameter, in order to accommodate the low quality Pu vector.

To improve shutdown margins, it was appropriate to increase the worth of control rods: the alternative approach of changing cycle length, whilst effective for PCR shutdown margin would not materially affect the BCR margins. The rod absorber already has $^{10}B$ enriched to 92%, so the only option was to increase the numbers of rods. An assessment of possible changes to the rod numbers and positions is presented in Section 5 below.

There were several reasons for also considering how to reduce the 'type B' peak pin ratings. Depending on to what degree the shutdown margins could be improved, the option of ZrH as non-absorber diluent (which produced the lower pin ratings) may not have been viable. The linear ratings quoted are from 2D calculations for a uniform burn-up; more detailed calculations will inevitably increase the peak ratings, so some margin to the 430 W/cm limit is required. With ZrH as non-absorber diluent, if this has to be segregated from

the absorber ($^{10}B_4C$) diluent, then there may be some distortion of ratings within S/As, further increasing peak values.

In Sub-section 4.2, there is a brief assessment of the introduction of hollow pellets to high quality Pu fuel with a 200% pin size - the case with most difficulty achieving pin rating limits.

## 4.2 RATING REDUCTION USING HOLLOW PELLETS

As the results summarized in Tables 4.7 and 4.8 showed, with either $^{11}B_4C$ as the non-absorber diluent material or the higher, 200%, pin size (and especially with both), the 'type B' pin ratings will exceed the 430 W/cm limit.

This Sub-section presents an extension of the sensitivity study, undertaken to demonstrate that mixing diluent material in fuel pellets could be effective in reducing pin ratings. The only diluent material which this study considered practicable to mix in the fuel pellet was void, included in the form of hollow pellets. The results in Part I of the study demonstrated that replacing $^{11}B_4C$ diluent with void should have little effect on the core characteristics, so a change of (part of) this diluent material to the void in hollow pellets would present no problem.

The peak pin ratings calculated in the sensitivity studies do not take into account the following factors. There are effects not modelled by the 2D (RZ) calculations of the sensitivity studies which will significantly increase peak ratings over the values in the tables. The peak ratings can show a significant imbalance between inner and outer core zones at BOC; it will to a large extent be possible to balance these ratings using different insertions for the different rings of rods (the sensitivity calculations balanced ratings at EOC, when rods are essentially fully out). These effects are addressed in Sub-section 6.4 and explicitly included in the final optimized calculations.

Calculated peak ratings can be adjusted by altering how many of the 217 pins are assumed to contain fuel: since the SLAROM cell model does not represent the fuel/diluent distribution within a S/A, the

total S/A power is unaffected by the fuel-diluent distribution and the peak pin rating is just inversely proportional to the number of pins that contain fuel. A 'type A' rating corresponds to fuel and diluent mixed together in all 217 pins, whereas a 'type B' rating has all fuel segregated in separate pins from the diluent.

The highest 'type B' pin rating of the cases in Tables 4.7 and 4.8 was 639 W/cm, for a 200% pin size with $^{11}B_4C$ non-absorber diluent, a case with 113.8 pins of $B_4C$ diluent, which corresponds to

$$(217 - 113.8) = 103.2$$

pins of fuel. Scaling the number of fuel pins by the inverse of the rating shows that to maintain peak ratings below 430 W/cm (for the present, neglecting any margin for modelling inaccuracies) would require the fuel to be present in at least

$$103.2 * {}^{639}/_{430} = 154$$

pins. Since there are only sufficient fuel to fill 103.2 pins, each fuel pellet would require a diluent fraction of at least

$$\frac{(154 - 103.2)}{154} = 0.330$$

This corresponds to a hollow pellet with a bore 0.574 of the outer diameter (assuming that the effect of replacing the requisite amount of $^{11}B_4C$ diluent with void is negligible).

A pellet bore of nearly 60% of the pellet diameter was judged to be rather too large to be practical. Based on the range of values that have been considered in the CAPRA project[4-1], it was decided to consider fuel pellets with a bore no greater than 45% of the pellet diameter, for which the central hole corresponds to 0.2025 of the pellet volume (the reference oxide CAPRA core[4-1] has a bore of 41%). Using the same type of scaling as in the previous paragraph: in the case of 150% pin size with $^{11}B_4C$ non-absorber diluent, adopting hollow fuel pellets of 45% bore would reduce the peak pin rating from 530 W/cm to 423 W/cm, within the limit but providing no margin for modelling inaccuracies.

With a pin size of 200%, when $^{11}B_4C$ non-absorber diluent was used then the pellet bore required to reduce pin ratings below the 430 W/cm limit was too large to be considered practical. In order to get pin ratings below limits with a 200% pin size it is necessary to have a mix of both ZrH and $B_4C$ diluent materials. Rather than just

using $^{10}B_4C$ absorber, considering a variable $^{10}B$ fraction - so that there is both ZrH and $^{11}B_4C$ as non-absorber diluent - gives an additional degree of freedom for optimizing core conditions.

A series of calculations were carried out based on the above considerations for reducing pin ratings: a 200% pin size was modelled, with hollow pellets of 45% bore; a mix of ZrH and $B_4C$ diluents was used, with a range of $^{10}B$ enrichments examined. A maximum of 30% $^{10}B$ was permitted, to ensure that unmodelled heterogeneity effects can be allowed for (this overcomes a shortcoming in the earlier calculations for ZrH non-absorber diluent, which used 92% $^{10}B$ in the absorber, making no allowance for heterogeneity).

Table 4.9 shows the results from the calculations; it includes the extreme cases of a single non-absorber diluent (from Table 4.8) for comparison. For each $^{10}B$ fraction, the ratio of ZrH to $B_4C$ diluent was varied to produce safety parameters close to the -285 void-to-Doppler ratio limit. For those limiting cases the 'type B' peak pin ratings decrease as the $^{10}B$ fraction increases, showing peak ratings of ~365 W/cm (~390 W/cm for imbalanced BOC ratings) for a $^{10}B$ fraction of 15% or greater. The shutdown margins are significantly improved over the cases where ZrH was the sole non-absorber diluent, though they remain negative.

To summarize, the results demonstrate that it is possible to produce peak pin ratings with a significant margin to the 430 W/cm limit even with the 200% pin size - by the expedient of both adopting hollow fuel pellets, and using a mixture of $B_4C$ and ZrH as diluent. For the less restrictive 150% pin size, although the use of hollow pellets together with just $B_4C$ as diluent would be unlikely to provide an adequate margin to the rating limit, a mixture of ZrH and $B_4C$ as diluent (even with solid fuel pellets) would provide a margin.

Table 4.1 Reactivity worth of thermal expansion to cold shutdown temperatures, for a range of cases

| Pu Quality | Control Rod Option | cycle length (months) | pin size | diluent material(s) | Diluent Fraction (pins) | Expansion Reactivity (%Δk/kk') |
|---|---|---|---|---|---|---|
| low | original | 12 | 180% | ZrH | 18 | 0.391 |
| low | original | 6 | 150% | ZrH | 12 | 0.446 |
| " | V | " | " | " | " | 0.447 |
| " | VII | " | " | " | " | 0.414 |
| ref. | original | 6 | 150% | ZrH & $^{10}B_4C$ | 32 / 5 | 0.493 |
| ref. | original | 6 | 200% | $B_4C$ | 95.7 | 0.580 |
| high | original | 6 | 150% | $B_4C$ | 93.1 | 0.445 |
| high | original | 6 | 150% | ZrH & $^{10}B_4C$ | 53 / 5 | 0.559 |
| high | original | 6 | 200% | ZrH & $B_4C$, hollow fuel | 32 / 24 | 0.582 |
| " | V | " | " | " | " | 0.594 |
| " | VII | " | " | " | " | 0.583 |

Table 4.2 Rod worths: sensitivity study and reference case for high quality Pu - cases optimized for 100% pin size

| Pu vector | | Reference | High | High | High | High |
|---|---|---|---|---|---|---|
| Diluent Material | | None | $ZrH\&^{10}B_4C$ | $ZrH\&^{10}B_4C$ | $B_4C$ | $B_4C$ |
| Case | | | uniform Pu | uniform diluent | 4*5month | 4*6month |
| Reactivity Loss per Cycle (%Δk/kk') | | 4.30 | 3.90 | 3.61 | 4.13 | 4.62 |
| Temperature Effect (%Δk/kk') | (nuc. data) | 0.60 | 0.72 | 0.53 | 0.50 | 0.42 |
| | (expansion) | 0.5 | 0.5 | 0.5 | 0.5 | 0.5 |
| Shutdown Worth | (PCR) | 7.18 | 6.82 | 6.29 | 6.87 | 7.38 |
| Required (%Δk/kk') | (BCR) | 1.54 | 1.66 | 1.47 | 1.44 | 1.36 |
| Rod Worth | (PCR) | 7.97 | 5.48 | 6.24 | 8.72 | 8.48 |
| (%Δk/kk') | (BCR) | 2.01 | 1.21 | 1.65 | 2.32 | 2.28 |
| Fraction of | (PCR) | 1.11 | 0.80 | 0.99 | 1.85 | 1.15 |
| Requirement | (BCR) | 1.30 | 0.73 | 1.13 | 1.61 | 1.67 |
| Shutdown Margin | (PCR) | +0.79 | -1.35 | -0.05 | +1.27 | +1.11 |
| (%Δk/kk') | (BCR) | +0.47 | -0.45 | +0.19 | +0.88 | +0.92 |

Table 4.3 Rod worths: sensitivity study for low quality Pu - various pin sizes and cycle lengths, for ZrH & $^{11}B_4C$ diluents

| Diluent Material | | ZrH | ZrH | ZrH | ZrH | $^{11}B_4C$ | $^{11}B_4C$ | $^{11}B_4C$ |
|---|---|---|---|---|---|---|---|---|
| Pin Size | | 140% | 150% | 180% | 180% | 160% | 200% | 220% |
| Cycle length | | 3*6 months | 6 months | 6 months | 12 months | 6 months | 6 months | 6 months |
| Reactivity loss per Cycle (%Δk/kk') | | 2.62 | 2.50 | 2.49 | 4.33 | 2.47 | 2.34 | 2.30 |
| Temperature effect (%Δk/kk') | (nuc. data) | 1.08 | 1.24 | 2.11 | 1.36 | 0.75 | 0.92 | 1.00 |
| | (expansion) | 0.5 | 0.5 | 0.5 | 0.5 | 0.5 | 0.5 | 0.5 |
| Shutdown Worth | (PCR) | 5.67 | 5.70 | 6.55 | 7.96 | 5.18 | 5.20 | 5.23 |
| Required (%Δk/kk') | (BCR) | 2.02 | 2.18 | 3.05 | 2.30 | 1.69 | 1.86 | 1.94 |
| Rod Worth | (PCR) | 5.86 | 5.31 | 3.66 | 4.12 | 5.96 | 5.18 | 4.81 |
| (%Δk/kk') | (BCR) | 1.41 | 1.25 | 0.86 | 1.00 | 1.39 | 1.15 | 1.05 |
| Fraction of | (PCR) | 1.03 | 0.93 | 0.56 | 0.52 | 1.15 | 1.00 | 0.92 |
| Requirement | (BCR) | 0.70 | 0.57 | 0.28 | 0.43 | 0.82 | 0.62 | 0.54 |
| Shutdown Margin | (PCR) | +0.18 | -0.39 | -2.89 | -3.84 | +0.78 | -0.02 | -0.42 |
| (%Δk/kk') | (BCR) | -0.61 | -0.93 | -2.19 | -1.30 | -0.30 | -0.71 | -0.89 |

Table 4.4 Rod worths: sensitivity study for reference Pu - ZrH & $^{11}B_4C$ non-absorber diluents, 4 batch * 6 month cycle - optimized cases for various pin sizes and various cases for 150% pin size

| Diluent Material | ZrH | ZrH | ZrH | ZrH | $^{11}B_4C$ | $^{11}B_4C$ | $^{11}B_4C$ | $^{11}B_4C$ |
|---|---|---|---|---|---|---|---|---|
| Pin Size | 150% | 150% | 150% | 200% | 150% | 150% | 200% | 220% |
| Diluent fraction (pins) | 2/57 | 4/38 | 5/29 | 6.5/41 | 76.4 (1.0) | 72.0 (1.6) | 95.7 (1.9) | 119 (0.4) |
| Void:Doppler ratio | -88 | -204 | -300 | -282 | -212 | -274 | -279 | -89 |
| Reactivity loss per Cycle (%Δk/kk') | 3.28 | 2.48 | 2.34 | 1.61 | 4.31 | 4.01 | 3.19 | 4.27 |
| Temperature effect (%Δk/kk') (nuc. data) | 1.36 | 0.79 | 0.61 | 0.49 | 0.71 | 0.64 | 0.58 | 0.98 |
| (%Δk/kk') (expansion) | 0.5 | 0.5 | 0.5 | 0.5 | 0.5 | 0.5 | 0.5 | 0.5 |
| Shutdown Worth (PCR) | 6.73 | 5.23 | 4.89 | 3.93 | 7.29 | 6.86 | 5.85 | 7.52 |
| Required (%Δk/kk') (BCR) | 2.30 | 1.73 | 1.55 | 1.43 | 1.65 | 1.58 | 1.52 | 1.92 |
| Rod Worth (PCR) | 3.69 | 3.93 | 4.02 | 2.73 | 6.70 | 6.60 | 5.17 | 5.33 |
| (%Δk/kk') (BCR) | 0.98 | 0.96 | 0.98 | 0.61 | 1.79 | 1.68 | 1.25 | 1.40 |
| Fraction of (PCR) | 0.55 | 0.75 | 0.82 | 0.69 | 0.92 | 0.96 | 0.88 | 0.71 |
| Requirement (BCR) | 0.42 | 0.56 | 0.63 | 0.43 | 1.09 | 1.07 | 0.82 | 0.73 |
| Shutdown Margin (PCR) | -3.04 | -1.30 | -0.87 | -1.20 | -0.59 | -0.26 | -0.69 | -2.19 |
| (%Δk/kk') (BCR) | -1.33 | -0.77 | -0.57 | -0.82 | +0.14 | +0.11 | -0.28 | -0.52 |

Table 4.5 Rod worths: sensitivity study for high quality Pu - ZrH & $^{11}B_4C$ non-absorber diluents, 4 batch * 6 month cycle, optimized cases for various pin sizes

| Diluent Material | | ZrH | ZrH | $^{11}B_4C$ | $^{11}B_4C$ | $^{11}B_4C$ |
|---|---|---|---|---|---|---|
| Pin Size | | 150% | 200% | 150% | 200% | 220% |
| Diluent Fraction (pins) | | 5.1 / 53 | 5.6 / 65 | 93.1 | 113.8 | 130.5 |
| Reactivity loss per Cycle (%Δk/kk') | | 2.10 | 1.42 | 4.08 | 3.23 | 3.83 |
| Temperature effect (%Δk/kk') | (nuc. data) | 0.50 | 0.37 | 0.49 | 0.42 | 0.65 |
| | (expansion) | 0.5 | 0.5 | 0.5 | 0.5 | 0.5 |
| Shutdown Worth | (PCR) | 4.49 | 3.59 | 6.80 | 5.73 | 6.67 |
| Required (%Δk/kk') | (BCR) | 1.44 | 1.31 | 1.43 | 1.36 | 1.59 |
| Rod Worth | (PCR) | 3.45 | 2.37 | 6.86 | 5.37 | 5.39 |
| (%Δk/kk') | (BCR) | 0.86 | 0.54 | 1.80 | 1.32 | 1.43 |
| Fraction of | (PCR) | 0.77 | 0.66 | 1.01 | 0.94 | 0.81 |
| Requirement | (BCR) | 0.60 | 0.41 | 1.26 | 0.97 | 0.90 |
| Shutdown Margin | (PCR) | -1.04 | -1.23 | +0.06 | -0.36 | -1.29 |
| (%Δk/kk') | (BCR) | -0.58 | -0.77 | +0.38 | -0.04 | -0.17 |

Table 4.6 Summary of sensitivity study results for low quality Pu - optimized cases for 4 batch * 6 months

| Diluent Material | ZrH | | $^{11}B_4C$ | |
|---|---|---|---|---|
| Pin Size | 140% * | 150% | 200% | (targets) |
| Na Void (%Δk/kk') | 2.917 | 2.707 | 2.146 | {1.631} |
| Doppler Constant | -.00992 | -.01147 | -.00794 | {-.00562} |
| Void:Doppler | -294 | -236 | -270 | (>-285) |
| Peak Pin Rating, BOC (A) | 281/278 | 283/278 | 286/285 | (<430) |
| (inner/outer) (W/cm) (B) | 292/289 | 299/294 | 391/390 | |
| Shutdown Margin (PCR) | +0.18 | -0.39 | -0.02 | (>0.0) |
| (%Δk/kk') (BCR) | -0.61 | -0.93 | -0.89 | (>0.0) |

* 3 batch fuel cycle

Table 4.7 Summary of sensitivity study results for reference Pu - optimized cases for 4 batch * 6 months

| Non-Absorber Diluent | ZrH | | $^{11}B_4C$ | |
|---|---|---|---|---|
| Pin Size | 150% | 200% | 150% | 200% |
| Na Void (%Δk/kk') | 2.077 | 1.610 | 1.699 | 1.569 |
| Doppler Constant | -.00693 | -.00571 | -.00618 | -.00562 |
| Void:Doppler | -300 | -282 | -274 | -279 |
| Peak Pin Rating, BOC (A) | 284/273 | 283/281 | 296/269 | 297/277 |
| (inner/outer) (W/cm) (B) | 342/330 | 363/359 | 442/403 | 532/495 |
| Shutdown Margin (PCR) | -0.87 | -1.2 | -0.26 | -0.69 |
| (%Δk/kk') (BCR) | -0.57 | -0.82 | +0.11 | -0.28 |

Table 4.8 Summary of sensitivity study results for high quality Pu - optimized cases for 4 batch * 6 months

| Non-Absorber Diluent | ZrH | | $^{11}B_4C$ | |
|---|---|---|---|---|
| Pin Size | 150% | 200% | 150% | 200% |
| Na Void (%Δk/kk') | 1.400 | 1.082 | 1.307 | 1.295 |
| Doppler Constant | -.00511 | -.00368 | -.00522 | -.00460 |
| Void:Doppler | -274 | -294 | -250 | -281 |
| Peak Pin Rating, BOC (A) | 288/270 | 288/277 | 303/265 | 304/274 |
| (inner/outer) (W/cm) (B) | 393/368 | 427/411 | 530/465 | 639/576 |
| Shutdown Margin (PCR) | -1.04 | -1.23 | +0.06 | -0.36 |
| (%Δk/kk') (BCR) | -0.58 | -0.77 | +0.38 | -0.04 |

Table 4.9 Hollow pellets with ZrH + $^{11}B_4C$ non-absorber diluent - 200% pin size, high quality Pu

| $^{10}B$ Fraction (%) | 2.1 | 5 | | 15 | | | 30 | | 92 |
|---|---|---|---|---|---|---|---|---|---|
| Diluent Fraction, $B_4C$/ZrH (pins) | 113.8/ 0 | 60 / 13 | 59 / 14 | 30 / 22 | 25 / 30 | 24 / 32 | 15 / 31 | 12 / 41 | 5.6 / 65 |
| Fuel Pellet Voidage | 0 | 0.2025 | 0.2025 | 0.2025 | 0.2025 | 0.2025 | 0.2025 | 0.2025 | 0 |
| Na Void (%Δk/kk') | 1.295 | 1.401 | 1.369 | 1.586 | 1.325 | 1.271 | | 1.170 | 1.082 |
| Doppler Constant | -.00460 | -.00451 | -.00466 | -.00298 | -.00408 | -.00435 | | -.00450 | -.00368 |
| Void:Doppler | -281 | -311 | -294 | -532 | -325 | -292 | | -260 | -294 |
| Reactivity Loss per Cycle (%Δk/kk') | 3.228 | 2.591 | 2.578 | 2.018 | 2.000 | 2.004 | | 1.894 | 1.419 |
| Peak Pin Ratings (BOC) (A) | 304/274 | 295/273 | 295/273 | 289/274 | 289/273 | 290/273 | 288/274 | 288/273 | 288/277 |
| (inner/outer) (W/cm) (B) | 639/576 | 445/411 | 445/411 | 380/361 | 387/366 | 390/368 | 366/347 | 381/361 | 427/411 |
| Pu Burning Rate (all) | 72.5 | 73.1 | 73.0 | 74.7 | 73.0 | 72.8 | | 72.5 | 72.4 |
| (kg/TWhe) (fissile) | 99.6 | 101.4 | 101.6 | 102.4 | 103.6 | 104.0 | | 108.9 | 107.1 |
| Ave. Irradiation (GWd/te) | 107.3 | 96.4 | 96.4 | 84.1 | 85.7 | 86.2 | 81.2 | 84.6 | 72.8 |
| Temperature Reactivity Effect (nuc. data) | 0.42 | 0.37 | 0.38 | | | 0.38 | | 0.41 | 0.370 |
| (%Δk/kk') (expansion) | 0.5 | 0.5 | 0.5 | | | 0.5 | | 0.5 | 0.5 |
| Shutdown Worth (PCR) | 5.73 | 4.94 | 4.94 | | | 4.27 | | 4.18 | 3.59 |
| Required (%Δk/kk') (BCR) | 1.36 | 1.31 | 1.32 | | | 1.32 | | 1.35 | 1.31 |
| Rod Worth (%Δk/kk') (PCR) | 5.37 | 4.48 | 4.43 | | | 3.52 | | 3.24 | 2.37 |
| (BCR) | 1.32 | 1.08 | 1.07 | | | 0.83 | | 0.77 | 0.54 |
| Fraction of (PCR) | 0.94 | 0.91 | 0.90 | | | 0.82 | | 0.78 | 0.66 |
| Requirement (BCR) | 0.97 | 0.83 | 0.81 | | | 0.63 | | 0.57 | 0.41 |
| Shutdown Margin (PCR) | -0.36 | -0.46 | -0.51 | | | -0.75 | | -0.93 | -1.23 |
| (%Δk/kk') (BCR) | -0.04 | -0.23 | -0.25 | | | -0.48 | | -0.59 | -0.77 |

# 5 ADDITIONAL CONTROL RODS

As was clearly demonstrated by the results discussed in Sub-section 4.1, there were severe difficulties encountered in trying to achieve the required shutdown margins. To offset this, variations of the original reference core design were examined in which the numbers of control rods were increased, with the aim of increasing rod group worths. The reference absorber design already included $B_4C$ enriched to 92% $^{10}B$, so the option of increasing $^{10}B$ enrichment was not available for increasing rod group worths. Whilst increasing the number of rods to some extent reduces the effectiveness of the existing rods, it was possible to produce the fairly modest increases in rod group worths necessary.

In examining possible rod positions, two design rules were observed. No rod was placed at the centre of the core. A minimum of at least 2 non-rod S/As separated each neighbouring pair of rods.

A total of 7 alternative core rod distributions were examined, as shown in Figure 5.1 The designs included variants where the core centre does not correspond to a point in the repeating pattern of rod positions. Where it was beneficial, a minor change in the core enrichment boundary, coinciding with the relocation of a ring of rods, was incorporated. The total number of rods was increased from 36 to between 45 and 54.

The suitability of the different rod distributions was examined using channel power distributions for PCRs at insertions of 0%, 50% and 100%. Important features of these rating distributions are summarized in Table 5.1. From examination of these results, the following conclusions were drawn: rod distributions III and IV were eliminated, because of the high rating peaks around BCR positions when PCRs are inserted; distribution VII is preferable to both V and VI, because it avoids a high (5 MW) peak with PCRs 100% inserted.

To further compare the different rod distributions, MOSES calculations of rod group worths, and the associated shutdown margins, were calculated for 3 different core states. These core states were chosen to represent a wide range of conditions, they encompassed the 3 Pu vectors assessed and the different diluent

material options. They are fairly typical of the cases for which rod worths must be improved, being:

low quality Pu, 4 * 6 months, 150% pin size, ZrH (12 pins) diluent

reference Pu, 4 * 6 months, 200% pin size, $B_4C$ (95.7 pins, 1.9% $^{10}B$) diluent

high quality Pu, 4 * 6 months, 200% pin size, ZrH (32 pins) & $B_4C$ (24 pins, 15% $^{10}B$) diluent, hollow pellet (45% bore).

The first two cases are taken from the limiting conditions identified in Tables 4.6 & 4.7. The third case is from Table 4.9, a case optimized for hollow fuel pellets.

Shutdown margins were calculated for each of the three cases described above, for the various rod position options. As with the initial calculations for Section 4, the thermal expansion coefficients of reactivity were not calculated for every case. The assumption of a fixed value (0.5%$\Delta k/kk'$) in the analysis will not materially affect the conclusions drawn. (Calculations for cores V and VII, in addition to those for the original core, showed only small variations in this reactivity coefficient - a maximum variation of 0.03%$\Delta k/kk'$, with <0.01%$\Delta k/kk'$ typical.)

The results of the shutdown margin calculations are shown in Tables 5.2 to 5.4, for the low, reference and high quality Pu cases respectively. Rod distribution options I and II both fail to meet shutdown requirements for BCRs, these options were therefore eliminated from further consideration. Of the options V, VI and VII, the latter is preferable because it results in rather larger PCR shutdown margins: the PCR shutdown requirement includes the reactivity loss, which is cycle length dependent, so a large PCR margin gives scope for increasing cycle lengths beyond 6 months. Therefore core option VII was chosen as the best variant to adopt for the optimized core calculations. However, the BCR margins are comparatively small for option VII; in the event of difficulties with BCR margins, core option V would be adopted as a fallback position.

Within each of the Tables 5.2 to 5.4 the calculations used fixed number density data, just altering the core map of fuel and rod S/As to evaluate the effects of different core geometries. Further calculations were done, to assess the effect of changing rod distribution when incorporated within the entire calculation route.

Table 5.5 shows the results of two sets of calculations, all for the same high quality Pu case as Table 5.4: first the diluent fraction is unaltered, just the Pu enrichment is increased to maintain the target criticality; in the second set of calculations the diluent fraction was adjusted to regain an ~45% peak Pu enrichment and safety parameters at the target. With the exception of shutdown margins, the variations in parameters (including diluent fractions) was small - rating variations with rod distribution are largely a consequence of the variation in the number of fuelled S/As. Comparing Table 5.5 with the equivalent cases of Table 5.4, the shutdown margin is seen to be somewhat sensitive to Pu enrichment, and also to ZrH diluent fraction.

A further set of variations are presented in Table 5.6, showing the effect of increasing the cycle length beyond 6 months. The PCR shutdown margin shows the expected strong dependence on cycle length, unlike the BCR value which is seen to be insensitive to cycle length.

Table 5.1 Effect of varying rod distribution on channel ratings

| Rod Distribution | Channel Power, MW | | | | | | | | | | | |
|---|---|---|---|---|---|---|---|---|---|---|---|---|
| | PCRs 0% inserted | | | | PCRs 50% inserted | | | | PCRs 100% inserted | | | |
| | centre S/A | inner core | outer core | core edge | centre S/A | inner core | outer core | core edge | centre S/A | inner core | outer core | core edge |
| original | 3.13 | 3.30 | 3.65 | 1.36 | 2.61 | 3.59 | 4.08 | 1.49 | 2.07 | 3.85 | 4.51 | 1.61 |
| I | 3.19 | 3.42 | 3.58 | 1.36 | 2.31 | 3.61 | 3.62 | 1.47 | 1.61 | 3.96 | 4.00 | 1.55 |
| II | 3.27 | 3.45 | 3.94 | 1.41 | | | | | | | | |
| III | 3.19 | 3.42 | 3.58 | 1.36 | 2.68 | 4.14 | 3.66 | 1.34 | 2.12 | 4.88 | 3.87 | 1.30 |
| IV | 3.27 | 3.45 | 3.94 | 1.41 | | | | | | | | |
| V | 4.36 | 4.36 | 3.26 | 1.39 | 3.70 | 3.70 | 3.76 | 2.11 | 2.82 | 3.63 | 4.97 | 3.04 |
| VI | 3.52 | 3.68 | 3.44 | 1.45 | 3.03 | 3.79 | 3.91 | 2.12 | 2.29 | 4.23 | 5.00 | 2.98 |
| VII | 3.52 | 3.68 | 3.44 | 1.45 | 3.55 | 3.84 | 3.85 | 1.78 | 3.34 | 4.06 | 3.71 | 2.18 |

inner & outer core are maximum values, edge is a minimum value

Table 5.2 Shutdown margin variation with rod distribution: low quality Pu case

| Rod Distribution | | Orig. | I | II | V | VI | VII |
|---|---|---|---|---|---|---|---|
| Reactivity loss per Cycle (%Δk/kk') | | 2.50 | 2.50 | 2.50 | 2.50 | 2.50 | 2.50 |
| Temperature Effect (%Δk/kk') | (nuc. data) | 1.24 | 1.27 | 1.25 | 1.27 | 1.21 | 1.23 |
| | (expansion) | 0.5 | 0.5 | 0.5 | 0.5 | 0.5 | 0.5 |
| Shutdown Worth Required (%Δk/kk') | (PCR) | 5.70 | 5.73 | 5.71 | 5.73 | 5.67 | 5.68 |
| | (BCR) | 2.18 | 2.21 | 2.19 | 2.21 | 2.15 | 2.17 |
| Rod Worth (%Δk/kk') | (PCR) | 5.31 | 6.67 | 7.28 | 7.77 | 7.32 | 9.29 |
| | (BCR) | 1.25 | 2.03 | 1.56 | 3.49 | 3.59 | 2.36 |
| Fraction of Requirement | (PCR) | 0.93 | 1.16 | 1.27 | 1.36 | 1.29 | 1.64 |
| | (BCR) | 0.57 | 0.92 | 0.71 | 1.58 | 1.67 | 1.09 |
| Shutdown Margin (%Δk/kk') | (PCR) | -0.39 | +0.94 | +1.57 | +2.04 | +1.66 | +3.61 |
| | (BCR) | -0.93 | -0.18 | -0.63 | +1.28 | +1.44 | +0.19 |

Table 5.3 Shutdown margin variation with rod distribution: reference quality Pu case

| Rod Distribution | | Orig. | I | II | V | VI | VII |
|---|---|---|---|---|---|---|---|
| Reactivity loss per Cycle (%Δk/kk') | | 3.19 | 3.19 | 3.19 | 3.19 | 3.19 | 3.19 |
| Temperature Effect (%Δk/kk') | (nuc. data) | 0.58 | 0.60 | 0.59 | 0.60 | 0.57 | 0.58 |
| | (expansion) | 0.5 | 0.5 | 0.5 | 0.5 | 0.5 | 0.5 |
| Shutdown Worth Required (%Δk/kk') | (PCR) | 5.85 | 5.87 | 5.86 | 5.87 | 5.84 | 5.85 |
| | (BCR) | 1.52 | 1.54 | 1.53 | 1.54 | 1.51 | 1.52 |
| Rod Worth (%Δk/kk') | (PCR) | 5.17 | 6.53 | 7.12 | 7.67 | 7.38 | 9.13 |
| | (BCR) | 1.25 | 2.01 | 1.50 | 3.34 | 3.45 | 2.31 |
| Fraction of Requirement | (PCR) | 0.88 | 1.11 | 1.22 | 1.31 | 1.26 | 1.56 |
| | (BCR) | 0.82 | 1.30 | 0.98 | 2.17 | 2.29 | 1.52 |
| Shutdown Margin (%Δk/kk') | (PCR) | -0.69 | +0.66 | +1.26 | +1.80 | +1.54 | +3.28 |
| | (BCR) | -0.28 | +0.47 | -0.03 | +1.80 | +1.94 | +0.79 |

Table 5.4 Shutdown margin variation with rod distribution: high quality Pu case

| Rod Distribution | | Orig. | I | II | V | VI | VII |
|---|---|---|---|---|---|---|---|
| Reactivity loss per Cycle (%Δk/kk') | | 2.00 | 2.00 | 2.00 | 2.00 | 2.00 | 2.00 |
| Temperature Effect (%Δk/kk') | (nuc. data) | 0.38 | 0.38 | 0.38 | 0.38 | 0.37 | 0.38 |
| | (expansion) | 0.5 | 0.5 | 0.5 | 0.5 | 0.5 | 0.5 |
| Shutdown Worth Required (%Δk/kk') | (PCR) | 4.27 | 4.27 | 4.27 | 4.27 | 4.26 | 4.26 |
| | (BCR) | 1.32 | 1.32 | 1.32 | 1.32 | 1.31 | 1.32 |
| Rod Worth (%Δk/kk') | (PCR) | 3.52 | 4.39 | 4.73 | 5.02 | 4.77 | 6.28 |
| | (BCR) | 0.83 | 1.33 | 1.00 | 2.35 | 2.46 | 1.53 |
| Fraction of Requirement | (PCR) | 0.82 | 1.03 | 1.11 | 1.18 | 1.12 | 1.47 |
| | (BCR) | 0.63 | 1.00 | 0.76 | 1.78 | 1.88 | 1.16 |
| Shutdown Margin (%Δk/kk') | (PCR) | -0.75 | +0.11 | +0.46 | +0.75 | +0.51 | +2.02 |
| | (BCR) | -0.48 | 0.0 | -0.32 | +1.03 | +1.15 | +0.22 |

Table 5.5 Effect of improved rod distribution on calculation of all parameters (high quality Pu)

| Rod Option | Original | V | VII | V | V |
|---|---|---|---|---|---|
| Pu Enrichment (inner/outer) (%) | 40.80/45.01 | 41.14/47.12 | 41.21/45.39 | 39.17/45.22 | 39.30/45.24 |
| Diluent Fraction ($B_4C$ / ZrH) (pins) | 24 / 32 | 24 / 32 | 24 / 32 | 24 / 27 | 23 / 29 |
| Na Void (%Δk/kk') | 1.271 | 1.227 | 1.230 | 1.314 | 1.260 |
| Doppler Constant | -.00435 | -.00421 | -.00425 | -.00434 | -.00462 |
| Void:Doppler ratio | -292 | -291 | -290 | -303 | -273 |
| Peak Pin Rating (B) (BOC) | 390.2/367.8 | 411.1/383.4 | 424.1/389.8 | 395.1/373.7 | 400.0/374.7 |
| (inner/outer) (W/cm) (EOC) | 371.0/370.8 | 386.4/386.7 | 392.5/392.6 | 375.4/375.7 | 377.1/377.5 |
| Reactivity Loss per Cycle (%Δk/kk') | 2.004 | 2.052 | 2.093 | 2.080 | 2.085 |
| EOC Keff (70 groups) | 1.01619 | 1.01477 | 1.01497 | 1.01350 | 1.01417 |
| (7 groups) | 1.00516 | 1.00492 | 1.00482 | 1.00505 | 1.00499 |
| Average Irradiation (GWd/te) | 86.2 | 88.5 | 88.6 | 85.9 | 86.5 |
| Shutdown Margin (PCR) | -0.75 | +0.11 | +1.89 | +0.29 | +0.20 |
| (%Δk/kk') (BCR) | -0.48 | +1.34 | +0.38 | +1.48 | +1.41 |

Table 5.6 Effect of varying cycle length for an improved rod distribution (high quality Pu)

| Rod Option | VII | VII | VII | VII |
|---|---|---|---|---|
| Pu Enrichment (%) | 41.21/45.39 | 43.11/45.09 | 43.43/45.06 | 44.22/44.89 |
| Diluent Fraction ($B_4C$/ZrH) (pins) | 24 / 32 | 25 / 27 | 24 / 29 | 24 / 27 |
| Fuel Cycle | 4*6 months | 4*9 months | 4*9 months | 4*10.5 mon |
| Na Void (%Δk/kk') | 1.230 | 1.338 | 1.285 | 1.319 |
| Doppler Constant | -.00425 | -.00432 | -.00459 | -.00466 |
| Void:Doppler ratio | -290 | -310 | -280 | -283 |
| Peak Pin Rating (BOC) | 424.1/389.8 | 481.8/361.0 | 492.8/360.9 | 500.3/351.2 |
| (B) (W/cm) (EOC) | 392.5/392.6 | 378.2/378.4 | 380.1/380.2 | 376.8/377.1 |
| Reactivity Loss per Cycle (%Δk/kk') | 2.093 | 3.444 | 3.485 | 4.219 |
| EOC Keff (70 gp) | 1.01497 | 1.01365 | 1.01440 | 1.01331 |
| (7 gp) | 1.00482 | 1.00481 | 1.00481 | 1.00434 |
| Average Irradiation (GWd/te) | 88.6 | 129.6 | 130.4 | 150.2 |
| Shutdown Margin (PCR) | +1.89 | +0.92 | +0.78 | +0.13 |
| (%Δk/kk') (BCR) | +0.38 | +0.39 | +0.33 | +0.33 |

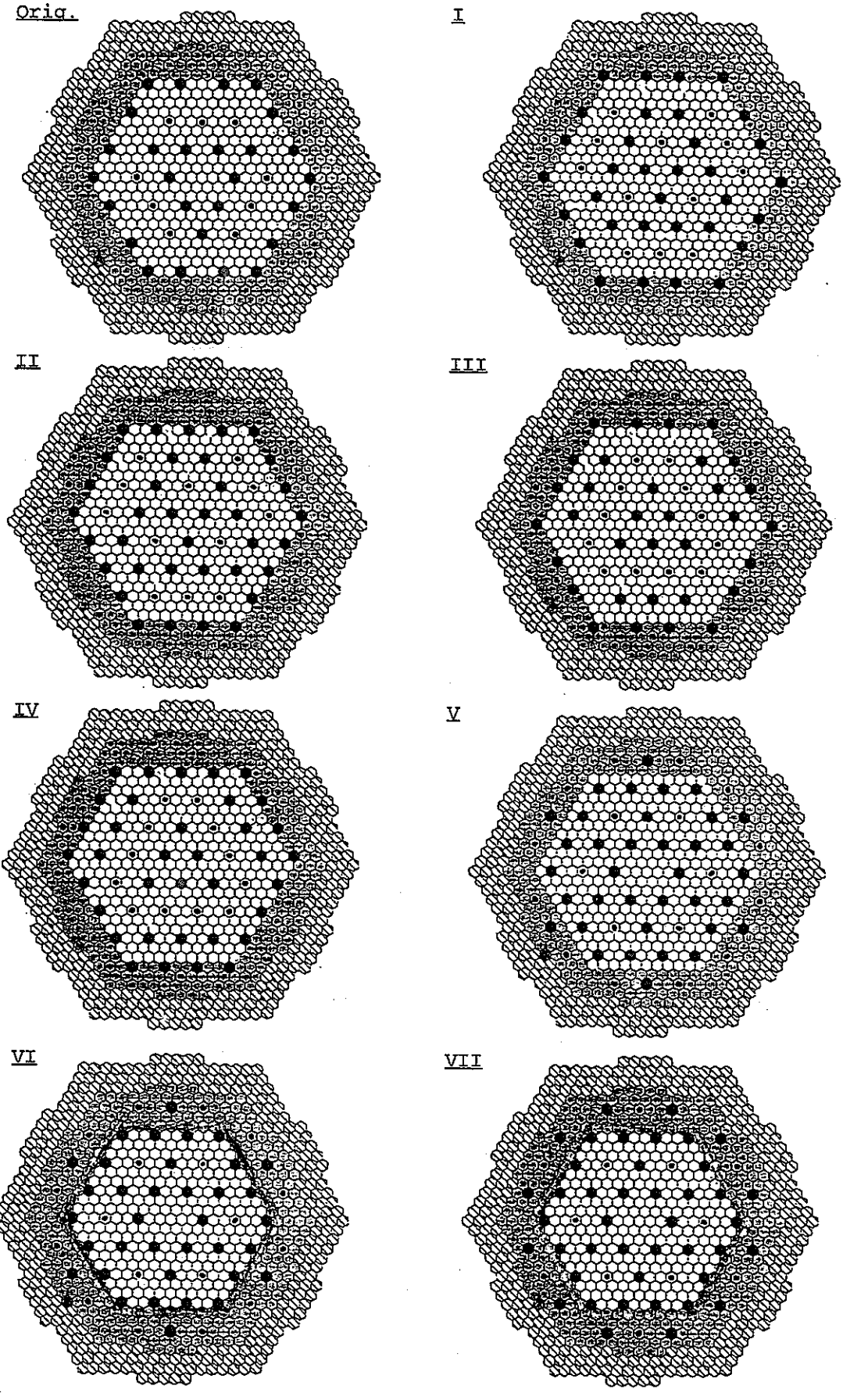


Figure 5.1 Alternative control rod configurations

# 6 OPTIMIZED DESIGN - METHODS

For the calculations that produced the final optimized designs of this study, a number of improvements in modelling methods and assumptions were made, with compared those used throughout the sensitivity survey. These changes represent both a response to conclusions drawn from the sensitivity survey, and also the adoption of more detailed and time-consuming calculations that would have been unsuitable for the wider ranging sensitivity survey.

The above and below core structure has been changed. The nominal uniform composition (80% steel, 20% Na) was replaced by a more detailed structure. This new structure was taken from the 600 MW(e) fast breeder reactor design study[6-1] carried out at PNC, with breeder regions deleted. This modelling improvement was instigated by calculations carried out by CEA, which showed that results can be sensitive to the axial reflector structure.

The rod absorber material is included in the model used for the RZ calculations. This requires the full core height to be modelled, rather than just half the core with a reflective boundary at the centre plane. It was considered appropriate to incorporate the absorber, both for the effect on Keff and because its presence may modify the fraction of $B_4C$ diluent required in the fuel S/As.

The PENCIL burn-up calculations that produce the BOC and EOC number densities were altered from 7 to 18 energy groups for the final calculations. This was done because the condensation (from 70 groups) that produced the 7 group nuclear data was seen to be unduly sensitive to small changes in core composition. Using a condensation to 18 groups improved the situation.

Peak pin ratings were taken from 3D (hex-Z) MOSES calculations, rather than 2D (RZ) CITATION calculations. These MOSES calculations incorporated 3D burn-up modelling. The individual fuel cycle batches were modelled explicitly. It was considered that such a detailed calculation was necessary to achieve a realistic assessment of peak pin ratings.

The model used to represent fuel in the SLAROM cell lattice program was altered. The homogeneous representation being replaced

by a 2 region RZ 'infinite pin' model, the inner region consisting of just the fuel pellet material (with the same radius as the fuel pellet). The main reason for adopting this model improvement was so that fuel and non-fuel materials could be given different temperatures and thus Doppler constants correctly calculated for just fuel temperatures changing. It also has the advantage of modelling fuel pin heterogeneity.

In the RZ calculations the radial meshes at the core edge were refined, making them of comparable size to the axial edge meshes. The improvement in accuracy from this change was not expected to be very great. The MOSES calculations of rod group worths used at first a coarse and later a more refined number density mesh representation of the core. Both these meshes differed from that in Figure 3.1 used for the sensitivity study calculations of Section 4.

## 6.1 ABOVE AND BELOW CORE STRUCTURE

The sensitivity study calculations used a very simplistic representation of the above and below core axial structures: a uniform composition of 80% steel / 20% Na was assumed. Calculations by CEA have shown that using a more realistic representation of above/below core structures can have a significant effect on the results: using axial structures based on the CAPRA core design caused a reduction in EOC Keff of ~7.5%, this required the fuel inventory to be increased by ~12% in order for criticality criteria to be re-attained (the comparison is complicated by the CEA calculations also including rod absorber in the above core region).

For the optimized calculations of the current study, a detailed axial structure for fuel S/As was taken from data for the 600 MW(e) breeder design of reference 6-1. Figure 6.1 is a S/A schematic diagram for the design of reference 6-1, it includes axial breeder regions, which are of course not wanted in a Pu burning core. Based on this source, the following axial structure was assumed:

| | |
|---|---|
| upper axial shield | 500 mm |
| above pin gap | 70 mm |

| | |
|---|---|
| upper pin plug | 30 mm |
| upper pin plenum | 50 mm |
| fuel | 600 mm |
| lower pin plug | 20 mm |
| lower pin plenum | 700 mm |
| lower axial shield | 330 mm. |

This structure is axially asymmetric: it is necessary to represent the whole core height, rather than just a half-height core with a reflective centre-plane boundary. The structure is somewhat different from that addressed by CEA.

The number densities for the various regions were calculated on the following basis. The plug and plena regions were taken to have the same composition as the fuel region, except that the fuel pins were taken to be filled with steel and void, respectively. The above pin gap comprises just Na and wrapper, the steel of the latter is 9.3% of the S/A volume. For the remaining regions, the design of reference 6-1 gives the following volume fractions: upper axial shield 20% Na, 80% steel; lower axial shield 29% Na, 31.5% steel, 39.5% natural $B_4C$ (at 90% of theoretical density).

To examine the effect of the changed axial structure, the final optimized cases for both high and low quality Pu vectors were re-run with all the above and below core shielding regions altered to the original composition of 20% Na, 80% steel. The result was an increase in EOC Keff values of ~1.4%.

## 6.2 ROD ABSORBER

In addition to the axial above/below core structures described in the previous Sub-section, the modelling of non-core structures was improved by the addition of rod absorber materials in all calculations. For the 2D (RZ) calculations, both burn-up and

reactivity (Keff), the absorber was placed immediately above the active core.

For the rod group worth calculations it was appropriate to use a homogeneous cell model for the absorber (as in the calculations of Section 4), since the adjustment factors applied to nominal rod group worths included an allowance for heterogeneity effects. For other purposes, it was more appropriate to use a heterogeneous cell model for the absorber, since this would result in a more accurate representation of the effects of the rods on reactivity and rating distribution.

It was therefore necessary for the calculations that produced condensed nuclear datasets (for 7 and 18 energy groups) to produce data for both homogeneous and heterogeneous models of absorber. Both condensations used the same flux, calculated in a 70 group SLAROM-JOINT-CITATION calculation which used the heterogeneous absorber model.

The heterogeneous absorber cell model represented the absorber from a complete absorber rod as a single cylinder, in a 1D 'infinite pin' model. The cell model used 6 separate regions, 5 of which represent the absorber S/A: $B_4C$ absorber, a voidage gap, a steel sheath, Na coolant, S/A wrapper and a surrounding fuel region. The region radii were - 4.7901, 4.9038, 5.7652, 7.9071, 8.3008 and 27.1527 cm. The outer region corresponds to 9.7 fuel S/A, its composition was taken from a typical equilibrium core case.

To examine the effect of the absorber material, the final optimized cases for both high and low quality Pu vectors were re-run with all the rod absorber regions altered to rod follower. The result was an increase in EOC Keff values of ~2.4%.

## 6.3 7/18 GROUP BURN-UP CALCULATIONS

In preparing data for the optimized cases, it was observed that calculated values of Keff showed an undue sensitivity to the core state for which the 7 group nuclear dataset had been condensed. For example, 7 group datasets were produced for two low quality Pu cores,

differing only in cycle length (9 and 10.5 months) and in the number of ZrH diluent pins in inner core fuel S/As (34 and 21). Using these 2 sets of nuclear data in 7 group PENCIL (burn-up) calculations for identical conditions produced EOC Keff values that differed by more than 0.6%, whilst 70 group CITATION calculations produced using number density data from these two conditions were virtually identical. More generally, any small change in the conditions of the convergence to 7 energy groups was liable to have a disproportionate effect on the resulting Keff value in PENCIL.

The minor differences in the conditions producing the 7 group datasets were insufficient to explain the variation in Keff. Later calculations demonstrated that the true effect of the diluent fraction changes on the nuclear data was only to alter Keff values by ~0.01%, a difference small enough to be neglected.

It was concluded that the instability in Keff values was a direct consequence of the 7 energy group structure used. The moderated flux spectrum associated with the presence of diluent in the Pu burning core designs requires more detail than the 7 group representation provides, if it is to be modelled accurately. It was decided to use a less coarse spectrum, a standard 18 group spectrum used within PNC (see Table 6.1).

Table 6.2 presents the results of a number of calculations, demonstrating the effect of changing the number of energy groups used. There is comparatively little variation - at most ~0.05%, generally much less - in Keff values from 70 group CITATION calculations, whichever nuclear data was used in the burn-up calculation. The difference between 7 and 18 group calculations using identical nuclear data was large - 0.35 to 1.0%. Keff values calculated for 18 groups and using nuclear data condensed for different conditions had only small differences - 0.02 to 0.07%. The results were sufficient to demonstrate that the use of an 18 group spectrum was both necessary and adequate to give an acceptable level of accuracy.

## 6.4 3D (MOSES) BURN-UP CALCULATIONS

In the sensitivity study, the calculated peak pin ratings were taken from 2D (RZ) models; this provides an acceptable comparison of different design options, but is inadequate for producing accurate values of peak rating. To provide more detailed modelling of peak ratings, 3D MOSES burn-up calculations were used to calculate peak ratings; they also produced values of peak irradiation.

The MOSES calculations explicitly represented the 4 separate batches of the fuel cycle, each being loaded in sequence in the burn-up transient. Each burn-up calculation modelled a total of 9 irradiation batches: 5 to reach fuel cycle equilibrium, then one step for each of the 4 distinct batches. Figure 6.2 shows the 4 batch loading scheme that was used for the core with rod distribution option VII - it was devised both to avoid (as far as possible) adjacent S/As in the same refuelling batch, and to avoid clusters of S/As with a mean irradiation much different from the enrichment zone average. A 120° rotational symmetry was obtained.

The MOSES calculations used a hexagonal-Z mesh with one mesh point per S/A, though an approximation based on Askew[3-3] was used to produce a pseudo-tri-Z representation of ratings. (An option to use a similar 6-point-per-S/A irradiation representation is yet to be implemented in MOSES.) Whilst MOSES possesses an option for full tri-Z calculations, the pseudo-tri-Z calculation is adequate for calculating peak rating values[3-1] and a full tri-Z calculation would make excessive demands on computing time. For similar reasons of economy, the MOSES burn-up calculations were done in 7 rather than 18 energy groups, whilst this may result in incorrect Keff values (see Sub-section 6.3), a test case with 18 groups showed the peak ratings to differ by no more than ~2%.

In addition to the above changes, the burn-up calculation differed from those of the sensitivity study by dividing the irradiation for each refuelling batch into two steps: BOC to MOC and MOC to EOC. For these 2 timesteps, different PCR insertions were used - BOC insertions for the first step and EOC (0% insertion) for the second step. This gives a more realistic representation of average rod positions during burn-up. The relative insertions of

different rings of PCRs were adjusted for the BOC steps, with the purpose of optimizing the inner:outer peak rating ratio at BOC. (The EOC rating ratio, with rods 0% inserted, is optimized by the choice of Pu enrichments and diluent fractions.)

## 6.5 HETEROGENEOUS FUEL LATTICE MODEL

In the sensitivity study, the fuel S/As were treated as homogeneous cells for the purposes of the SLAROM calculations evaluating nuclear data. This had 2 main effects on the calculations: because the heterogeneity of the fuel was not modelled, fuel self-shielding effects were under estimated; Doppler coefficients were calculated for all the S/A materials increasing in temperature, rather than just fuel pellet materials.

For the optimized calculations, a heterogeneous fuel cell model was used in SLAROM: a 1D cylindrical 'infinite pin' model, with 2 regions. The inner region comprised the fuel materials and had the same radius and mean density as the fuel pellet. The outer region comprised a mix of all other materials, to the amount and volume associated with a single fuelled pin. The inner zone had a temperature of 1373 K (increasing to 1873 K for Doppler calculations), the outer zone was fixed at 703 K.

Perturbation analysis in Part I of the sensitivity study showed that non-fuel isotopes (principally Fe and Cr) contributed typically 10-30% of the calculated Doppler effect. Doppler feedback from structural materials is of dubious value, since it will only occur with some heat transfer time delay. Therefore the optimized calculations excluded structural materials from the assessment of Doppler constants

The target for safety parameters was not altered when the Doppler calculation was changed to excluding structural materials, so the final optimized calculations effectively used a limit for the safety parameters that was in the region of 20% more restrictive than the limit used for the sensitivity studies.

Some of the final optimized calculations of Section 7 were for hollow fuel pellets. An attempt was made to represent hollow pellet fuel with a 3 region SLAROM cell model, the additional region being the void at the centre of the pellet. The calculations encountered difficulties, as exemplified by the Doppler constants, all for the same core, shown in Table 6.3. The table shows values of Doppler constant calculated for 3, 2 and 1 region models, and with non-fuel temperatures set to either 703 K or the same temperature as the fuel. From these and other calculations it was concluded that the representation of different temperatures in the 3 region SLAROM model was faulty. The optimized calculations were restricted to using the 2 region model.

Table 6.3 shows that compressing the fuel into its actual annular volume (rather than smearing it over the whole pellet) had the effect of reducing the Doppler constant by one third, it also reduced the EOC Keff by 0.16%. It is not certain whether this is a real effect of the fuel self-shielding, or related to problems with temperature modelling in SLAROM. However, given the apparently disproportionate effect of changing from 2 to 3 regions (compared with the difference between 1 and 2 regions), and the temperature errors identified above, it seems most likely that the results are an artifact of the calculation. These phenomena should be the subject of further investigation, since the reduction of Doppler constant for hollow fuel pellets (should it be a real effect) was significant.

## 6.6 MESH REPRESENTATION

With the absorber explicitly modelled and the above/below core structure modelled in detail, there is no longer axial symmetry and it became necessary to use a full core height model in the 2D calculations. The core radial number density mesh was modified from that used in the sensitivity study: two narrow meshes of 3 and 6 cm were created from the outside of the outer enrichment zone, other than this there was a single radial region for each enrichment zone. With the core axial number density mesh doubled to 8 meshes, this gives a total of 32 core number density regions. The purpose of this change was to mimic the axial edge mesh modelling at the core radial

edge - it was demonstrated in Part I of the study that this level of detail was necessary to effectively model axial leakage effects. Figure 6.3 is a representation of the 2D mesh structure used.

All the MOSES calculations used a radial S/A distribution taken from the map for case VII in Figure 5.1 (for the MOSES burn-up calculations, only a 120° segment is modelled, with 4 separate fuel batches represented, as in Figure 6.2). All the MOSES calculations used the same axial structure for the non-core regions: a simplified version of that for the 2D calculations, shown in Figure 6.3, but with no differentiation between different areas with identical compositions.

Twenty meshes were used for the core axial flux representation in MOSES. Two different core number density representations were used for the rod worth MOSES calculation, both are shown in Figure 6.4. At first a simple mesh structure was used, with just 4 different sets of number densities for each enrichment zone, arranged with reflective symmetry about the core centre plane. Later calculations used a more detailed representation of 3 radial groups of S/As, the extra group being 48 outer S/As corresponding to the outer 2 meshes in the 2D representation; each group had a full 8 mesh number density representation. The MOSES burn-up calculations also used 8 axial number density meshes, but the radial modelling represented each S/A separately.

Table 6.1 Energy group structure

| Groups 7G | 18G | 70G | Upper Energy |
|---|---|---|---|
| 1 | 1 | 1 | 10.0 (MeV) |
| | | 2 | 7.7880 |
| | 2 | 3 | 6.0653 |
| | | 4 | 4.7237 |
| 2 | 3 | 5 | 3.6788 |
| | | 6 | 2.8650 |
| | 4 | 7 | 2.2313 |
| | | 8 | 1.7377 |
| 3 | 5 | 9 | 1.3534 |
| | | 10 | 1.0540 |
| | 6 | 11 | 0.82085 |
| | | 12 | 0.63928 |
| | | 13 | 0.49787 |
| | 7 | 14 | 0.38774 |
| | | 15 | 0.30197 |
| | | 16 | 0.23518 |
| | 8 | 17 | 0.18316 |
| | | 18 | 0.14264 |
| | | 19 | 0.11109 (MeV) |
| 4 | 9 | 20 | 86.517 (keV) |
| | | 21 | 67.379 |
| | | 22 | 52.475 |
| | 10 | 23 | 40.868 |
| | | 24 | 31.828 |
| | | 25 | 24.788 |
| | 11 | 26 | 19.305 |
| | | 27 | 15.034 |
| | | 28 | 11.709 |
| 5 | 12 | 29 | 9.1188 |
| | | 30 | 7.1017 |
| | | 31 | 5.5308 |
| | 13 | 32 | 4.3074 |
| | | 33 | 3.3546 |
| | | 34 | 2.6126 |
| | 14 | 35 | 2.0347 |
| | | 36 | 1.5846 |
| | | 37 | 1.2341 (keV) |

| Groups 7G | 18G | 70G | Upper Energy |
|---|---|---|---|
| 6 | 15 | 38 | 961.12 (eV) |
| | | 39 | 748.52 |
| | | 40 | 582.95 |
| | 16 | 41 | 454.00 |
| | | 42 | 353.58 |
| | | 43 | 275.36 |
| | 17 | 44 | 214.45 |
| | | 45 | 167.02 |
| | | 46 | 130.07 |
| 7 | 18 | 47 | 101.30 |
| | | 48 | 78.893 |
| | | 49 | 61.442 |
| | | 50 | 47.851 |
| | | 51 | 37.267 |
| | | 52 | 29.023 |
| | | 53 | 22.603 |
| | | 54 | 17.603 |
| | | 55 | 13.710 |
| | | 56 | 10.677 |
| | | 57 | 8.3153 |
| | | 58 | 6.4760 |
| | | 59 | 5.0435 |
| | | 60 | 3.9279 |
| | | 61 | 3.0590 |
| | | 62 | 2.3824 |
| | | 63 | 1.8554 |
| | | 64 | 1.4450 |
| | | 65 | 1.1254 |
| | | 66 | 0.87642 |
| | | 67 | 0.68256 |
| | | 68 | 0.53158 |
| | | 69 | 0.41399 |
| | | 70 | 0.32242 (eV) |

Minimum energy, $10^{-5}$ eV

Table 6.2 The variation of Keff with no. of energy groups for the nuclear data and the conditions of it is condensation

| Conditions of Condensation Calculation | No. of groups | Conditions of Keff Calculation | | | |
|---|---|---|---|---|---|
| | | 10.5 month cycle, 21/0 pins ZrH diluent | | 9 month cycle, 34/0 pins ZrH diluent | |
| | | Keff Calculation Type | | Keff Calculation Type | |
| | | PENCIL (7/18 gp) | CITATION (70 group) | PENCIL (7/18 gp) | CITATION (70 group) |
| 9 month cycle 31/4 pins ZrH | 7 | 1.01573 | 1.00446 | 1.00557 | 0.99830 |
| 〃 | 18 | 1.00564 | 1.00477 | 1.00023 | 0.99824 |
| 10.5 month cycle 21/0 pins ZrH | 7 | 1.00933 | 1.00444 | - | - |
| 〃 | 18 | 1.00579 | 1.00436 | 1.00093 | 0.99778 |

Table 6.3 Effect of fuel cell model on Doppler constant for hollow fuel pellets

| Temperature of Non-fuel Regions | 3 Region Model | 2 Region Model | 1 Region Model |
|---|---|---|---|
| 703 K (fixed) | -0.00394 | -0.00499 | - |
| same as fuel | -0.00395 | -0.00589 | -0.00620 |

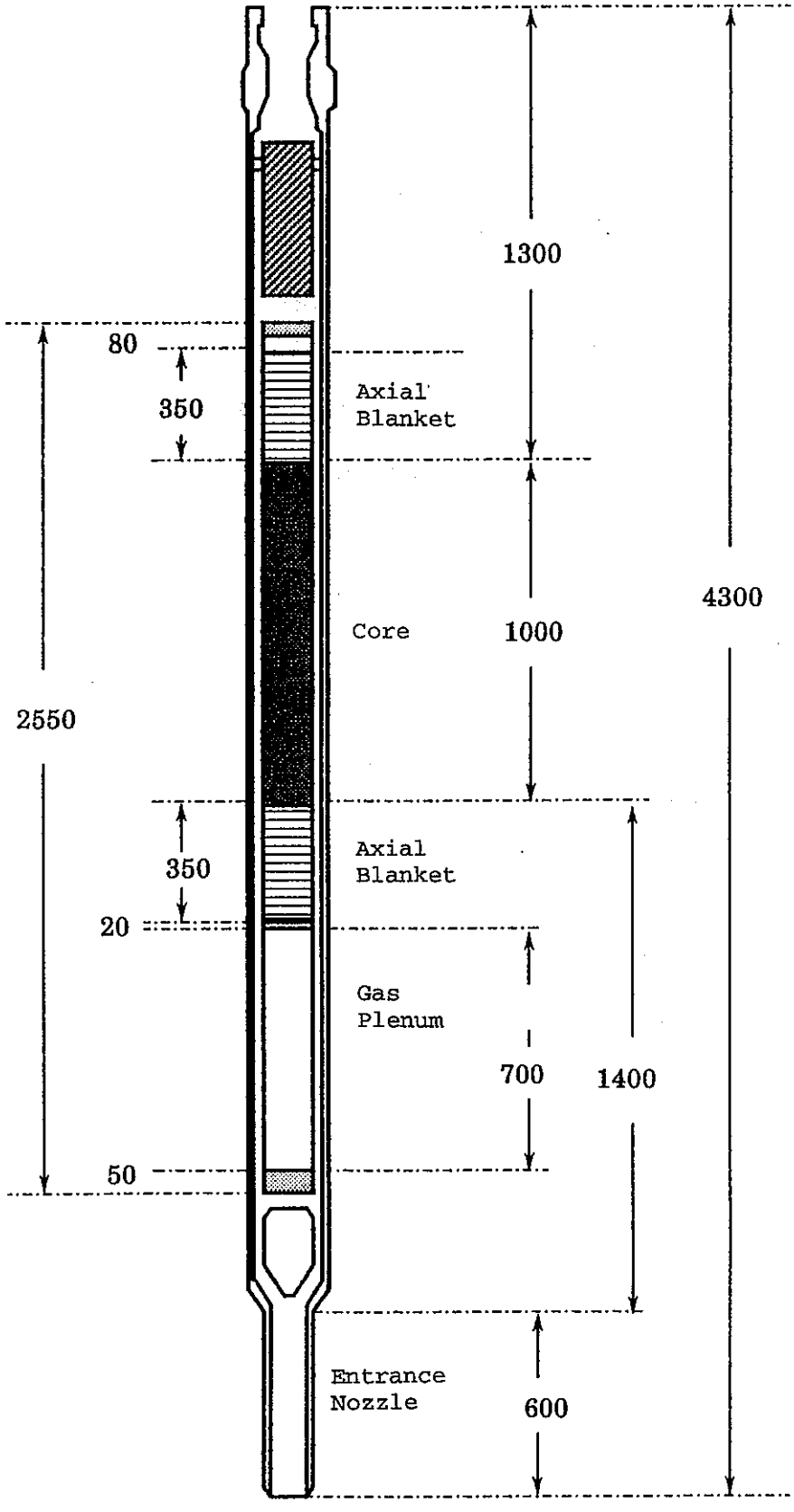


Figure 6.1 S/A schematic used as basis for above/below core structures

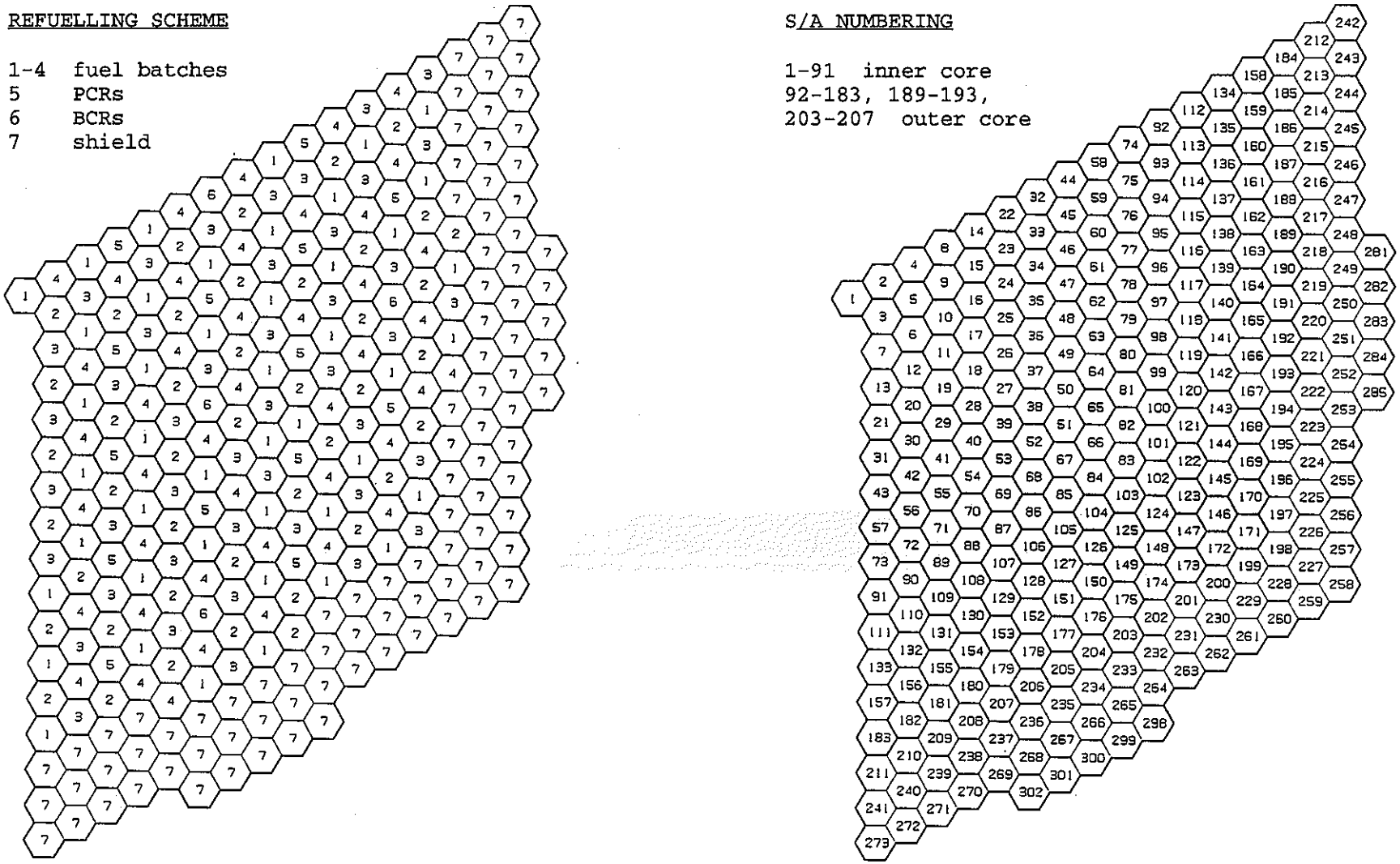


Figure 6.2 4 batch refuelling pattern and S/A numbering scheme (120° model)

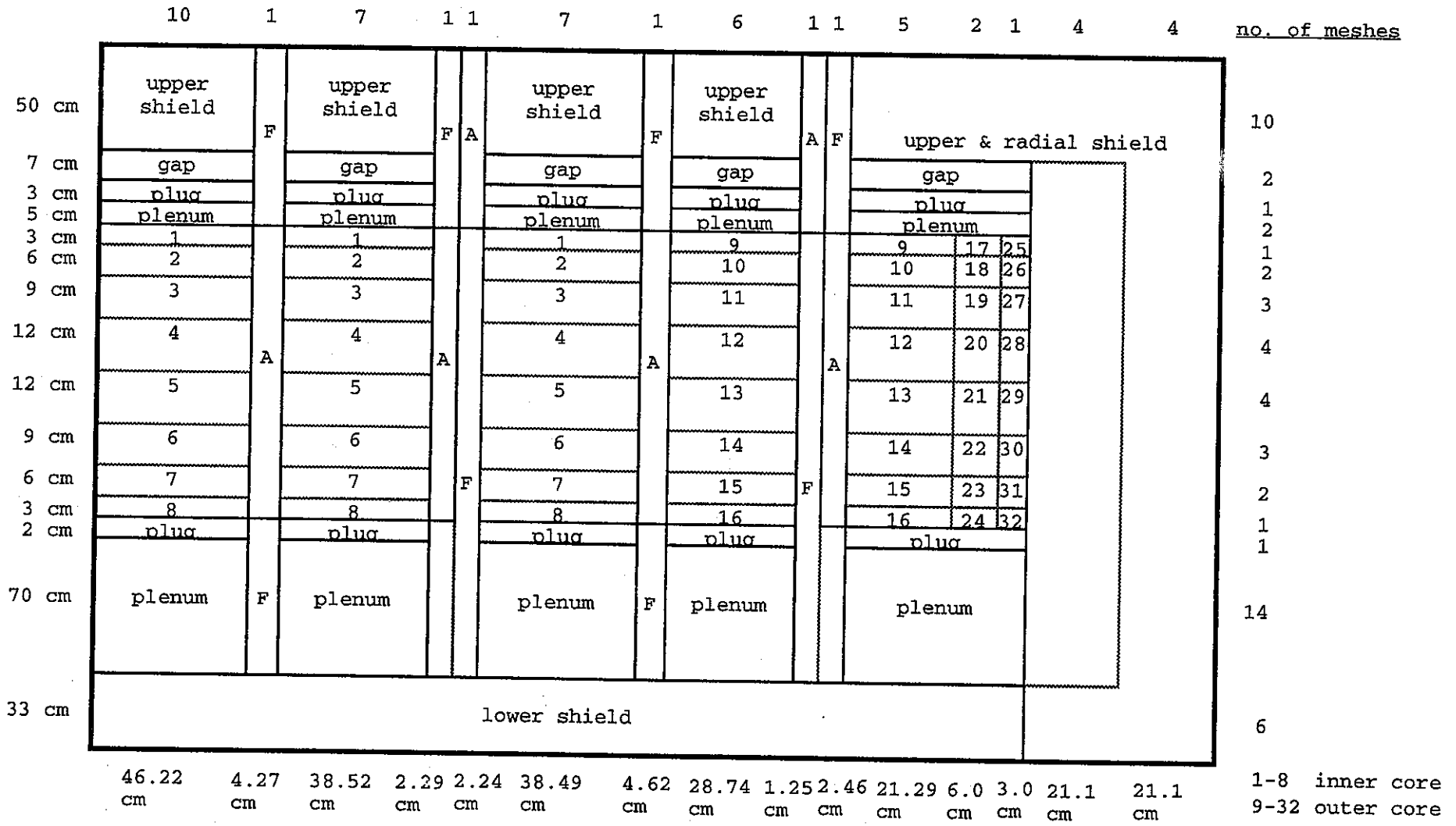


Figure 6.3 2D mesh representation for optimized calculations

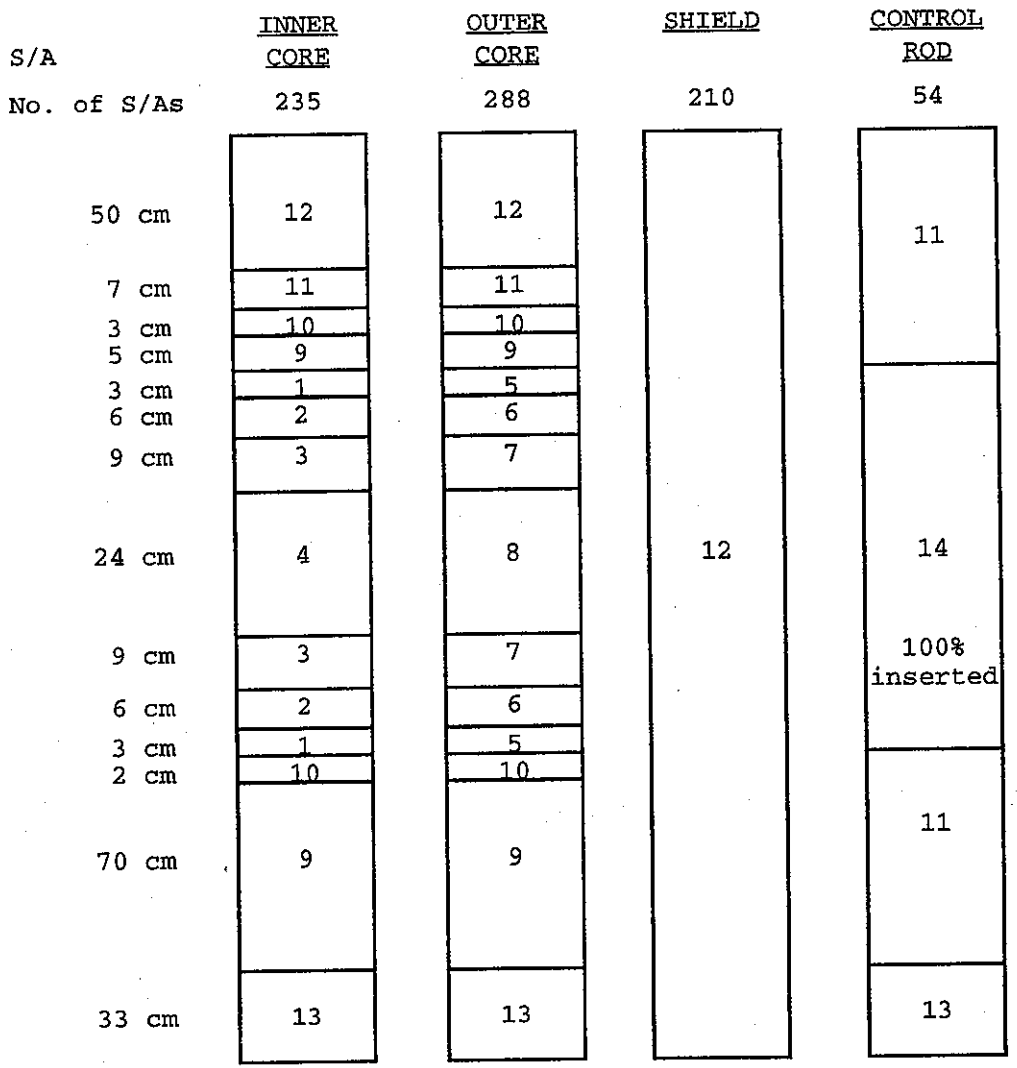


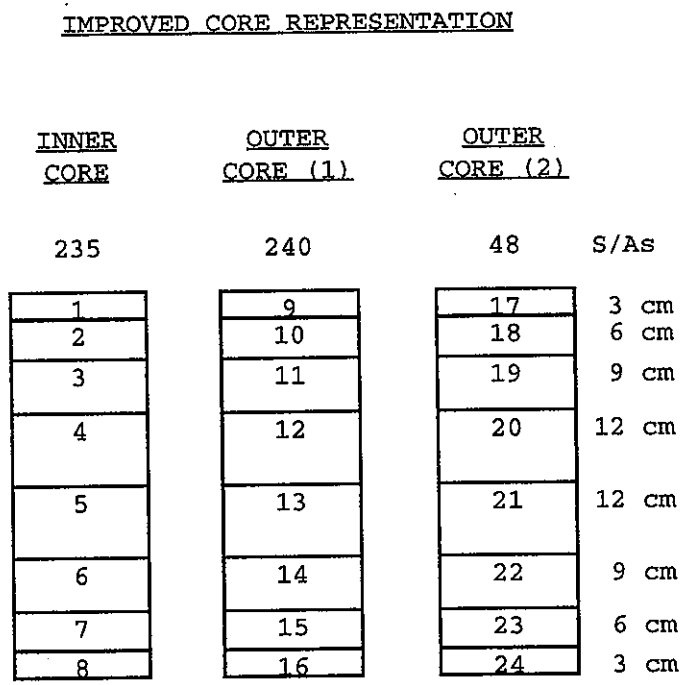


Materials (original representation)

| | | | |
|---|---|---|---|
| 1-4 | inner fuel | 11 | gap/follower |
| 5-8 | outer fuel | 12 | upper/radial shield |
| 9 | plenum | 13 | lower shield |
| 10 | plug | 14 | rod absorber |

Figure 6.4 Axial mesh representations for optimized MOSES rod worth calculations

# 7 OPTIMIZED DESIGN - CALCULATIONS

The calculations to produce an optimized core design are readily described in 3 stages, as represented by the following Sub-sections. First are preliminary scoping calculations using the modified calculational route, to confirm values for parameters common to the different Pu vectors - primarily the fuel pin size. For each of the extreme Pu vector, there are calculations to identify an optimized condition, demonstrating that margins to safety criteria exist providing for design flexibility; each optimized condition is examined in detail.

## 7.1 PRELIMINARY CALCULATIONS

The main aim of the initial calculations was to define the fuel pin size to be adopted. The sensitivity study calculations for low quality Pu had identified two workable minimum pin sizes - 150% and 200% of the reference design value - depending on the diluent material adopted for use with that Pu vector. The increase in peak pin ratings associated with the use of the more accurate 3D MOSES burn-up calculations (see below) effectively precludes the viability of the 200% pin size option, since peak ratings were already marginal for this pin size. As a result, the low quality Pu options were restricted to ZrH as diluent. The changes to above/below core structure and absorber rod modelling required an increase in fuel inventory by around 10% in order for criticality to be maintained without reducing cycle lengths.

The minimum effective pin size was expected to be in the range 160 - 170%. Table 7.1 shows the results of cases that were examined to identify an optimum pin size. The first 2 cases were for low quality Pu, using ZrH diluent. As with the optimized low quality Pu calculations, a uniform Pu enrichment was used, with diluent fraction being used to control the inner:outer zone rating ratio (the balance that is sought is of 'type A' ratings, effectively balancing channel powers).

The first case of Table 7.1 was for a pin size of 170% with a cycle length of 12 months. The peak pin ratings are acceptably low,

a maximum of 337 W/cm ('type B') and the safety parameters are within the limits adopted for the study (though the Na void worth is fairly high at 2.02%Δk/kk'). The PCR shutdown margin is negative, but this should be rectified by reducing the cycle length to around 9 months. Of some concern is the BCR shutdown margin, which though positive is rather small.

The second case in Table 7.1 has the pin size reduced to 165% and the cycle length reduced to 9 months. As can be seen, these changes are sufficient to increase the shutdown margins to an acceptable level (there is sufficient PCR margin to allow a cycle somewhat longer than 9 months). The safety parameters are improved over the previous case - Na void worth reduces to 1.81%Δk/kk' - but there is a notable increase in peak pin rating to 366 W/cm.

Considering the above results in the light of Figure 2.3 from the sensitivity study, it was concluded that 165% was the most suitable pin size as far as the low quality Pu was concerned. Any higher size would bring BCR margins that were too small to be acceptable, whilst any smaller pin size would prejudice the capability to maximize cycle length without producing unacceptable safety parameters. The high peak pin rating corresponds to the limit of acceptable values, taking into account the expected effects of more detailed 3D burn-up calculations (see below).

The third case in Table 7.1 is for the high quality Pu vector, a calculation intended to demonstrate that the 165% pin size will also be acceptable for this second extreme Pu composition. With this Pu vector there is a greater scope for optimizing core conditions, represented by the relative fractions of ZrH, $B_4C$ and void (hollow pellets) comprising the diluent. Table 7.1 shows a single case, the hollow pellet bore was set at 45% of the pellet diameter, with 16 pins of ZrH and 12 pins of $B_4C$ (30% $^{10}B$ enrichment), for a 6 month cycle. The results show good shutdown margins, indicating that a cycle length significantly longer than 6 months should be possible. The peak pin rating is 358 W/cm, similar to the low quality Pu case for the same pin size. Whilst the safety parameters are outside targets, this would be readily corrected by adjusting the diluent composition - Figure 2.2 from the sensitivity study indicates that

this would only result in a small decrease in the ample PCR shutdown margin.

A 3D MOSES burn-up calculation was done for the high quality Pu case from Table 7.1, to determine the magnitude of the difference in peak pin ratings between 2D and 3D calculations, and hence an effective pin rating limit appropriate to 2D calculations. In the 3D calculation, no attempt was made to modify the BOC rod insertions to balance the rating distribution, a uniform 50% insertion was used. Table 7.2 shows the peak pin ratings produced by the 3D burn-up calculation; the maximum values are 403.1 W/cm at BOC and 390.0 W/cm at EOC, these are 16.7% and 13.0% higher than the equivalent values in the 2D burn-up PENCIL calculation. It was concluded that a peak rating limit of 380-365 W/cm should be adopted for the 2D calculations used to identify the optimized core conditions, to ensure that the more accurate 3D calculations do not exceed the 430 W/cm rating limit.

The initial calculations identified 165% as the most appropriate pin size to use. It was confirmed that the rod distribution option VII provided adequate BCR shutdown margins, and that PCR shutdown margins would be acceptable with cycle lengths in the region of 9 months. The effect of the 3D burn-up calculations on peak ratings was to effectively reduce the rating limit for 2D calculations to ~365 W/cm (the limit should not apply to imbalanced BOC ratings, since the 3D calculations will use PCR insertions to bring those into balance).

## 7.2 LOW QUALITY Pu VECTOR

In this Sub-section are presented a series of calculations used to identify the most suitable conditions for the optimized core with the low quality Pu vector. There is then a full set of calculations for the identified optimized condition. A 165% fuel pin size was used, as identified in Sub-section 7.1.

The first step was to condense a 7 group nuclear dataset for conditions not too dissimilar from what will be the final optimized

design. A case with a 6 month cycle and 31/4 ZrH diluent pins was used.

A series of 2D PENCIL burn-up calculations were done, varying the cycle length over the range 9 to 12 months, and with ZrH diluent fractions chosen to give appropriate values of Keff. Since in all cases the difficulty was to reduce the inner zone rating sufficiently to produce a balanced distribution, all cases used a zero diluent fraction for the outer enrichment zone. A small number of 70 group reactivity calculations demonstrated that in order for the 70 group EOC Keff to achieve the target of 1.0048, then the target for the equivalent 7 group PENCIL value should be approximately in the range 1.012 to 1.016.

Table 7.3 shows the key results of the PENCIL burn-up calculations. Note that the unbalanced BOC ratings are not significant, since these would be controlled by PCR insertions (as in the 3D MOSES burn-up calculation of the final optimized case). The following conclusions were drawn. Whatever the cycle length, there were difficulties over providing sufficient inner zone diluent to produce balanced channel powers (i.e. balanced 'type A' ratings) at EOC. For the shorter cycle lengths, ~9 months, the amount of diluent required to achieve criticality targets is at its largest, this restricts the number of fuelled pins and thus results in 'type B' pin ratings approaching the 365 W/cm limit identified in Sub-section 7.1. For longer cycle lengths, around 12 months, the amount of diluent that produces target criticalities is insufficient to produce balanced EOC ratings - this imbalance results in peak 'type B' ratings that again approach the 365 W/cm limit. A cycle length of 10.5 months was identified as the longest that was compatible with approximately balanced EOC ratings ('type A' values within 15 W/cm) and thus providing a reasonable margin to ('type B') peak pin rating limits.

Calculations of safety parameters and rod group worths were done for 3 of the cases from Table 7.3, including the 10.5 month cycle case; the results are shown in Table 7.4. For a 10.5 month cycle length, the shutdown margins for both PCR and BCR are seen to be reasonable, with safety parameters within criteria (though Na void worth is high at 2.01%$\Delta$k/kk').

The case with a 10.5 month cycle and 21/0 ZrH diluent pins was identified as the most suitable to use for the low quality Pu final optimized case. New 7 and 18 group nuclear datasets were condensed using this case. An 18 group 2D PENCIL burn-up calculation, followed by 70 group CITATION calculations, produced a 70 group EOC Keff of 1.00436. An adjustment was made to bring this Keff closer to the 1.0048 target: the Pu enrichment was increased from 45% to 45.05%. Using the adjusted Pu enrichment, a complete series of calculations was carried out for the optimized condition.

Table 7.5 provides a summary of the results of the calculations for the final optimized condition, it includes the equivalent case for the high quality Pu vector. A full set of calculations was carried out: first an 18 group 2D PENCIL burn-up calculation, then 70 group 2D CITATION reactivity calculations, a mass balance calculation, various PERKY perturbation calculations, 7 group 3D MOSES calculations of rod group worths (including calculations of core expansion factors), and finally a 7 group 3D MOSES burn-up calculation. The main points to note in the results are: all safety parameters are within targets, though Na void worth is high at 2.01%$\Delta$k/kk', so is the Doppler constant at -0.00821; good shutdown margins are demonstrated of 0.55%$\Delta$k/kk' and 0.36%$\Delta$k/kk' for PCRs and BCRs respectively; although the peak (3D) rating of 417 W/cm is as much as 24% higher than the value from the 2D calculation, there is an acceptable margin to the 430 W/cm limit.

Table 7.6 shows the peak pin ratings for each timestep in the 3D MOSES burn-up calculation. The small differences between cycles 5 and 9 demonstrate that the calculation had essentially achieved fuel cycle equilibrium. The variation in BOC Keff between different refuelling batches, 0.17%, is a result of small differences in the number of channels refuelled, varying between 129 and 133 (in practise these should instead lead to minor variations in cycle length - the effect is not significant). Channel power distributions for the 4 batches are shown in Figures 7.1 to 7.4 for BOC conditions and Figures 7.5 to 7.8 for EOC.

To enable balanced BOC ratings to be produced in the 3D MOSES burn-up calculation, PCR insertions were used that varied with rod position, PCRs being considered as 4 different rings. The effect of

rod insertion pattern was examined using 2D CITATION calculations, then using 3D MOSES snapshot calculations, and finally using the 3D MOSES burn-up calculation itself. The effect of rod insertions on rating distribution differed somewhat between these 3 types of calculation, hence the use of 3D burn-up calculations to finally identify a suitable rod distribution. Figure 7.9 shows radial rating distributions from 2D calculations: they clearly show the need to reduce core centre ratings (exacerbated by the insertion of absorber rods), which can be achieved by inserting the inner PCR ring ~20% more than the rest. Steady-state 3D calculations showed two distinct rating peaks, at the core centre and around the innermost BCRs, both in the inner enrichment zone; as shown in Figure 7.10, a 10% extra insertion of the inner PCRs sufficed to balance peak channel ratings. Examining the peak pin ratings for the 3D burn-up calculation, it was found that to produce a balance between the 2 above mentioned peak areas a rather larger difference in rod insertions was required - the final BOC rod insertion used was 75% for the innermost ring and 50% for all others.

## 7.3 HIGH QUALITY Pu VECTOR

In this Sub-section are presented a series of calculations used to identify the most suitable conditions for the optimized core with the high quality Pu vector. There is then a full set of calculations for the identified optimized condition. A 165% fuel pin size was used, as identified in Sub-section 7.1.

It was decided to fix the pellet bore at 45%, and the diluent $^{10}B$ enrichment at 30%. The high bore value ensures a low diluent fraction, and hence minimizes peak pin ratings. The $^{10}B$ enrichment is low enough to correspond to a practical level of $^{10}B$ enrichment when unmodelled heterogeneity effects are allowed for.

The first step was to condense a 7 group nuclear dataset for conditions not too dissimilar from what will be the final optimized design. A case with a 12 month cycle and hollow pellets of 45% bore with 16 ZrH and 12 $B_4C$ (30% $^{10}B$) diluent pins was used.

A series of 2D PENCIL burn-up calculations were done, along with the associated 70 group reactivity calculations and rod group worth calculations. The cycle length was varied over the range 10 to 12 months, along with variations in the ratio of ZrH to $B_4C$ diluent. The PENCIL calculations used a Keff target of 1.0089, with Pu enrichments adjusted by PENCIL to meet the target (the corresponding 70 group Keff values varied between 1.004 and 1.009). The total numbers of diluent pins were chosen to result in peak Pu enrichments close to the 45% limit. The rod worth calculations used a fixed thermal expansion reactivity factor of 0.6%$\Delta$k/kk', taken from the high quality Pu case in Table 7.1.

Table 7.7 shows the results of the various calculations. The void-to-Doppler ratio safety parameter is seen to be a function of the number of $B_4C$ diluent pins; to ensure that the safety parameter target is met, there should be less than 10 $B_4C$ diluent pins. In some of the cases the shutdown margins are not met; increasing the number of $B_4C$ diluent pins improves the shutdown margins, for the PCRs the shutdown margin is also improved by reducing the cycle length. At least 6 $B_4C$ diluent pins are required to ensure that there is a reasonable BCR shutdown margin. It was decided that the final optimized case should use 8 $B_4C$ diluent pins - anything less would unnecessarily shorten the cycle length required to produce an acceptable PCR shutdown margin. The peak pin ratings (ignoring imbalanced BOC values, which will be offset by differential PCR insertions in the 3D burn-up calculations) remain below the 365 W/cm limit identified in Sub-section 7.1, provided that the total number of diluent pins remains below ~40.

It was estimated that a cycle length of 9.75 months would be short enough to give an adequate PCR shutdown margin with 8 $B_4C$ diluent pins, and that in addition 23 ZrH diluent pins would result in the reactivity target being achieved with a peak Pu enrichment closest to 45%. New 7 and 18 group nuclear datasets were condensed using this case. An 18 group 2D PENCIL burn-up calculation produced a peak Pu enrichment of 44.76%. An adjustment was made to bring this Pu enrichment closer to the 45% target: the number of ZrH diluent pins was increased from 23 to 24. Using the adjusted diluent

fraction, a complete series of calculations was carried out for the optimized condition.

Table 7.5 provides a summary of the results of the calculations for the final optimized condition, it also includes the equivalent case for the low quality Pu vector. A full set of calculations was carried out: first an 18 group 2D PENCIL burn-up calculation, then 70 group 2D CITATION reactivity calculations, a mass balance calculation, various PERKY perturbation calculations, 7 group 3D MOSES calculations of rod group worths (including calculations of core expansion factors), and finally a 7 group 3D MOSES burn-up calculation. The key points of the results are: safety parameters well within targets, with a Na void worth of only 0.822%$\Delta$k/kk' and a Doppler constant of -0.00499; there is a good BCR shutdown margin of 0.67%$\Delta$k/kk', that for PCRs is just sufficient at 0.14%$\Delta$k/kk'; the peak pin rating of 428 W/cm is only just below the 430 W/cm rating limit.

Table 7.8 shows the peak pin ratings for each timestep in the 3D MOSES burn-up calculation. As with the low quality Pu case (Sub-section 7.2), the transient produces a good approximation to fuel cycle equilibrium, and the Keff variations between refuelling batches are consistent with the variation in numbers of channels refuelled. Unlike the low quality Pu case, there were significant variations in peak pin ratings between the different refuelling batches: this made it necessary to adopt different BOC PCR insertions for different batches - the inner PCR ring varied between 55% and 65% inserted, with the remainder fixed at 50% in. Channel power distributions for the 4 batches are shown in Figures 7.11 to 7.14 for BOC conditions and Figures 7.15 to 7.18 for EOC.

## 7.4 MARGINS TO LIMITS

For both the extreme Pu vectors examined in the previous two Sub-sections, it proved possible to produce a design which resulted in the values of key parameters - peak pin rating, shutdown margins and safety parameters (represented by the void-to-Doppler ratio) - that were within limits. A reasonable margin to limits was

demonstrated for at least one parameter; shutdown margin for low quality Pu and void-to-Doppler ratio for high quality Pu. The final optimized conditions are each representative of a set of similar conditions, all of which would give acceptable results.

The final calculations were optimized for the calculation route used in this study. The use of yet more detailed/accurate methods may lead to some variation in the calculated core characteristics: thus there may be some need for further adjustment of the optimized conditions.

The diluent fraction is used to ensure criticality with a peak (45%) Pu enrichment. For the high quality Pu case the diluent composition can be varied to ensure a good balance between the safety parameters and shutdown margins; however, only a very restricted range of compositions is possible, since the balance between these parameters is very sensitive to small changes in the absorber diluent fraction. After diluent parameters are set, the cycle length and pin size are used to define the optimized core condition.

Any shortfall in PCR shutdown margin could be offset by a small reduction in cycle length. Reducing the fuel pin size would have the effect of both reducing pin ratings and improving shutdown margins. For the low quality Pu case the margin for adjusting either of these parameters is limited. Cycle length has only a restricted range before either the diluent fraction increases or an inner-outer zone imbalance is caused, both increase the peak rating. A reduction in pin size of at most a few percent is all that would be possible before difficulties are encountered with the inner-outer zone rating balance.

In addition to the above, there are other parameters which could be used to optimize core conditions. A comparatively small increase in core height (~10-20%) could be beneficial: the proportionate decrease in pin ratings may well be more significant than the associated increase in Na void worth. A reduction in peak Pu enrichment below 45% would reduce the diluent fraction required, thus reducing pin ratings. Neither of these options were considered in the current study: they were not found to be necessary, and were therefore not used since they represent respectively a departure

from the reference core design and a reduction in the rate of Pu burning.

Table 7.1 Cases identifying the most suitable pin size for the optimized calculations

| Pu Quality | low | low | high |
|---|---|---|---|
| Pu Enrichment (%) | 45/45 | 45/45 | 37.96/44.03 |
| Pin Size (%) | 170 | 165 | 165 |
| Diluent Material(s) | ZrH | ZrH | ZrH & $B_4C$ |
| Diluent Fraction (pins) | 22 / 0 | 30 / 0 | 16 & 12 |
| Pellet Bore (%) | (solid) | (solid) | 45 |
| Cycle Length (months) | 12 | 9 | 6 |
| Na Void Worth (%Δk/kk') | 2.021 | 1.811 | 1.141 |
| Doppler Constant | -0.00812 | -0.00912 | -0.00294 |
| Void:Doppler ratio | -249 | -199 | -388 |
| Peak Pin Rating (BOC) | 337 / 290 | 366 / 284 | 358 / 345 |
| ('type B') (W/cm) (EOC) | 327 / 295 | 355 / 291 | 346 / 345 |
| Shutdown Margin (PCR) | -1.49 | +1.10 | +3.50 |
| (%Δk/kk') (BCR) | +0.05 | +0.22 | +0.99 |

Table 7.2 3D burn-up peak pin ratings: high quality Pu, 165% pin size, 6 month cycle, hollow pellets, 16/12 pins ZrH/$B_4C$ diluent

| Irradiation Cycle | Time in Cycle | Peak Pin Rating ('type B') | |
|---|---|---|---|
| | | inner core | outer core |
| 6 | BOC | 389.9 | 392.6 |
| | MOC | 367.2 | 392.3 |
| | EOC | 364.8 | 388.9 |
| 7 | BOC | 387.0 | 397.4 |
| | MOC | 363.9 | 380.8 |
| | EOC | 361.5 | 378.0 |
| 8 | BOC | 370.7 | 403.1 |
| | MOC | 357.2 | 393.7 |
| | EOC | 355.3 | 390.0 |
| 9 | BOC | 382.9 | 399.1 |
| | MOC | 360.9 | 385.0 |
| | EOC | 358.8 | 381.9 |
| 2D values | BOC | 358 | 345 |
| | EOC | 346 | 345 |

Table 7.3 Low quality Pu, optimized calculations: rating and Keff variation with cycle length and ZrH diluent fraction

| Cycle Length (months) | Diluent Fraction (inner/outer) (pins) | EOC Keff (7 group) | Peak Pin Rating (inner/outer core) (W/cm) | | |
|---|---|---|---|---|---|
| | | | 'type A' EOC | 'type B' BOC | 'type B' EOC |
| 9 | 30 / 0 | 1.01271 | 307/294 | 362/289 | 356/294 |
| 9 | 34 / 0 | 1.00557 | 310/297 | 373/292 | 368/297 |
| 9.5 | 27 / 0 | 1.01317 | 304/292 | 355/286 | 347/292 |
| 9.5 | 28 / 0 | 1.01117 | 305/293 | 357/287 | 350/293 |
| 10.5 | 21 / 0 | 1.01573 | 301/288 | 385/280 | 334/288 |
| 11 | 19 / 0 | 1.01534 | 310/287 | 395/278 | 340/287 |
| 11 | 21 / 0 | 1.01043 | 298/288 | 383/280 | 330/288 |
| 12 | 12 / 0 | 1.02448 | 350/282 | 434/271 | 371/282 |
| 12 | 16 / 0 | 1.01273 | 323/285 | 408/276 | 348/285 |
| 12 | 22 / 0 | 0.99761 | 297/290 | 372/282 | 330/290 |

Table 7.4 Low quality Pu, optimized calculations: shutdown margin and safety parameter variation with cycle length

| Cycle Length (months) | 9 | 9.5 | 10.5 |
|---|---|---|---|
| ZrH Fraction (pins) | 34 / 0 | 27 / 0 | 21 / 0 |
| EOC Keff (7 group) | 1.00557 | 1.01317 | 1.01573 |
| (70 group) | 0.99830 | 1.00457 | 1.00446 |
| Na Void (%Δk/kk') | 1.762 | 1.877 | 2.009 |
| Doppler Constant | -0.00964 | -0.00919 | -0.00830 |
| Void:Doppler ratio | -183 | -204 | -242 |
| Shutdown Margin (PCR) | +0.56 | +0.77 | +0.57 |
| (%Δk/kk') (BCR) | +0.08 | +0.23 | +0.40 |

Table 7.5 Final optimized cases - general results

| Pu Vector | | Low quality Pu | High quality Pu |
|---|---|---|---|
| Pu Enrichment (inner/outer) (%) | | 45.05/45.05 | 40.25/45.03 |
| Diluent Material | | ZrH | ZrH & $B_4C$ (30% $^{10}B$) |
| Diluent Fraction (in/out) (pins) | | 21 / 0 | 24 / 8 |
| Pellet Type | | Solid | Hollow (45% bore) |
| Fuel Cycle | | 4 * 10.5 months | 4 * 9.75 months |
| 18 group 2D burn-up | | | |
| EOC Keff | | 1.00629 | 1.00317 |
| Reactivity Loss/Cycle (%Δk/kk') | | 4.509 | 5.124 |
| Peak Pin Rating ('type A') (W/cm) | (BOC) | 356.6 / 281.0 | 332.6 / 293.3 |
| | (EOC) | 303.3 / 290.1 | 296.9 / 297.3 |
| Peak Pin Rating ('type B') (W/cm) | (BOC) | 394.8 / 281.0 | 390.2 / 344.1 |
| | (EOC) | 335.8 / 290.1 | 348.2 / 349.1 |
| Average Irradiation (GWd/te) | | 116.9 | 152.8 |
| 70 group 2D reactivity | | | |
| EOC Keff | | 1.00490 | 1.00455 |
| Reactivity Loss/Cycle (%Δk/kk') | | 4.545 | 4.878 |
| Peak Pin Rating ('type B') (W/cm) | (BOC) | 396.2 / 281.7 | 388.3 / 344.8 |
| | (EOC) | 337.3 / 290.7 | 350.2 / 349.8 |
| Na Void (%Δk/kk') | | 2.013 | 0.822 |
| Doppler Constant | | -0.00821 | -0.00499 |
| Void:Doppler ratio | | -245 | -165 |
| mass balance | | | |
| Pu Burning Rate (kg/TWhe) | (all Pu) | 74.2 | 71.9 |
| | (fissile Pu) | 39.4 | 97.9 |
| perturbation | | | |
| Delayed Neutron Fraction (%) | | 0.3176 | 0.2613 |
| Prompt Neutron Lifetime (sx$10^{-6}$) | | 0.5432 | 0.6220 |
| Safety | V/D.τ | -451 | -265 |
| Comparators | β/D.τ | -71 | -84 |
| Na Void Components (% of total) | fission | -10.1 | -36.2 |
| | capture | +22.4 | +73.9 |
| | scatter | +168.7 | +262.0 |
| | leakage | -81.0 | -199.7 |
| Doppler Main Isotopes (% of total) | $^{239}Pu$ | -11.1 | -56.2 |
| | $^{240}Pu$ | +31.4 | +13.6 |
| | $^{242}Pu$ | +6.0 | - |
| | $^{238}U$ | +73.5 | +147.7 |
| | $^{10}B$ | n/a | -5.5 |
| rod group worths (3D) | | | |
| Reactivity Loss/Cycle (%Δk/kk') | | 4.548 | 4.878 |
| Temperature Effect (%Δk/kk') | (nuc. data) | 0.947 | 0.519 |
| | (expansion) | 0.465 | 0.491 |
| Shutdown Requirements (%Δk/kk') | (PCR) | 7.777 | 7.785 |
| | (BCR) | 1.852 | 1.450 |
| Rod Group Worth (%Δk/kk') | (PCR) | 8.328 | 7.905 |
| | (BCR) | 2.215 | 2.117 |
| Fraction of Requirements | (PCR) | 1.071 | 1.018 |
| | (BCR) | 1.196 | 1.460 |
| Shutdown Margins (%Δk/kk') | (PCR) | +0.551 | +0.138 |
| | (BCR) | +0.363 | +0.667 |
| 7 group 3D burn-up | | | |
| Peak Pin Rating (W/cm) | | 416.9 | 428.0 |
| Peak Pin Irradiation (GWd/te) | | 171.9 | 195.6 |

Table 7.6 3D burn-up peak pin ratings: low quality Pu, final optimized case

| Irradiation Cycle | Time in Cycle | Keff | Inner Core | | Outer Core | |
|---|---|---|---|---|---|---|
| | | | Peak Rating (B) (W/cm) | Pos'n (S/A) | Peak Rating (B) (W/cm) | Pos'n (S/A) |
| 1 | BOC | 1.06580 | | | | |
| | MOC | 1.10341 | | | | |
| | EOC | 1.07843 | | | | |
| 2 | BOC | 1.02976 | | | | |
| | MOC | 1.06616 | | | | |
| | EOC | 1.04246 | | | | |
| 3 | BOC | 1.00685 | | | | |
| | MOC | 1.04239 | | | | |
| | EOC | 1.01925 | | | | |
| 4 | BOC | 0.99715 | 415.0 | 67 | 339.4 | 107 |
| | MOC | 1.03221 | 394.4 | 5 | 320.4 | 107 |
| | EOC | 1.00920 | 389.2 | 5 | 317.5 | 107 |
| 5 | BOC | 0.99553 | 413.2 | 44 | 326.2 | 117 |
| | MOC | 1.03020 | 402.5 | 2 | 312.5 | 110 |
| | EOC | 1.00724 | 396.7 | 2 | 310.2 | 110 |
| 6 | BOC | 0.99423 | 411.9 | 1 | 329.9 | 94 |
| | MOC | 1.03002 | 413.3 | 1 | 317.7 | 94 |
| | EOC | 1.00696 | 406.2 | 1 | 315.1 | 94 |
| 7 | BOC | 0.99344 | 408.8 | 3 | 320.5 | 118 |
| | MOC | 1.02871 | 411.0 | 3 | 311.3 | 101 |
| | EOC | 1.00576 | 404.4 | 3 | 309.2 | 101 |
| 8 | BOC | 0.99508 | 416.9 | 67 | 340.2 | 107 |
| | MOC | 1.03009 | 397.9 | 7 | 321.1 | 107 |
| | EOC | 1.00706 | 392.4 | 7 | 318.3 | 107 |
| 9 | BOC | 0.99471 | 413.7 | 44 | 327.0 | 117 |
| | MOC | 1.02933 | 401.9 | 2 | 313.0 | 110 |
| | EOC | 1.00638 | 396.1 | 2 | 310.7 | 110 |

Table 7.7 High quality Pu, optimized calculations: effect of varying cycle length and ZrH & $B_4C$ diluent fractions

| Cycle Length (months) | 12 | 11 | 11 | 11 | 10 | 10 |
|---|---|---|---|---|---|---|
| Diluent Fraction $ZrH/B_4C$ (pins) | 16 / 12 | 14 / 10 | 26 / 6 | 36 / 4 | 22 / 8 | 29 / 6 |
| Pu Enrichments (%) | 40.68/45.82 | 40.00/45.06 | 40.90/44.97 | 42.46/45.06 | 40.11/45.08 | 40.54/44.97 |
| EOC Keff (70 gp) | 0.98726 | 1.00597 | 1.00930 | 1.00642 | 1.00911 | 1.00885 |
| (7 gp) | 0.99137 | 1.00888 | 1.00890 | 1.00892 | 1.00892 | 1.00905 |
| Na void (%Δk/kk') | 1.323 | 1.113 | 0.675 | 0.497 | 0.825 | 0.625 |
| Doppler | -0.00280 | -0.00360 | -0.00615 | -0.00775 | -0.00496 | -0.00638 |
| Void:Doppler ratio | -473 | -308 | -110 | -64 | -166 | -98 |
| Peak Pin Rating (BOC) | 365.6/332.0 | 368.5/331.2 | 402.6/340.2 | 451.6/347.5 | 381.2/341.6 | 402.2/348.0 |
| (B) (W/cm) (EOC) | 332.1/334.4 | 334.2/334.1 | 347.2/347.0 | 361.6/361.0 | 345.4/344.8 | 354.1/353.5 |
| Shutdown Margin (PCR) | +0.025 | +0.275 | -1.367 | -2.952 | +0.012 | -0.967 |
| (%Δk/kk') (BCR) | +1.064 | +0.870 | +0.353 | -0.052 | +0.550 | +0.248 |

Table 7.8 3D burn-up peak pin ratings: high quality Pu, final optimized case

| Irradiation Cycle | Time in Cycle | Keff | Inner Core | | Outer Core | |
|---|---|---|---|---|---|---|
| | | | Peak Rating (B) (W/cm) | Pos'n (S/A) | Peak Rating (B) (W/cm) | Pos'n (S/A) |
| 1 | BOC | 1.08013 | | | | |
| | MOC | 1.11054 | | | | |
| | EOC | 1.08464 | | | | |
| 2 | BOC | 1.04183 * | | | | |
| | MOC | 1.07133 * | | | | |
| | EOC | 1.04518 | | | | |
| 3 | BOC | 1.01736 | | | | |
| | MOC | 1.04475 | | | | |
| | EOC | 1.01842 | | | | |
| 4 | BOC | 1.00677 @ | 417.4 | 7 | 421.3 | 97 |
| | MOC | 1.03229 @ | 404.0 | 7 | 404.7 | 105 |
| | EOC | 1.00578 | 398.0 | 7 | 399.1 | 105 |
| 5 | BOC | 1.00318 | 415.5 | 2 | 419.2 | 117 |
| | MOC | 1.02953 | 411.4 | 2 | 394.3 | 110 |
| | EOC | 1.00298 | 405.2 | 2 | 388.9 | 110 |
| 6 | BOC | 1.00044 * | 421.1 | 1 | 415.7 | 96 |
| | MOC | 1.02870 * | 427.5 | 1 | 405.7 | 96 |
| | EOC | 1.00203 | 419.4 | 1 | 400.0 | 96 |
| 7 | BOC | 1.00033 | 428.0 | 3 | 417.5 | 118 |
| | MOC | 1.02718 | 417.2 | 3 | 391.7 | 101 |
| | EOC | 1.00061 | 410.2 | 3 | 387.0 | 101 |
| 8 | BOC | 1.00305 @ | 422.1 | 7 | 424.3 | 97 |
| | MOC | 1.02842 @ | 408.0 | 7 | 407.3 | 105 |
| | EOC | 1.00186 | 401.6 | 7 | 401.6 | 105 |
| 9 | BOC | 1.00161 | 415.4 | 2 | 420.7 | 117 |
| | MOC | 1.02788 | 411.5 | 2 | 395.5 | 110 |
| | EOC | 1.00131 | 405.3 | 2 | 390.1 | 110 |

* PCRs inserted 65/50/50/50%
@ PCRs inserted 55/50/50/50%
all other SOC/MOC cases PCRs 60/50/50/50% inserted

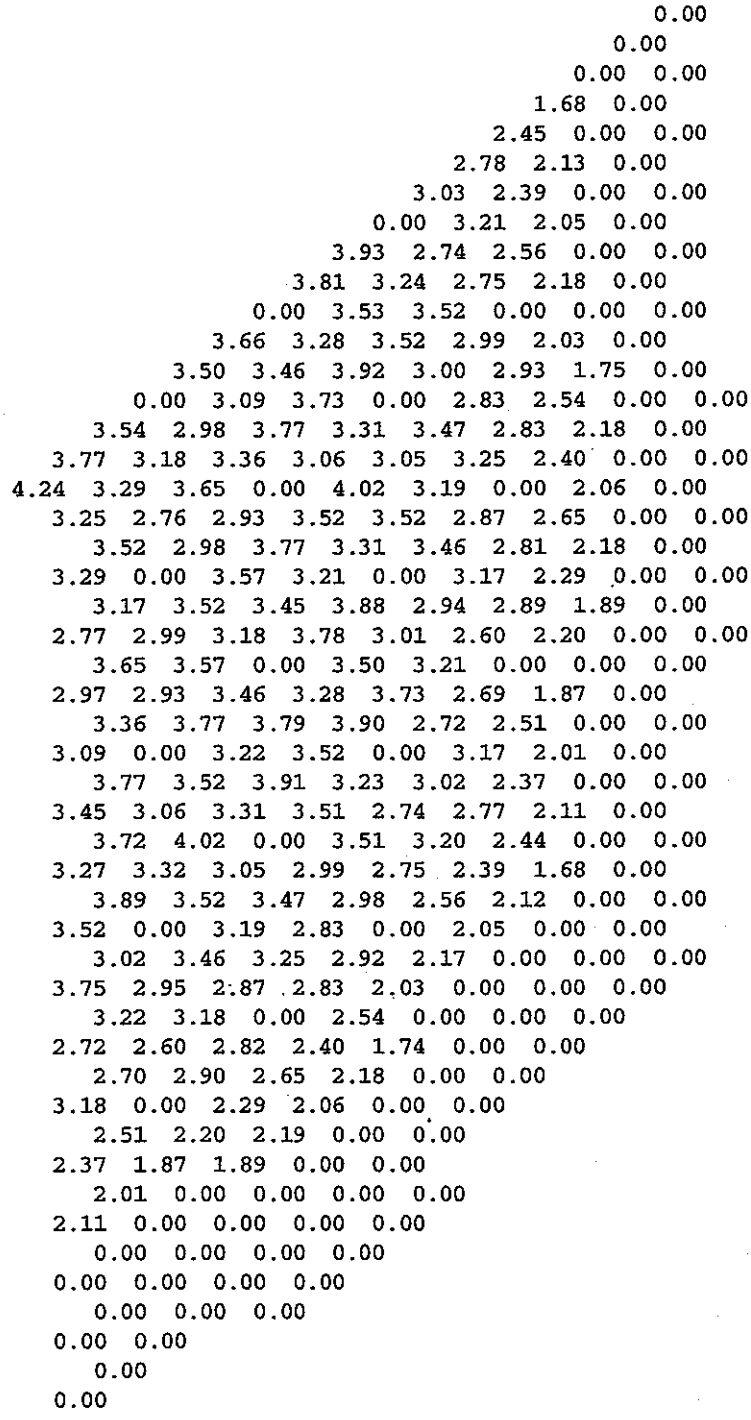


Figure 7.1 Channel power distribution: low quality Pu final optimized case, refuelling batch 1, BOC

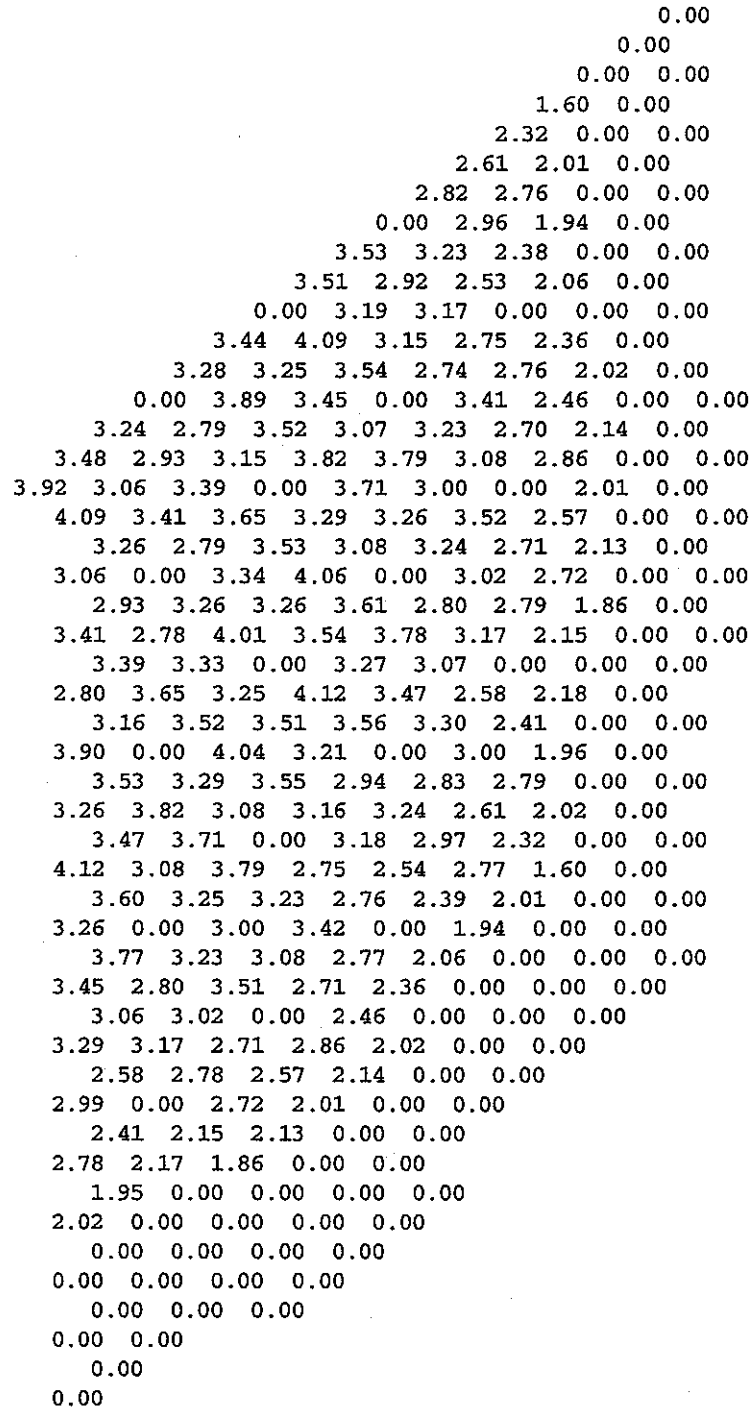


Figure 7.2 Channel power distribution: low quality Pu final optimized case, refuelling batch 2, BOC

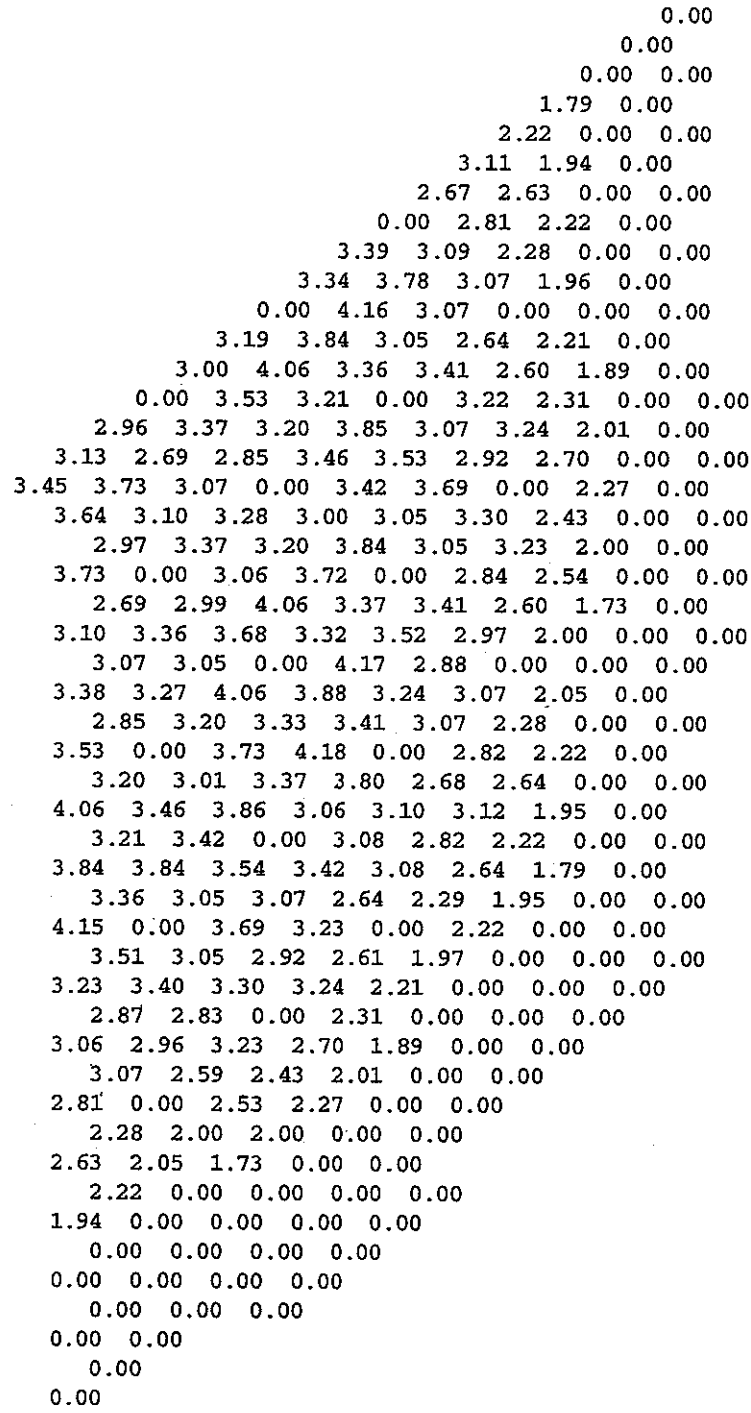


Figure 7.3 Channel power distribution: low quality Pu final optimized case, refuelling batch 3, BOC

```
                                                    0.00
                                                 0.00
                                              0.00  0.00
                                           1.71  0.00
                                        2.55  0.00  0.00
                                     2.91  1.85  0.00
                                  3.18  2.48  0.00  0.00
                               0.00  2.63  2.10  0.00
                            3.09  2.86  2.66  0.00  0.00
                         4.17  3.44  2.87  1.88  0.00
                      0.00  3.80  2.86  0.00  0.00  0.00
                   4.02  3.57  3.77  3.16  2.11  0.00
                2.81  3.78  3.13  3.18  2.48  1.83  0.00
             0.00  3.31  4.05  0.00  3.03  2.72  0.00  0.00
          2.77  3.15  3.02  3.54  2.86  3.08  1.95  0.00
       3.99  3.34  3.58  3.25  3.26  3.56  2.60  0.00  0.00
    3.26  3.46  2.88  0.00  3.18  3.45  0.00  2.21  0.00
       3.40  2.88  3.09  3.77  3.81  3.14  2.91  0.00  0.00
          2.76  3.14  3.02  3.55  2.88  3.09  1.98  0.00
       3.46  0.00  3.86  3.45  0.00  3.47  2.48  0.00  0.00
          3.34  2.83  3.77  3.09  3.18  2.51  2.03  0.00
       2.88  3.16  3.45  4.14  3.20  2.81  2.37  0.00  0.00
          2.88  3.86  0.00  3.74  3.46  0.00  0.00  0.00
       3.13  3.09  3.78  3.55  2.94  2.88  2.00  0.00
          3.57  3.02  4.16  3.07  2.85  2.68  0.00  0.00
       3.30  0.00  3.46  3.78  0.00  2.63  2.12  0.00
          3.02  3.77  3.12  3.42  3.17  2.48  0.00  0.00
       3.78  3.24  3.54  3.76  2.85  2.90  1.85  0.00
          4.04  3.18  0.00  2.85  2.62  2.54  0.00  0.00
       3.55  3.55  3.26  3.17  2.86  2.47  1.71  0.00
          3.10  3.81  2.86  3.16  2.65  1.84  0.00  0.00
       3.76  0.00  3.45  3.03  0.00  2.10  0.00  0.00
          3.21  2.88  3.56  2.48  1.87  0.00  0.00  0.00
       2.96  3.19  3.14  3.07  2.11  0.00  0.00  0.00
          3.47  3.48  0.00  2.71  0.00  0.00  0.00
       2.86  2.82  3.10  2.60  1.83  0.00  0.00
          2.89  2.51  2.91  1.95  0.00  0.00
       2.64  0.00  2.48  2.21  0.00  0.00
          2.68  2.38  1.98  0.00  0.00
       2.49  2.00  2.04  0.00  0.00
          2.13  0.00  0.00  0.00  0.00
       1.86  0.00  0.00  0.00  0.00
          0.00  0.00  0.00  0.00
       0.00  0.00  0.00  0.00
          0.00  0.00  0.00
       0.00  0.00
          0.00
       0.00
```

Figure 7.4 Channel power distribution: low quality Pu final optimized case, refuelling batch 4, BOC

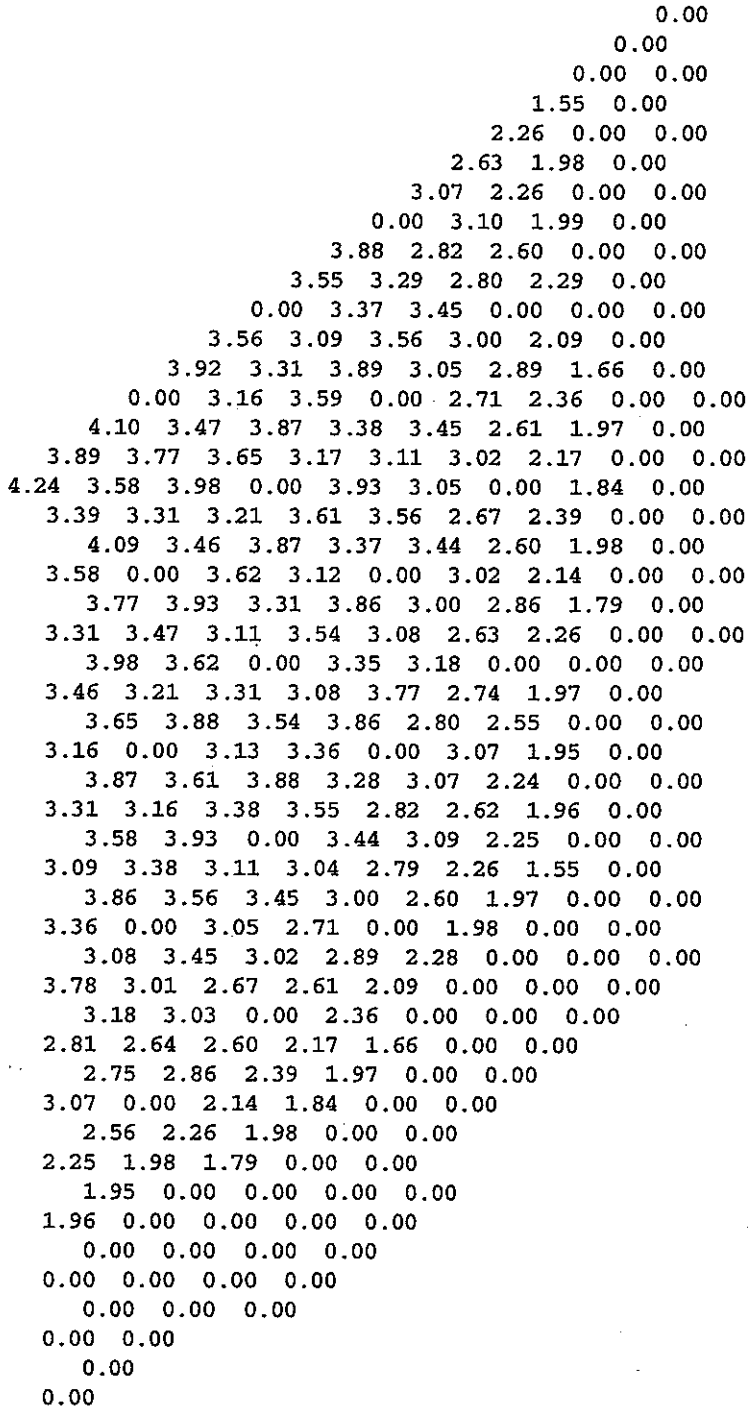


Figure 7.5 Channel power distribution: low quality Pu final optimized case, refuelling batch 1, EOC

```
                                                    0.00
                                                 0.00
                                              0.00  0.00
                                           1.48  0.00
                                        2.15  0.00  0.00
                                     2.48  1.88  0.00
                                  2.89  2.61  0.00  0.00
                               0.00  2.89  1.89  0.00
                            3.54  3.32  2.44  0.00  0.00
                         3.29  3.01  2.60  2.17  0.00
                      0.00  3.08  3.15  0.00  0.00  0.00
                   3.34  3.81  3.23  2.79  2.41  0.00
                3.66  3.11  3.55  2.82  2.74  1.90  0.00
             0.00  3.91  3.34  0.00  3.24  2.29  0.00  0.00
          3.77  3.23  3.62  3.15  3.23  2.50  1.93  0.00
       3.59  3.48  3.42  3.90  3.82  2.86  2.57  0.00  0.00
    3.91  3.32  3.69  0.00  3.65  2.87  0.00  1.80  0.00
       4.18  4.01  3.93  3.39  3.31  3.25  2.32  0.00  0.00
          3.78  3.24  3.63  3.16  3.24  2.51  1.93  0.00
       3.32  0.00  3.39  3.89  0.00  2.89  2.53  0.00  0.00
          3.49  3.64  3.12  3.61  2.87  2.76  1.76  0.00
       4.01  3.23  3.86  3.32  3.82  3.19  2.21  0.00  0.00
          3.69  3.38  0.00  3.14  3.04  0.00  0.00  0.00
       3.24  3.93  3.11  3.82  3.52  2.65  2.29  0.00
          3.42  3.62  3.30  3.56  3.37  2.47  0.00  0.00
       3.91  0.00  3.87  3.09  0.00  2.92  1.91  0.00
          3.63  3.38  3.56  3.02  2.90  2.63  0.00  0.00
       3.12  3.90  3.15  3.24  3.33  2.49  1.89  0.00
          3.35  3.65  0.00  3.16  2.90  2.16  0.00  0.00
       3.83  3.16  3.82  2.83  2.61  2.62  1.49  0.00
          3.60  3.31  3.23  2.80  2.45  1.89  0.00  0.00
       3.13  0.00  2.87  3.25  0.00  1.89  0.00  0.00
          3.81  3.23  2.86  2.74  2.18  0.00  0.00  0.00
       3.50  2.86  3.24  2.50  2.41  0.00  0.00  0.00
          3.03  2.88  0.00  2.29  0.00  0.00  0.00
       3.36  3.18  2.50  2.57  1.91  0.00  0.00
          2.64  2.76  2.32  1.93  0.00  0.00
       2.91  0.00  2.53  1.80  0.00  0.00
          2.46  2.21  1.93  0.00  0.00
       2.63  2.29  1.76  0.00  0.00
          1.90  0.00  0.00  0.00  0.00
       1.89  0.00  0.00  0.00  0.00
          0.00  0.00  0.00  0.00
       0.00  0.00  0.00  0.00
          0.00  0.00  0.00
       0.00  0.00
          0.00
       0.00
```

Figure 7.6 Channel power distribution: low quality Pu final optimized case, refuelling batch 2, EOC

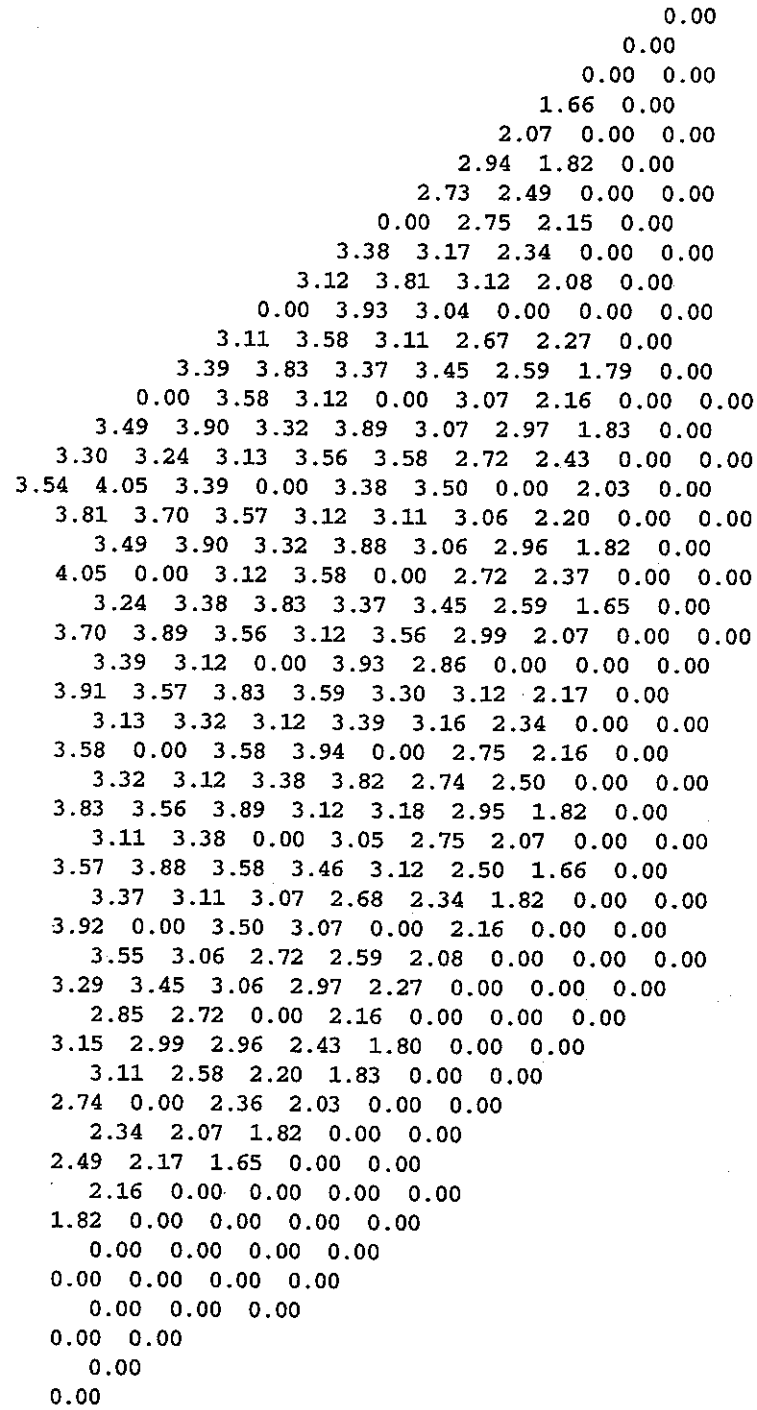


Figure 7.7 Channel power distribution: low quality Pu final optimized case, refuelling batch 3, EOC

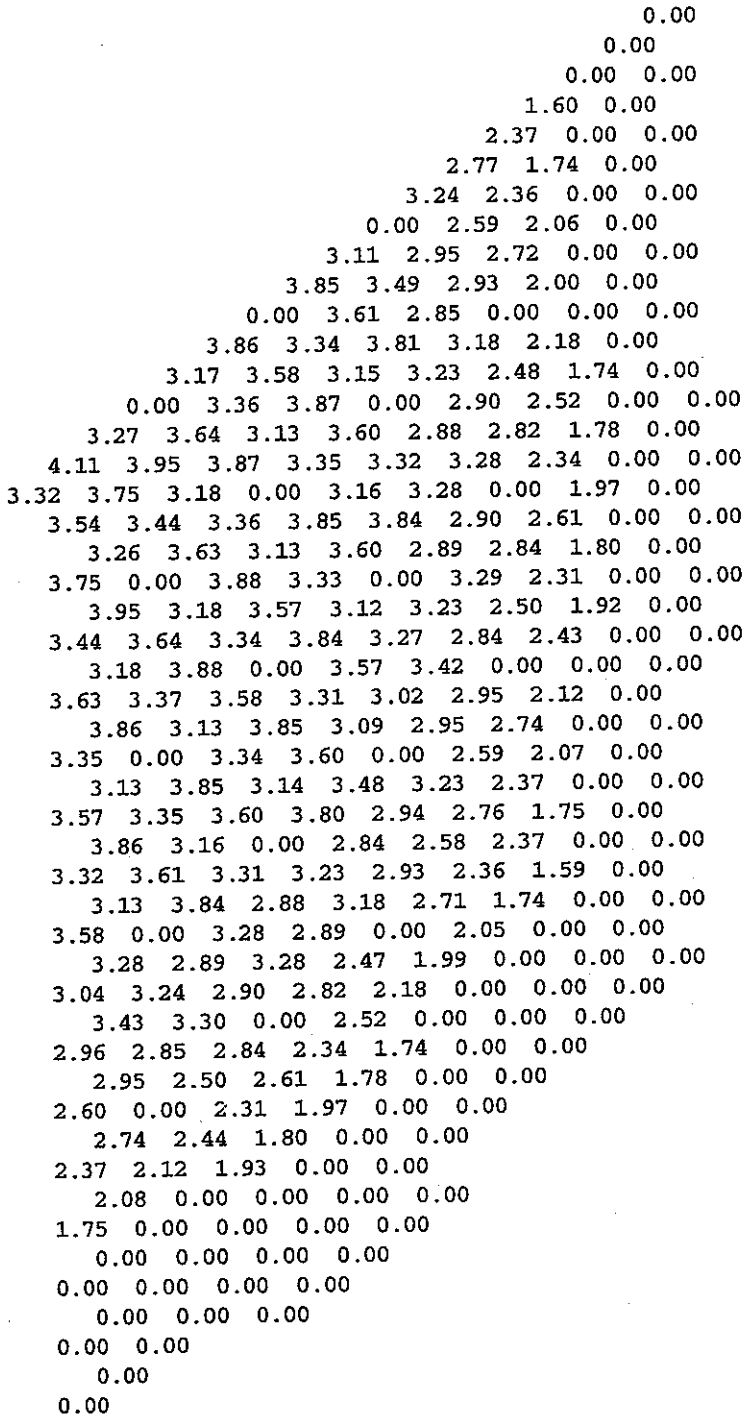


Figure 7.8 Channel power distribution: low quality Pu final optimized case, refuelling batch 4, EOC

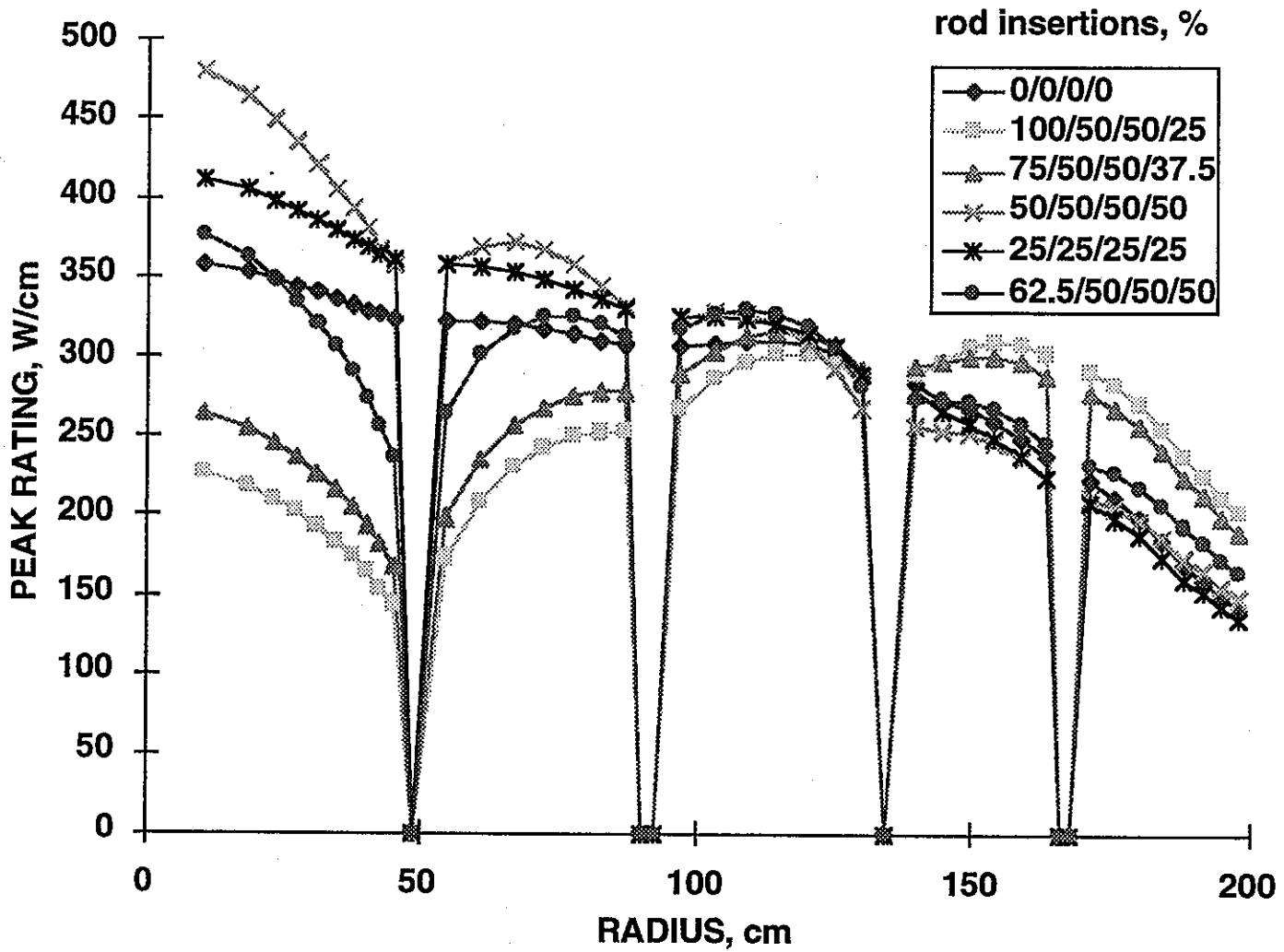


Figure 7.9 Low quality Pu optimized case - variation of BOC 2D radial rating distribution with PCR distribution

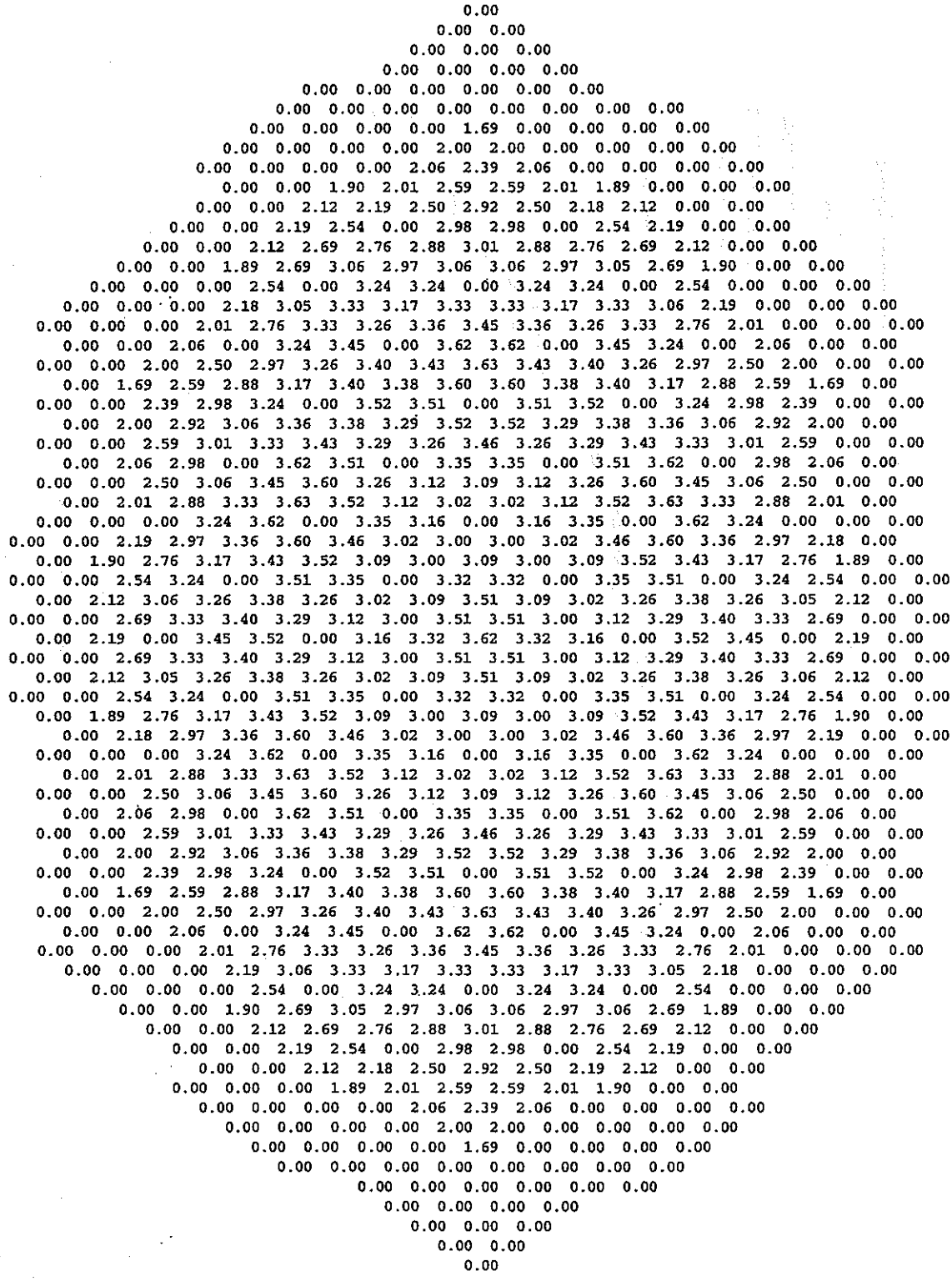


Figure 7.10 Low quality Pu optimized case - MOSES snapshot BOC channel power distribution for PCRs 60/50/50/50% in

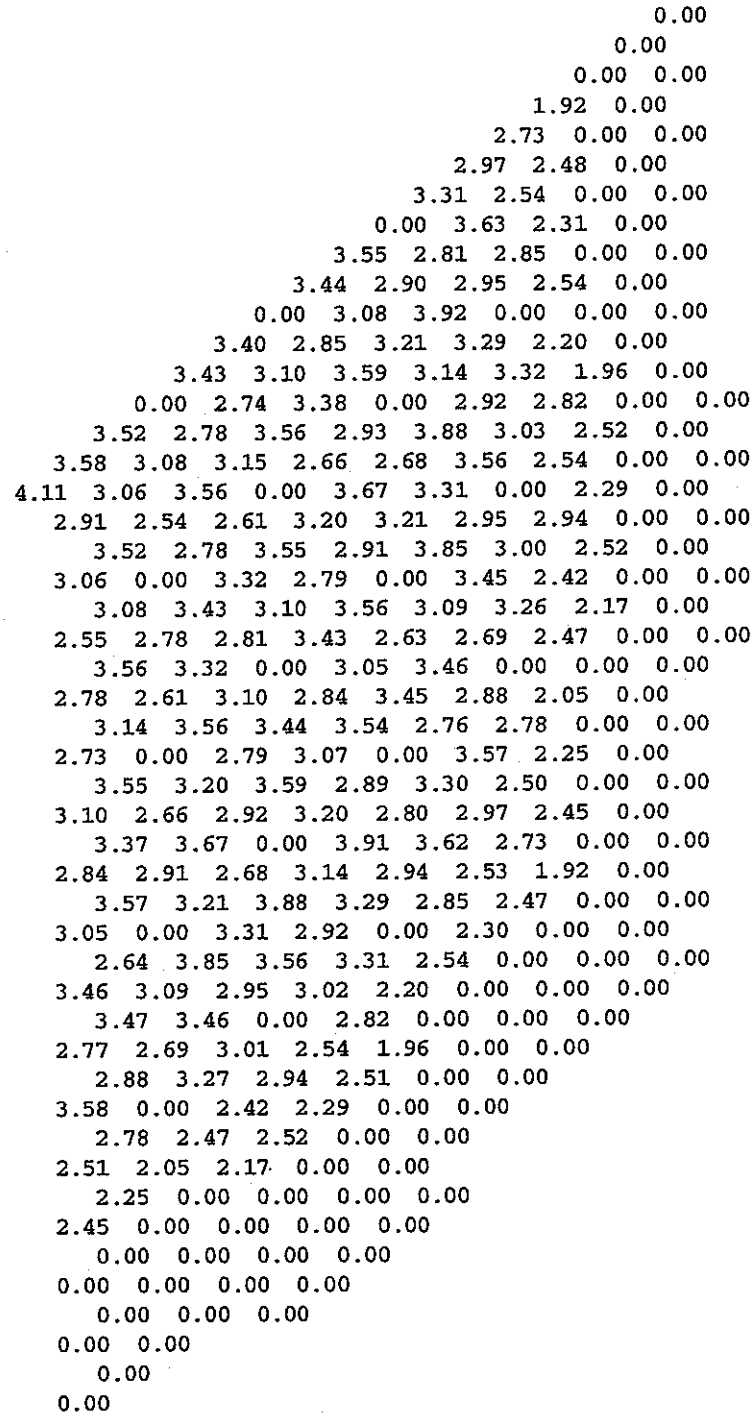


Figure 7.11 Channel power distribution: high quality Pu final optimized case, refuelling batch 1, BOC

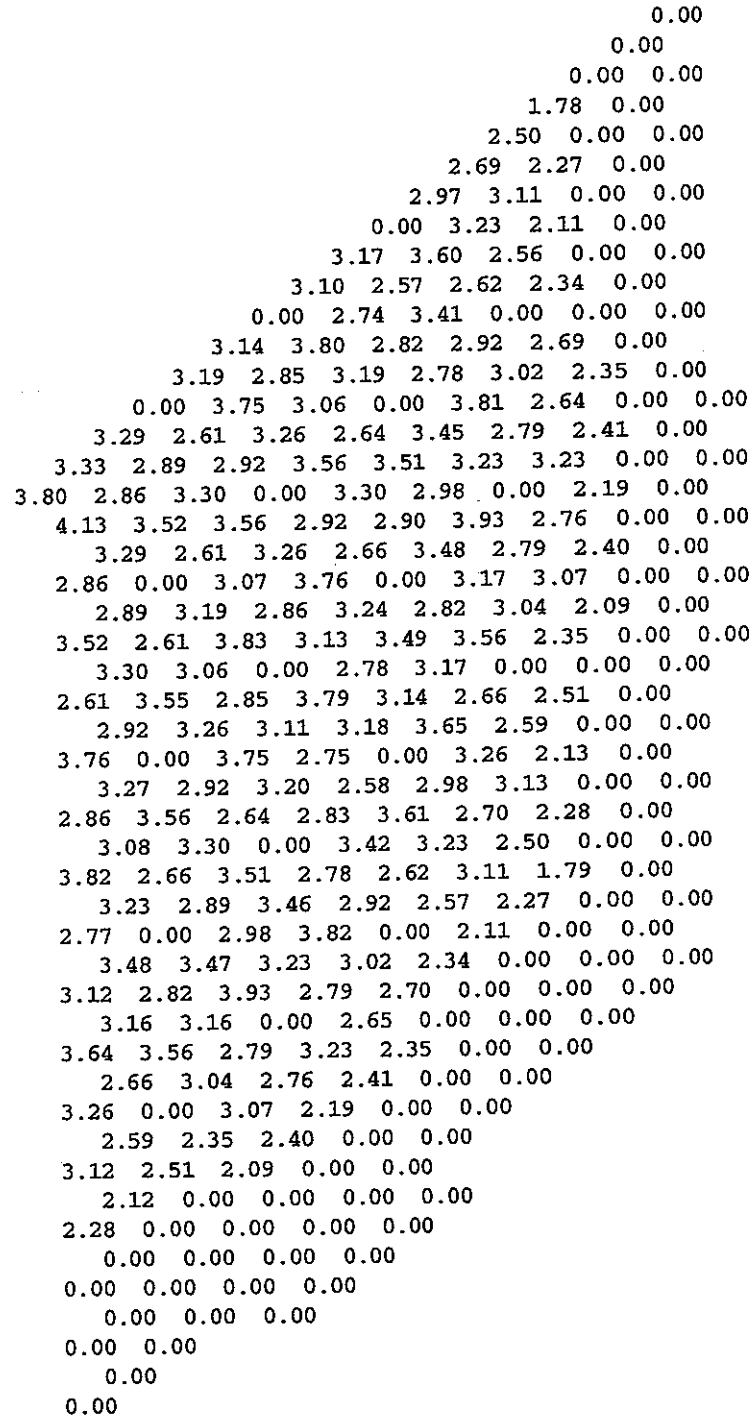


Figure 7.12 Channel power distribution: high quality Pu final optimized case, refuelling batch 2, BOC

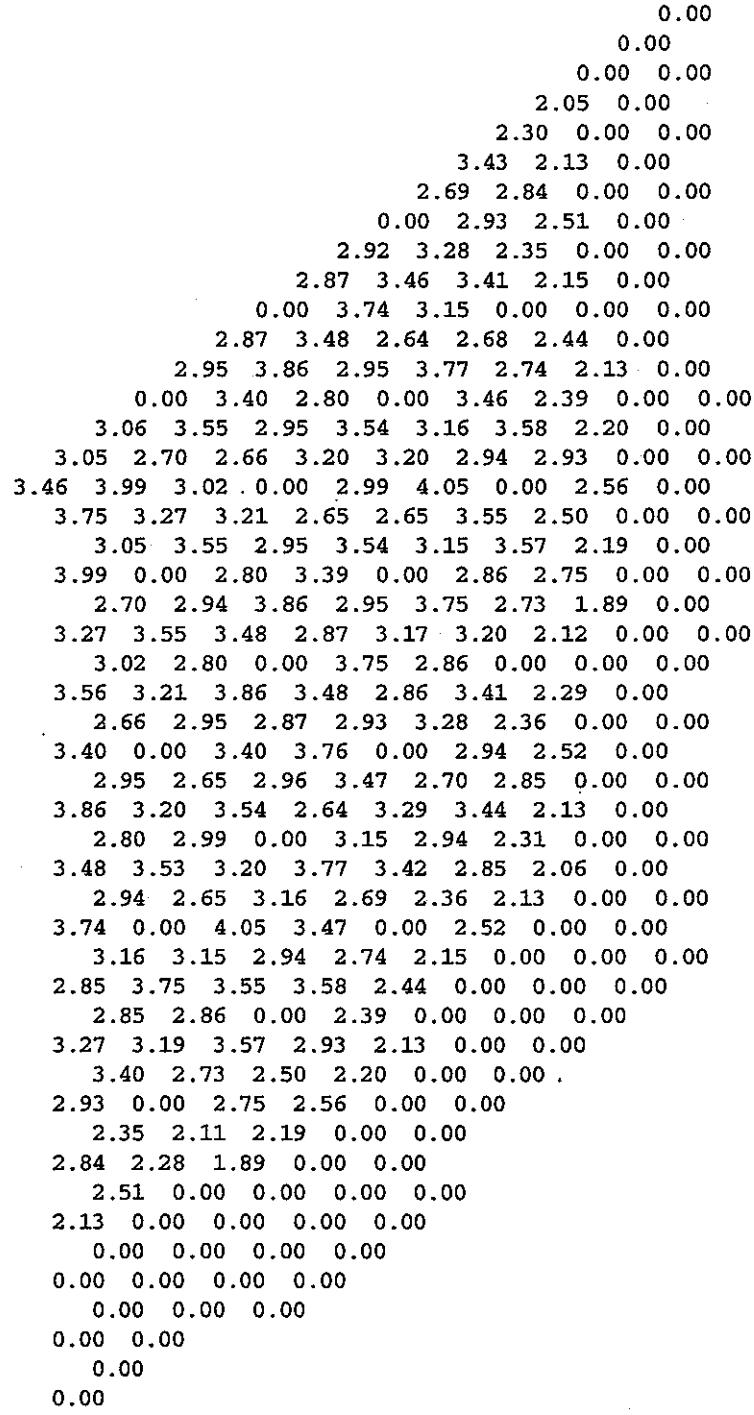


Figure 7.13 Channel power distribution: high quality Pu final optimized case, refuelling batch 3, BOC

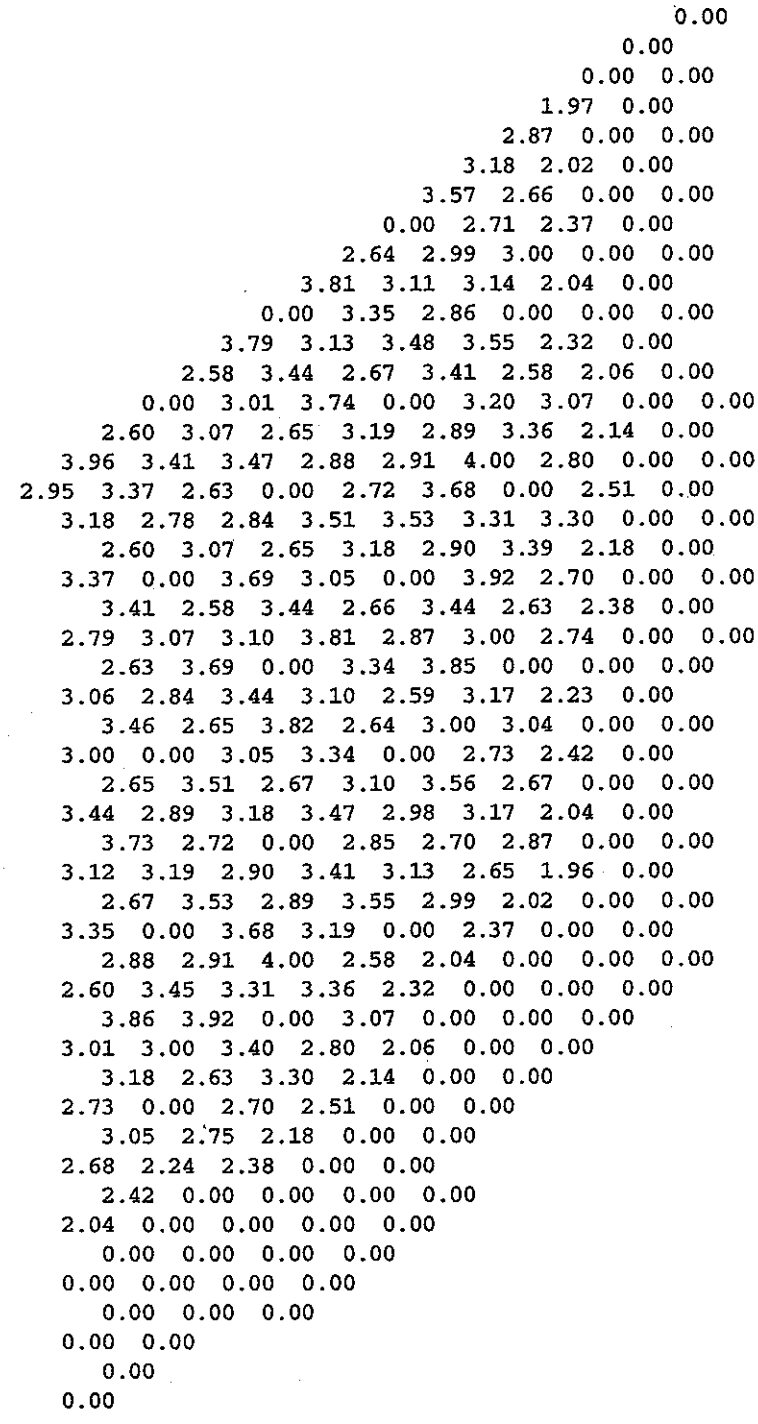


Figure 7.14 Channel power distribution: high quality Pu final optimized case, refuelling batch 4, BOC

```
                                                    0.00
                                                  0.00
                                                0.00  0.00
                                              1.74  0.00
                                            2.47  0.00  0.00
                                          2.75  2.25  0.00
                                        3.30  2.35  0.00  0.00
                                      0.00  3.42  2.18  0.00
                                    3.58  2.86  2.83  0.00  0.00
                                  3.31  2.97  2.94  2.60  0.00
                                0.00  3.01  3.79  0.00  0.00  0.00
                              3.41  2.79  3.28  3.25  2.23  0.00
                            3.86  3.08  3.66  3.18  3.22  1.82  0.00
                          0.00  2.89  3.37  0.00  2.76  2.57  0.00  0.00
                        4.04  3.24  3.77  3.07  3.84  2.74  2.24  0.00
                      3.73  3.62  3.50  2.86  2.78  3.25  2.26  0.00  0.00
                    4.17  3.34  3.92  0.00  3.69  3.15  0.00  2.02  0.00
                      3.08  3.03  2.93  3.40  3.30  2.72  2.60  0.00  0.00
                        4.04  3.25  3.77  3.06  3.81  2.72  2.24  0.00
                      3.34  0.00  3.46  2.81  0.00  3.24  2.22  0.00  0.00
                        3.62  3.87  3.08  3.64  3.13  3.17  2.02  0.00
                      3.03  3.25  2.85  3.32  2.73  2.69  2.49  0.00  0.00
                        3.92  3.46  0.00  2.99  3.38  0.00  0.00  0.00
                      3.24  2.94  3.08  2.76  3.52  2.88  2.12  0.00
                        3.50  3.78  3.33  3.57  2.82  2.77  0.00  0.00
                      2.89  0.00  2.82  3.01  0.00  3.38  2.13  0.00
                        3.77  3.40  3.66  2.97  3.29  2.32  0.00  0.00
                      3.08  2.86  3.07  3.28  2.85  2.74  2.23  0.00
                        3.36  3.69  0.00  3.78  3.41  2.47  0.00  0.00
                      2.78  3.06  2.78  3.17  2.94  2.35  1.74  0.00
                        3.64  3.30  3.83  3.25  2.83  2.25  0.00  0.00
                      3.00  0.00  3.15  2.75  0.00  2.18  0.00  0.00
                        2.74  3.81  3.25  3.22  2.60  0.00  0.00  0.00
                      3.52  3.14  2.72  2.74  2.22  0.00  0.00  0.00
                        3.39  3.24  0.00  2.57  0.00  0.00  0.00
                      2.83  2.70  2.72  2.26  1.82  0.00  0.00
                        2.89  3.17  2.60  2.24  0.00  0.00
                      3.38  0.00  2.22  2.02  0.00  0.00
                        2.78  2.49  2.25  0.00  0.00
                      2.32  2.12  2.02  0.00  0.00
                        2.14  0.00  0.00  0.00  0.00
                      2.23  0.00  0.00  0.00  0.00
                        0.00  0.00  0.00  0.00
                      0.00  0.00  0.00  0.00
                        0.00  0.00  0.00
                      0.00  0.00
                        0.00
                      0.00
```

Figure 7.15 Channel power distribution: high quality Pu final optimized case, refuelling batch 1, EOC

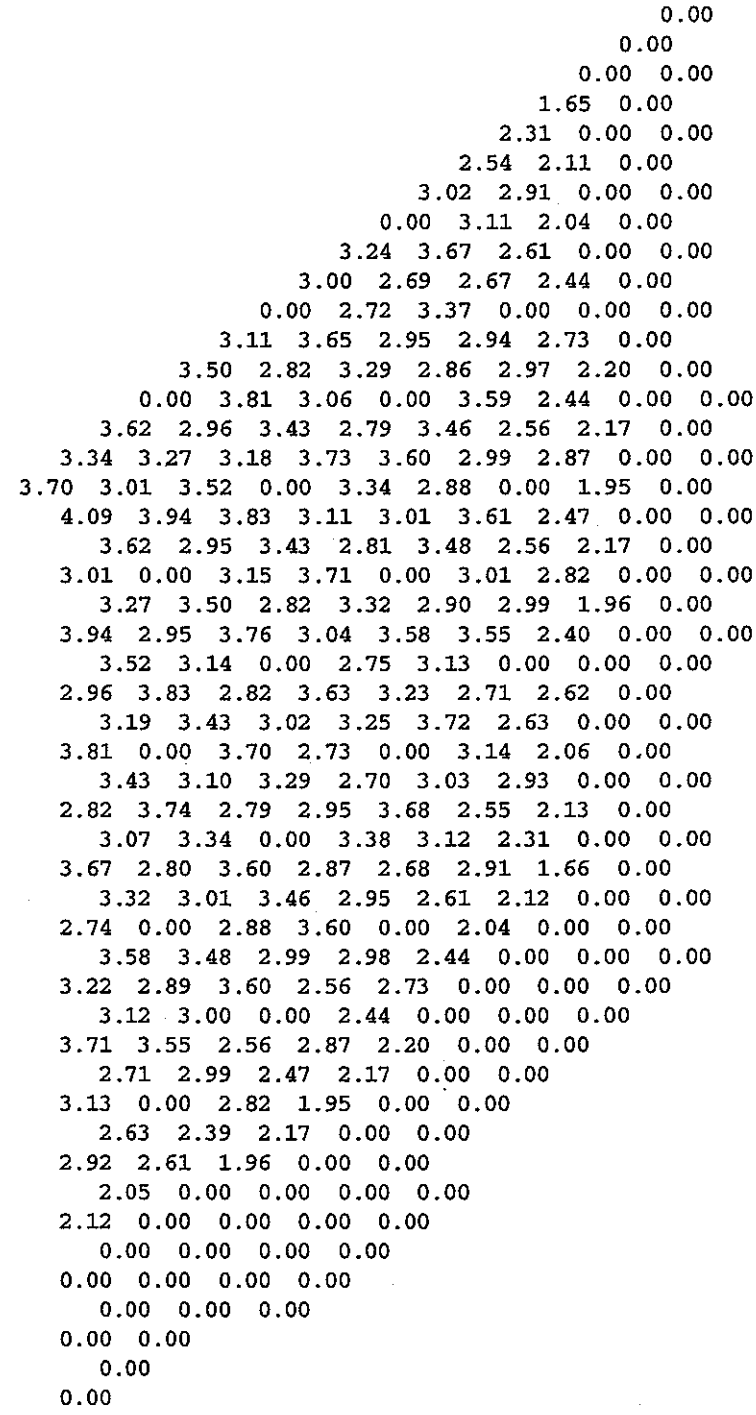


Figure 7.16 Channel power distribution: high quality Pu final optimized case, refuelling batch 2, EOC

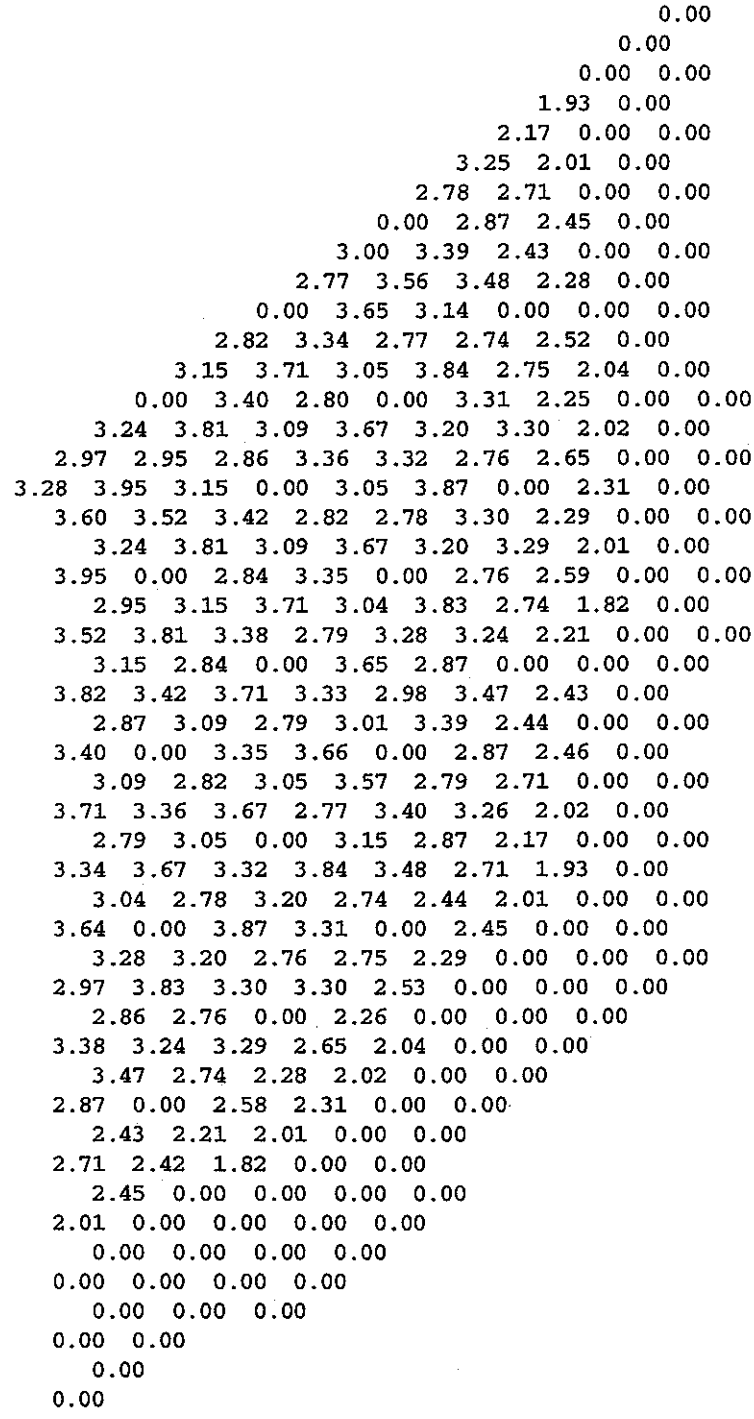


Figure 7.17 Channel power distribution: high quality Pu final optimized case, refuelling batch 3, EOC

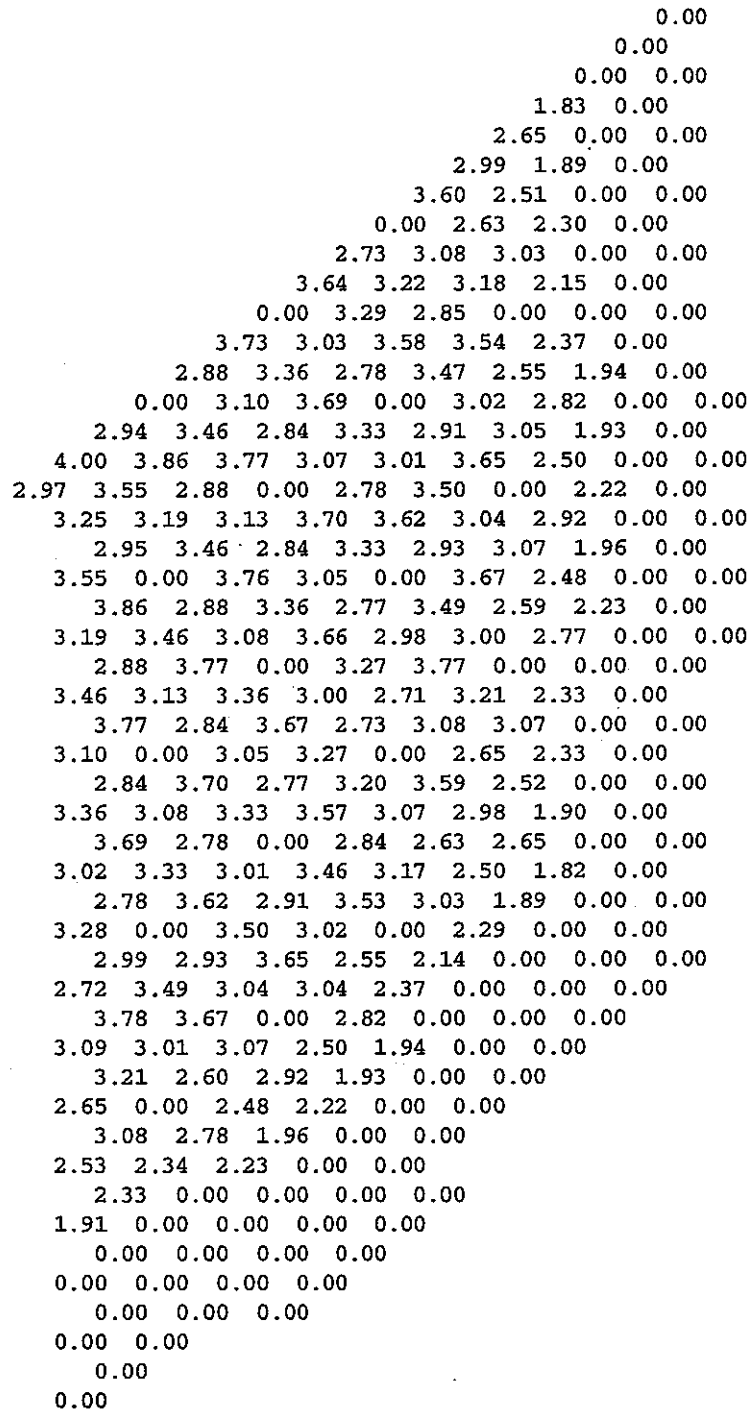


Figure 7.18 Channel power distribution: high quality Pu final optimized case, refuelling batch 4, EOC

# 8 CONCLUSIONS

The effects of varying the Pu vector in a 600 MW(e) design of Pu burning fast reactor have been examined. A series of sensitivity studies was carried out, culminating in the production of a design optimized for a full range of Pu vectors. The conclusions encompass both the work of the current document and that reported as Part I of the study, including some revision of previous conclusions in the light of more recent results.

The study adopted as a reference a core design which had been optimized for Pu burning with a fixed, intermediate quality Pu vector. The Pu vector was varied from military grade Pu (high quality), to Pu multiply recycled in a Pu burner reactor (low quality). Methods of modifying the core design that were effective in offsetting the consequences of Pu vector variation were those that altered the fuel inventory appropriately: replacing some fuel with a diluent material; altering the fuel pin size.

Two different groups of diluent materials were identified, classified by their effects on certain significant reactor parameters:

non-absorber : improves the Na void/Doppler parameters
but degrades the shutdown margin

absorber : improves the shutdown margin
but degrades the Na void/Doppler parameters.

Just one absorber diluent material was examined, $^{10}B_4C$. One non-absorber diluent - ZrH - was identified as having a significantly better performance than any of the others examined. All the remaining non-absorber diluents examined were rather similar in effect; $^{11}B_4C$ and BeO were a little better than MgO, $Al_2O_3$, $CeO_2$ or 'void'. Because of its compatibility with the absorber diluent, $^{11}B_4C$ was considered further, along with ZrH. The use of a mixture of absorber and non-absorber diluents gives an extra degree of freedom for defining the fuel cycle design, optimizing the combination of shutdown margin and Na void/Doppler values by adjusting the ratio of absorber:non-absorber diluent.

To achieve criticality with a low quality Pu vector, the fuel pin size had to be increased from that of the reference core. In

addition, a small amount of non-absorber diluent was included, so that acceptable values of Na void/Doppler parameters were produced. The minimum fuel pin size required was ~150% or ~200% of the reference pin volume, depending on whether ZrH or $^{11}B_4C$ was used as the diluent.

If, for high quality Pu, the same increased pin sizes are used as were necessary for the low quality Pu, then the amount of diluent material required (to maintain criticality) is so high that the 430 W/cm pin limit can only be met if some fraction of the diluent is mixed in the fuel pellets. The minimum proportion of diluent needed in the fuel pellet increases as the pin size increases; if ZrH rather than $^{11}B_4C$ is used as non-absorber diluent the ratings decrease and the limit can just be met without any diluent in the fuel pellet. Increasing the pin size also decreases the shutdown margins; however, there is a decrease in shutdown margins if $^{11}B_4C$ is replaced by ZrH.

An alternative to using fuel pellets that incorporate diluent material (as an inert matrix) is to replace some of the diluent material with 'void', and place the 'void' in the fuelled pins (as hollow fuel pellets). Since 'void' and $^{11}B_4C$ have similar effects as diluents, reactor characteristics need be little changed. Fuel pellet integrity considerations will limit the size of hole in a hollow pellet; a maximum bore of 45% of pellet diameter was assumed. For a 150% pin size, the hollow pellet reduced peak ratings to just below 430 W/cm. For a 200% pin size with $^{11}B_4C$ non-absorber diluent, peak ratings remained well above the limit - adopting a mix of ZrH and $^{11}B_4C$ as non-absorber diluent allowed a good margin to the rating limit (without the sizable decrease in shutdown margin that occurs if just ZrH is used).

With the increased pin sizes, the rod group worth shutdown margins were generally inadequate (i.e. negative). It was shown that, by increasing the number of absorber rods above that of the reference core, the shutdown margins could be increased to an acceptable level

Following the sensitivity assessment, the study was completed by producing a single core design suitable for and optimized with the range of Pu vectors. These calculations used models and calculation

methods more detailed than would have been practical for the sensitivity survey. The effects of the changes included a reduction in core reactivity (compensated for by an increase in pin size), and most significantly an increase in peak pin ratings by in the region of 20% (from replacing a 2D model buy a 3D model). This latter resulted in the option of a larger (~200%) pin size considered in the sensitivity studies not being viable.

The optimized design was generally limited to considering options that are within the scope of current operational experience, rather than incorporating some of the design proposals whose feasibility is the subject of ongoing R & D. Thus the final optimized designs were produced subject to the following restrictions:

MOX fuel, with a peak Pu enrichment ~45%

no inert matrix included in the fuel pellet

the same pin size for all Pu vectors.

The optimized reactor/core design required some modifications to the reference core designated as the starting point of the study (which reference core had itself been optimized for Pu burning, with a fixed, intermediate quality Pu vector). One of the aims of the study was to make as few alterations to the original reference core design as possible - the intention was to provide a demonstration of the flexibility of fast reactors in a Pu burning role, by showing that we could still meet our other aims with this self-imposed rigidity. The following modifications were made:

fuel pin volume increased, by 65%

number of absorber rods increased, from 36 to 54.

With just these two modifications, it proved possible to produce a design capable of accommodating the range of Pu vectors - thus demonstrating the flexibility of fast reactors in a Pu burning role.

The first of these changes was necessary to achieve criticality with the lower qualities of Pu; the second change was required for the rod shutdown requirements to be met with the increased pin size - it was more than sufficient and allowed cycle lengths to increase to ~10 months (a significant economic advantage, compared with a 6 month

cycle). The pin size of 165% corresponds to a pin diameter of 7.422 mm, a fuel pellet diameter of 6.141 mm and a clad thickness of 0.538 mm. With these dimensions the core region has the following volume fractions: coolant 47.37%, wrapper 9.26% and fuel pin 43.37%, the latter includes 11.66% clad and 29.69% fuel. There are 235 fuel S/As in the inner enrichment zone and 288 in the outer zone. Otherwise, the reference design remains unaltered: a core of 0.6 m height x ~4.0 m radius, a S/A design with 217 pins and a pitch of 158.1 mm (a/f).

Optimized conditions were produced for the two extreme Pu vectors. The low quality Pu case was for a fuel cycle of 4 batches of 10.5 month, a uniform 45.1% Pu enrichment and 21 ZrH diluent pins (only in the inner zone). The high quality Pu case was for a fuel cycle of 4 batches of 9.75 months, hollow fuel pellets of 45% bore with Pu enrichments of 40.3% and 45.0% in the 2 zones, a diluent of 24 ZrH pins and 8 $B_4C$ pins (30% $^{10}B$). All limits on parameters were met, a comprehensive set of results is shown in Table 7.5, the key parameters are:

| | low quality Pu | high quality Pu |
|---|---|---|
| Na void worth | 2.01%Δk/kk' | 0.83%Δk/kk' |
| Doppler constant | -0.00820 | -0.00499 |
| Void:Doppler ratio | -245 | -165 |
| peak pin rating | 417 W/cm | 428 W/cm |
| PCR shutdown margin | +0.55%Δk/kk' | +0.14%Δk/kk' |
| BCR shutdown margin | +0.36%Δk/kk' | +0.67%Δk/kk'. |

The optimized core design was achieved with some margin to limits in one or other of the parameters.

Some conclusions were drawn regarding the calculation methods and these may be relevant to other studies:

- peak pin ratings are only modelled effectively by using a full 3D representation. Peak pin ratings can be underestimated by around 20% (for otherwise identical conditions) if a 2D (RZ) geometry is modelled, rather than a 3D (pseudo-tri-Z) geometry (used in the calculation of burn-up as well as flux/rating distributions). There

is an additional effect (of a few percent) from the explicit representation of the separate fuel irradiation batches.

- the 7 group energy spectrum is not really adequate for a core, such as the Pu burner with diluent, in which there is significant moderation: uncertainties in Keff are increased by more than half a percent. The 18 group structure is a significant improvement.

- in a breederless core the above and below core structures can have a significant effect on reactivity, they should be modelled in some detail. A breederless core also requires a detailed mesh at the core edge, for number density as well as flux, if leakage is to be modelled accurately - this can have a significant effect on Na void worth.

- using a 2-region model for fuel in SLAROM can significantly alter the Doppler constant. Since this is the more realistic option - it excludes any effect of structural materials at the same temperature as fuel - it should be preferred.

- reactivity loss per cycle is inadequate as a quantitative (rather than qualitative) indicator of shutdown margin variations. To properly assess shutdown margins, 3D calculations of rod worth are necessary.

Two areas were identified where further investigation is warranted:

- the effect of unfuelled diluent pins on the within S/A rating distribution and on thermohydraulics considerations.

- the apparent effect of fuel cell modelling, whereby changing from solid to annular fuel pellet geometry altered the Doppler constant by a third (see Sub-section 6.5).

ACKNOWLDGEMENT

The author wishes to express his thanks to PNC for being given the opportunity under the International Fellowship scheme to come to work in Japan and undertake the task reported herein.

The work was carried out under the supervision of the General Manager of the Reactor Physics Research Section, Dr, Wakabayashi, who provided the right level of support to allow the task to be carried out in an effective and rewarding manner. Both Dr. Wakabayashi and the Deputy General Manager of the Reactor Physics Research Section, Mr. Ishikawa, participated in technical discussions which were essential to guiding the direction of the work as it progressed.

The work would have been immeasurably more onerous, if not impossible, without the willing contributions of all the members of the Reactor Physics Research Section, in helping me understand the various computer systems and programs used, and particularly in facilitating access to various Japanese reports and data sources.

REFERENCES

1-1 M.Yamaoka, M.Ishikawa, T.Wakabayashi. Feasibility study of TRU transmutation by LMFBRs. Proc. Int. Conf. on Fast Reactors and Related Fuel Cycles (FR'91), Vol.IV, Oct.28-Nov.1, Kyoto (1991)

1-2 T.Wakabayashi, M.Yamaoka, M.Ishikawa, H.Hirao. Status of study on TRU transmutation in LMFBRs. Trans. Am. Nucl. Soc., 64, 556 (1992)

1-3 M.Yamaoka, T.Wakabayashi. Design study of a super long life core loaded with TRU fuel. Proc. Int. Conf. on design and safety of advanced nuclear power plants (ANP'92), Vol.I, Oct.25-29, Tokyo (1992)

1-4 T.Wakabayashi, T.Ikegami. Characteristics of an LMFBR core loaded with minor actinide and rare earth containing fuels. Proc. Int. Conf. on Future Nuclear Systems: Emerging Fuel Cycles and Waste Disposal Options (GLOBAL'93), Vol.1, Sep.12-17, Seattle (1993)

1-5 T.Wakabayashi, S.Okhi, T.Ikegami. Feasibility studies of an optimized fast reactor core for MA and FP transmutation. Proc. Int. Conf. on Evaluation of Emerging Nuclear Fuel Cycle Systems (GLOBAL'95), Vol.I, Sep.11-14, Versailles (1995)

1-6 L.Koch. Formation and recycling of minor actinides in nuclear power stations, Handbook on the physics and chemistry of the actinides, Chapter 9. North-Holland publishing (1986)

1-7 Committee on International Security and Arms Control, US National Academy of Sciences, Management and disposition of excess weapons plutonium. National Academy Press (1994)

1-8 A.Languille et al. CAPRA core studies - the oxide reference option. Proc. Int. Conf on Evaluation of Emerging Nuclear Fuel Cycle Systems (GLOBAL'95), Vol.I, Sep.11-14, Versailles (1995)

1-9 J.C.Garnier, A.Shono, T.Wakabayashi. Parametrical Studies on Pu burning in fast reactors. Proc. Int. Conf. on Evaluation of Emerging Nuclear Fuel Cycle Systems (GLOBAL'95), Vol.I, Sep.11-14, Versailles (1995)

3-1 MOSES manual PNC N9520 89-018 (1989)

3-2 T.Takeda, Y.Komano. Extension of Askew's coarse mesh method to few-group problems for calculating two-dimensional power distribution in fast breeder reactors. J.Nucl.Sci.Technol. 15[7], 523 (1978)

4-1 A.Languille et al. CAPRA core studies - the oxide reference option. Proc. Int. Conf. on Evaluation of Emerging Nuclear Fuel Cycle Systems (GLOBAL'95), Vol.I, Sep.11-14, Versailles (1995)

6-1 Status of fast breeder reactor research and development. PNC TN 1410 92-011 (1992)